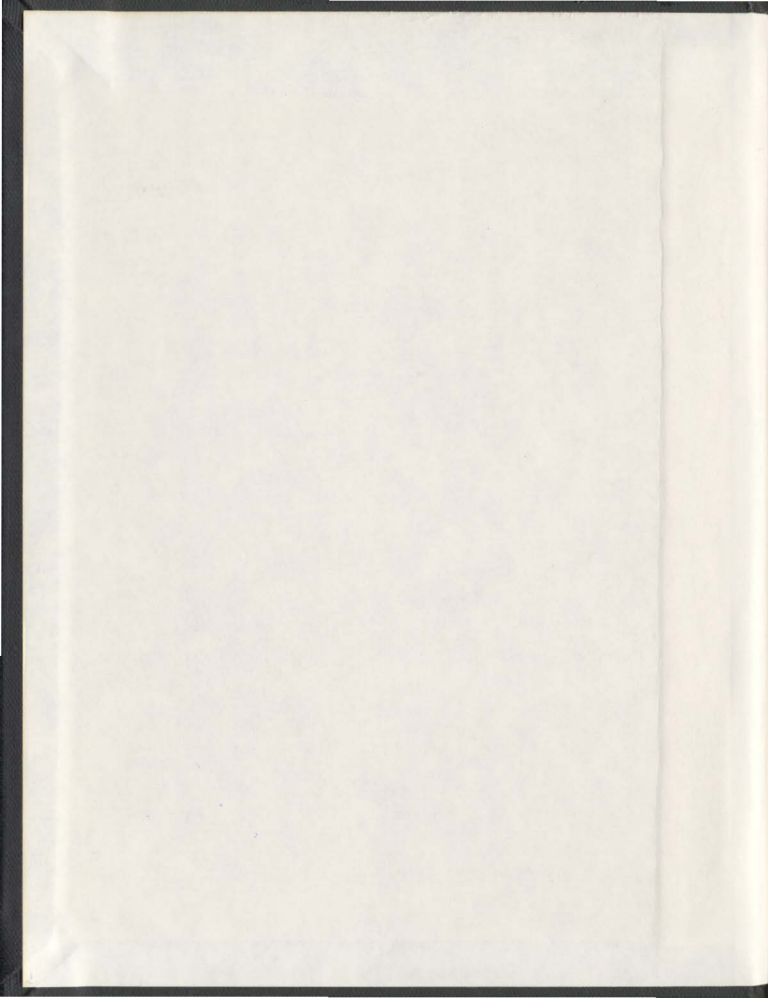


STRUCTURE-FUNCTION OF NATIVE AND
AMINO-TERMINALLY TRUNCATED STRIATED
MUSCLE TROPOMYOSINS

CHARITHA LAKSHINI GOONASEKARA



**STRUCTURE-FUNCTION OF NATIVE AND AMINO-
TERMINALLY TRUNCATED STRIATED MUSCLE
TROPOMYOSINS**

by

Charitha Lakshini Goonasekara. B.Sc. (University of Colombo, Sri Lanka)

**A thesis submitted to the School of Graduate Studies in partial fulfillment of the
requirements for the degree of Doctor of Philosophy**

Department of Biochemistry

**Memorial University
St. John's, Newfoundland
May, 2008**

Abstract

Tropomyosin is a polymeric protein found in the muscle thin filament together with actin and troponin. The end regions, which encompass the first and last 10-11 amino acids, are vital to its function. We have analyzed the role of the amino-terminal region by selective removal of the first six amino acids. A method describing the hydrolysis of the sixth peptide bond of tropomyosin by bacterial outer membrane protease T (Omp T) is described.

Compared to the native counterparts, shortened forms of rabbit skeletal and Atlantic salmon fast skeletal tropomyosins (residues 7 - 284), as well as the unacetylated (residues 1 - 284) version of the latter, all display reduced affinity for both troponin and the amino-terminal fragment of rabbit skeletal troponin-T (N-Tn-T, residues 1 - 158), as judged by affinity chromatography. Thus, loss of the hexapeptide, together with the blocking group, weakens the binding of tropomyosin and troponin-T. Omp T-digested tropomyosin binds weakly to F-actin in the micromolar concentration range, but this interaction is restored by troponin. At moderate ionic strength (50mM KCl), the apparent Kds are: 0.26 μ M (+EGTA) and 1.6 μ M (+Ca²⁺). The inductive property of troponin is attributable, in part, to troponin-I. But whereas the amino-terminal fragment of troponin-T (residues 1-158) enhances troponin-I-induced F-actin binding of two other tropomyosin products which have weak affinity for F-actin, specifically, recombinant unacetylated tropomyosin (residues 1 - 284) and carboxypeptidase-digested tropomyosin (residues 1 - 273, Heeley, D. H. et al (1987) J. Biol. Chem. 262,9971-9978), it is ineffective in the case of the Omp T-digested protein. These data are evidence for a troponin-T binding site within the amino-terminal region of tropomyosin.

In assays that contain myosin, thin filaments composed of Omp T-digested tropomyosin are less cooperative than native thin filaments, consistent with the disruption of physical continuity within the filament. At the same time, however, the truncated system (+Ca²⁺,

ionic strength, 22mM) activates myosin to a greater extent than native tropomyosin, and has stronger affinity for myosin-S1-ADP (+EGTA; ionic strength, 70mM), the reverse of what has been observed with the carboxy-terminally-shortened protein. These results suggest that the amino-terminal region of tropomyosin is an inhibitory thin filament element, which stabilizes the off-state of the thin filament via an interaction with the tail section of troponin-T, and that the two ends at the overlap complex have opposing regulatory roles.

Finally, the conformational stability of tropomyosins from Atlantic salmon was characterized under a variety of conditions (salt, pH and osmolyte). The most variable sections of sequence encompass residues 9-49, 73-87 and 172-216. In two of these hotspots there is a pair of closely-spaced glycines, namely at residues 24 and 27 in fast skeletal tropomyosin and residues 83 and 87 in cardiac tropomyosin. Further, the isoform from fast muscle does not have a "d" position alanine between residues 172-216 due to the isomorphism Ala179Thr and thus lacks the fifth alanine cluster. These substitutions have reduced the conformational stability of the fish protein compared to the mammalian counterpart and provide insight into the adaptation of tropomyosin to cold temperature.

Acknowledgement

I would like to express my deepest gratitude to my supervisor Dr. David Heeley for allowing me the opportunity to work in his lab and for his guidance throughout the project. I will always value the kindness, patience and understanding you have shown towards me, which made me feel at home thousands miles away from my family. I am very much thankful to my supervisory committee, Dr. Martin Mulligan and Dr. Valerie Booth, for their valuable suggestions and guidance in my study and the thesis. I would also like to express my gratitude to Ms. Donna Jackman for her expert technical support, guidance throughout my research and valuable comments on all my manuscripts and thesis. I am also thankful to Ms. Linda Winsor for helping me with Mass spectrometric analysis, Dr. Dawn Marshall for helping me with phylogenetic analysis and Dr. Howard White for providing me with valuable proteins samples. My appreciation also goes to Mr. Craig Skinner and Mr. Roy Ficken for all your technical support in generating computer graphics for my manuscripts and thesis. For all my lab mates and people in the Biochemistry department, your friendship and company are greatly appreciated; you have made a pleasant environment to work. I also like to express my deepest gratitude to my dear husband Sampath Seneviratne and friends Chandrika Liyanapatirane, Wasana Mudalige, Lisa Gallivan, Robert Mercer, Kanta Chechi and Pratibha Dubey for their technical and moral support given to me to succeed in this program. Finally, my loving family – my parents, brother and husband, without your love and support this thesis would not have been possible and I am deeply indebted to you.

Contents

Abstract	ii
Acknowledgement	iv
Contents	v
List of figures	x
List of tables	xiii
List of abbreviations	xiv

Chapter 1. Introduction

1.1 Striated muscle and its architecture	1
1.2 Thin Filament	4
1.2.1 Tropomyosin	4
1.2.1.1 Genes, isoforms and distribution	5
1.2.1.2 Structure	9
1.2.1.3 Stability	15
1.2.2 Actin	16
1.2.3 Troponin	21
1.2.3.1 Troponin C	23
1.2.3.2 Troponin I	24
1.2.3.3 Troponin T	25
1.3 Myosin	26
1.4 Muscle contraction	28
1.4.1 Regulation of muscle contraction	31
1.4.1.1 Calcium induced changes in the troponin complex	31
1.4.1.2 Structural changes in the thin filament	34
1.4.1.3 Thin filament cooperativity	38
1.5 Objectives of the study	39

Chapter 2. Materials and methods

2.1 Extraction of muscle proteins	44
2.1.1 Tropomyosin	44
2.1.1.1 Acetone powder preparation	44

2.1.1.2	Tropomyosin isolation	45
2.1.2	Troponin	46
2.1.2.1	Acetone powder preparation	47
2.1.2.2	Troponin isolation	47
2.1.2.3	Separation of troponin subunits	48
2.1.3	Actin	48
2.1.3.1	Acetone powder preparation	48
2.1.3.2	Actin isolation	49
2.2	Expression of tropomyosin in bacteria	50
2.3	Preparation of amino-terminally truncated tropomyosin	51
2.3.1	Expression of tropomyosin in <i>E. coli</i> JM109	51
2.3.1.1	Cloning tropomyosin cDNA in to the expression vector	52
2.3.1.2	Transformation and Induction	53
2.3.2	Cleavage of isolated tropomyosin with a cell suspension of <i>E. coli</i> JM109	53
2.3.2.1	Analytical-scale digestion	53
2.3.2.2	Large-scale digestion	54
2.4	Electrophoretic methods	55
2.4.1	Sodium dodecyl sulfate polyacrylamide gel electrophoresis (SDS PAGE)	55
2.4.2	Isoelectric focusing gel electrophoresis	55
2.4.3	Agarose gel electrophoresis	56
2.5	Spectroscopic methods	56
2.5.1	UV-Visible absorbance	56
2.5.2	Matrix Assisted Laser Desorption Ionization – time of flight (MALDI-tof) Mass spectrometry	57
2.5.3	Circular Dichroism	57
2.6	Protein blotting	59
2.7	Affinity chromatography	59
2.7.1	Bradford assay	61
2.8	Tropomyosin binding to Actin	61
2.8.1	Labeling tropomyosin with Iodo[1- ¹⁴ C]acetamide	61
2.8.2	Actin binding assay	62
2.9	ATPase activity measurements	63
2.10	Myosin binding assay	63

2.11	Data fitting	64
------	--------------	----

Chapter 3. Preparation and analysis of amino terminally truncated tropomyosin

3.1	Introduction	65
3.2	Results	66
3.2.1	Induction of tropomyosin expression in <i>E. coli</i> JM 109	66
3.2.2	Treatment of tropomyosin with <i>E. coli</i> JM109 cell suspension	69
3.2.2.1	Time course and temperature.	69
3.2.2.2	Effect of pH, divalent cations and cell lysate over cell suspension	72
3.2.2.3	Digestion of other tropomyosins	73
3.2.2.4	Effect of acetylation on digestion	73
3.2.2.5	Preparative scale digestion	76
3.2.3.	Analysis of truncated tropomyosins.	79
3.2.3.1	Edman-based sequencing	79
3.2.3.2	Mass analysis	79
3.2.3.3	Circular Dichroism spectrometry of truncated tropomyosins.	84
3.2.3.4	Ability to form thin filaments	87
4.3.	Discussion	91

Chapter 4. Binding of Omp T digested tropomyosin to other thin filament proteins

4.1	Introduction	100
4.2	Results	101
4.2.1	Binding of truncated tropomyosin to troponin or its constituents	101
4.2.1.1	Binding to whole troponin	101
4.2.1.2	Binding to N-troponin T	105
4.2.2	Binding of truncated tropomyosin to actin	105
4.2.2.1	Effect of whole troponin	105
4.2.2.2	Effect of troponin sub-components Troponin-I and N-troponin T	114

4.3	Discussion	119
-----	------------	-----

Chapter 5. Effects of removal of the amino terminal six amino acids of tropomyosin on the regulatory properties and myosin binding of the striated muscle thin filament

5.1	Introduction	125
5.2	Results	125
	5.2.1 Activation of myosin subfragment 1	125
	5.2.1.1 Effect of varying tropomyosin concentration	126
	5.2.1.2 Effect of varying myosin-S1 concentration	128
	5.2.1.3 Effect of varying thin filament concentration	132
	5.2.2 Myosin-S1 binding to thin filaments containing truncated or full-length tropomyosin.	132
5.3	Discussion	137

Chapter 6. Sequence diversity and the structural properties of salmon tropomyosins

6.1	Introduction	142
6.2	Results	143
	6.2.1 Characterizing the thermostabilities of wild type and recombinant salmon fast tropomyosins	143
	6.2.1.1 Effect of differential heating and cooling on the minor transition of salmon fast tropomyosin.	150
	6.2.1.2. Thermostabilities of the two cyanogen bromide fragments	153
	6.2.1.3. Thermostability of the oxidized protein	155
	6.2.1.4. Near UV Circular Dichroism	158
	6.2.2 Effect of pH, salt, trimethylene N-amino oxide, divalent cations, on the stability of salmon fast tropomyosin.	159
	6.2.3 Thermostability of salmon cardiac and slow tropomyosins	167

6.2.4	Sequence comparisons of tropomyosin isoforms	170
6.2.5	Constructing a phylogenetic tree for tropomyosin	180
6.3	Discussion	183
Chapter 7. General discussion		193
Publications and papers presented at conferences		203
References		205

List of figures

Figure 1.1:	The architecture of the striated muscle and its components	3
Figure 1.2:	The gene organization and structure of tropomyosin	7
Figure 1.3:	Actin structure	19
Figure 1.4:	Structure of the head region of skeletal troponin complex.	22
Figure 1.5:	Structure of myosin	27
Figure 1.6:	The crossbridge cycle (Lynn and Taylor 1971)	30
Figure 1.7:	Regulation of muscle contraction	32
Figure 3.1:	SDS PAGE analysis of salmon fast tropomyosin expressed in <i>E. coli</i> JM109	67
Figure 3.2:	Truncation of rabbit and salmonid tropomyosin with a <i>E. coli</i> JM109 cell suspension.	70
Figure 3.3:	Digestion of various vertebrate muscle tropomyosins	74
Figure 3.4:	The effect of acetylation on Omp T digestion.	75
Figure 3.5:	Preparative scale truncation of rabbit skeletal tropomyosin.	77
Figure 3.6:	Matrix Assisted Laser Desorption Ionization, linear time-of-flight mass spectral analysis of truncated tropomyosins.	82
Figure 3.7:	Circular Dichroism spectrometry of truncated tropomyosins.	85
Figure 3.8:	Binding of tropomyosins to actin in the presence and absence of troponin.	88
Figure 3.9:	Sequences of salmon fast and rabbit alpha tropomyosins.	93
Figure 4.1:	Affinity chromatography.	102
Figure 4.2:	The induction of binding of truncated rabbit skeletal tropomyosin to F-actin by troponin (in the presence or absence of Ca^{2+}) at 70mM ionic strength.	107

Figure 4.3:	The induction of binding of various salmon fast tropomyosins to F-actin by troponin (in the presence or absence of Ca^{2+}) at 70mM ionic strength	110
Figure 4.4:	The effect of ionic strength on the induction of binding of rabbit truncated tropomyosin to F-actin by troponin (in the presence or absence of Ca^{2+}).	112
Figure 4.5:	The effect of potassium acetate on the induction of binding of truncated rabbit tropomyosin to F-actin by troponin (in the presence or absence of Ca^{2+}).	115
Figure 4.6:	The effects of troponin-I and N-troponin-T on binding of truncated tropomyosin to F-actin.	116
Figure 5.1:	Comparison of regulatory properties of thin filaments containing either truncated or wild type full-length rabbit tropomyosin.	127
Figure 5.2:	Activation of myosin-S1 by different thin filaments as a function of myosin-S1 concentration.	130
Figure 5.3:	Dependence of the actomyosin MgATPase activity on the concentration of thin filaments containing either truncated or intact tropomyosin.	133
Figure 5.4:	Binding of myosin-S1 to thin filaments containing truncated or full-length rabbit tropomyosins.	135
Figure 6.1:	Thermostability of wild type salmon fast muscle tropomyosin	144
Figure 6.2:	Thermostability of recombinant salmon fast muscle tropomyosin	147
Figure 6.3:	The effect of differential heating and cooling on the minor transition of salmon fast muscle tropomyosin	151
Figure 6.4:	Thermostability of the CNBr fragments of salmon fast muscle tropomyosin.	154
Figure 6.5:	Effect of disulphide bond formation on the thermostability of salmon fast tropomyosin in far and near UV range	156
Figure 6.6:	Effect of pH on the stability of type salmon fast muscle	160

tropomyosin

Figure 6.7:	Effect of salt and osmolytes on the stability of wild type salmon fast muscle tropomyosin	162
Figure 6.8:	The effect of divalent cations on the stability of salmon fast muscle tropomyosin.	165
Figure 6.9:	Thermostability of salmon cardiac and slow tropomyosins and the effect of pH.	168
Figure 6.10:	The effect of salt and TMAO on the stability of salmon cardiac and slow muscle tropomyosins.	171
Figure 6.11:	Distribution of amino acid substitutions in salmonid and rabbit-alpha muscle tropomyosins	175
Figure 6.12:	Amino acid sequence comparisons of salmonid tropomyosins	177
Figure 6.13:	Alanine clusters of tropomyosins	178
Figure 6.14:	The phylogenetic analysis of tropomyosin	181
Figure 7.1:	A model to show the consequence of removing amino-terminal six residues of tropomyosin on the state of thin filament	198

List of tables

Table 3.1:	The amino-terminal sequences of various tropomyosins	80
Table 3.2:	Omp T susceptible sequences in rabbit alpha and salmon fast muscle tropomyosins showing P4,P3,P2,P1',P2',P3',P4' positions.	94
Table 3.3:	Omp T cleavage sites showing their positions in the heptad-repeat of the tropomyosin coiled-coil.	96
Table 6.1:	Comparison of relative ellipticity changes between wild type and recombinant salmon fast tropomyosins.	149
Table 6.2:	A summary of the melting temperatures of three salmonid fast, cardiac and slow isoforms.	173

List of abbreviations

ADP	Adenosine di phosphate
ATP	Adenosine tri phosphate
CAPS	N-cyclohexyl-3-aminopropanesulfonic acid
CD	Circular dichroism
dH ₂ O	Distilled water
DTT	Dithiothreitol
EDTA	Ethylene diamine tetraacetic acid
EGTA	Ethylene glycol tetraacetic acid
ϵ_{280} 1mg/ml	Extinction coefficient of a 1mg/ml protein at 280nm
HEPES	4-(2-hydroxyethyl)-1-piperazineethanesulfonic acid
IPTG	Isopropyl β -D-thiogalactopyranoside
LB	Lauria broth
MALDI-tof	Matrix assisted laser desorption ionization – time of flight mass
MOPS	3-Morpholinopropanesulfonic acid
Myosin-S1	myosin subfragment 1
NP40	Nonyl phenoxypolyethoxyethanol 40
N-TnT	Amino terminal fragment of troponin T
pI	Isoelectric precipitation point
PIPES	Piperazine-1,4-bis(2-ethanesulfonic acid)
PMSF	Phenylmethylsulphonylfluoride
PVDF	Polyvinylidene Difluoride
SDS PAGE	Sodium dodecyl sulfate polyacrylamide gel electrophoresis spectrometry
TBE	Tris/Borate/EDTA buffer
TE	Tris/EDTA buffer
TEMED	N, N, N, N-tetramethylethylenediamine
TM	Tropomyosin
Tn	Troponin
Tris	Tris(hydroxymethyl)aminomethane

Chapter 1. Introduction

1.1 Striated muscle and its architecture

Muscle is the contractile tissue of the body that produces force and causes motion. In vertebrates, voluntary movements such as locomotion depend on the ability of skeletal muscle to contract on its scaffolding of bone (Figure 1.1A), whereas involuntary movements such as heart pumping or peristalsis depend on the contraction of cardiac and smooth muscles, respectively.

Skeletal muscle fibers have been further divided into three types based on several criteria such as the number of mitochondria present, the use of oxidative or glycolytic pathways for ATP production, contraction time and their resistance to fatigue (Aidley 1971). These are, slow oxidative, fast oxidative and fast glycolytic muscle fibers. The two types of fast fibers constitute most of the skeletal muscle cells in vertebrates. The fast glycolytic fibers are large in diameter, light in colour, contain large glycogen reserves and relatively few mitochondria, and use anaerobic metabolism. Therefore, fast fibers produce powerful but short-term contractions and can fatigue rapidly. In contrast, slow oxidative fibers are smaller in diameter, contain the pigment myoglobin, mitochondria and a higher supply of oxygen for aerobic metabolism, and are red in colour. They produce slow contractions for an extended period and are resistant to fatigue. The properties of fast oxidative fibers are intermediate between the other two, for they have a red colour, large amount of

mitochondria, high fatigue resistance, high glycogen and short contraction times. The percentages of the three fiber types in a skeletal muscle can be quite variable. Most mammalian muscles contain an intermingled mixture of all three and so appear pink. However, in certain vertebrate classes, like fish (round bodied), they are anatomically segregated. The slow muscle is confined to a seam along the lateral line running from the back of the head to the caudal fin while the remainder of the trunk muscle is made up of the fast muscle fibers.

Cardiac and skeletal muscles are also termed striated muscles. The long thin muscle fibers of striated muscle are multinucleated single cells (Figure 1.1B). Immersed in the cytoplasm are many parallel myofibrils (Figure 1.1C and D), which run along the fibril axis. Each myofibril consists of a chain of sarcomeres, or the contractile units, which comprise a precisely arranged assembly of parallel and partly overlapping thick and thin filaments (Hanson and Huxley 1953, Huxley 1957) (Figure 1.1D). At high magnification, the thick and thin filaments in each sarcomere can be seen as a series of dark and light bands respectively, which gives the muscle its striated appearance. A dense line in the center of each light band separates one sarcomere from the next and is known as the 'z' line (Figure 1.1E). Thin filaments comprised of actin, tropomyosin and troponin are attached to the 'z' discs at either end of the sarcomere with opposite polarity and extend towards the middle where they overlap with the thick filaments, made up of myosin. During muscle contraction, these two filaments slide past each other, due to a mechanical

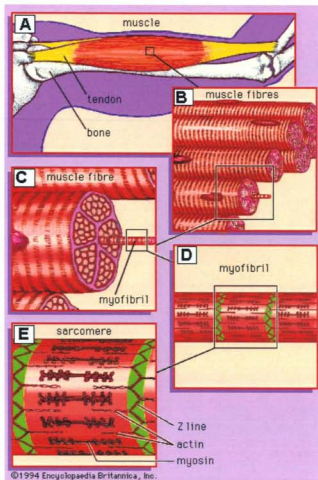


Figure 1.1. The architecture of the striated muscle and its components

A schematic representation of the skeletal muscle (A), muscle fibers (cells) (B and C), myofibrils (D), the sarcomere (E), and the thin filament (F) are shown (Adapted from Encyclopaedia Britannica with permission).

force generated by the cyclic interaction of actin and myosin (Huxley 1969, Huxley 1971) coupled to the energy of ATP hydrolysis (Davies 1964).

1.2 Thin Filament

The striated muscle thin filament is an assembly of three proteins, actin, tropomyosin and the troponin complex, that regulate acto-myosin ATPase activity (Figure 1.1F). Actin monomers polymerize into a double stranded helix making the core of thin filament. Tropomyosin also exists in a polymeric form, involving a head to tail aggregate of individual molecules, which is located in each of the two grooves of the actin helix. One tropomyosin molecule spans seven actin monomers. To each tropomyosin molecule is then bound one complex of troponin composed of troponin C (TnC), troponin T (TnT), and troponin I (TnI). The core of the troponin complex is positioned at one third of the distance from the carboxy-terminal end of tropomyosin. Actin serves as a catalyzer of the Mg-ATPase activity of myosin by accelerating ATP-hydrolysis product release (phosphate and ADP). Tropomyosin, together with troponin, regulates the productive interaction between actin and myosin in accordance with the ligands, Ca^{2+} and rigor myosin (Weber and Murray 1973, Heeley et al. 2002).

1.2.1 Tropomyosin

Striated muscle tropomyosin is a coiled-coil molecule of approximately 66,000 Da that dissociates into two 33,000 Da chains in denaturing media under reducing conditions

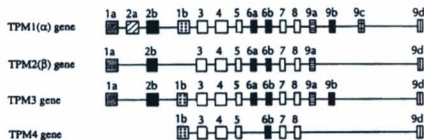
(Woods 1966, 1967, Smillie 1979). It was discovered by Bailey in 1946 (Bailey, 1946, 1948 and 1951). Each tropomyosin chain consists of 284 pairs of amino acid residues (Stone et al., 1975) and has a α -helical content exceeding 90%. Tropomyosin has an isoelectric precipitation point (pI) of 4.6, and, therefore, is negatively charged at neutral pH. It is a heat stable protein and binds end-to-end to itself at low salt concentrations, to troponin T and to F-actin.

1.2.1.1 Genes, isoforms and distribution

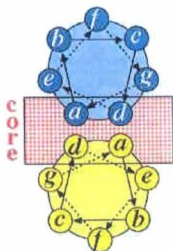
Tropomyosin exists in multiple isoforms. This isoform diversity which was first observed electrophoretically (Cummins and Perry 1973) was later found to originate from different combinations of expressing multiple genes, using alternative promoters, and alternative splicing of primary RNA transcripts. Based on the size of the translation product, tropomyosins are categorized into two main groups; a high molecular weight group containing ~284 amino acid residues; and a low molecular weight group containing ~248 amino acids, the result of expression from alternative promoters. All muscle tropomyosins so far identified belong to the former group while the latter group contains some of the non-muscle tropomyosins. In yeast, tropomyosins with even lower molecular weights containing 199 and 161 residues exist (Drees et al., 1995). Despite these differences in size, every isotropomyosin is built up from segments of approximately 40 residues, each of which interacts with an actin monomer in the actin filament. So far there is no evidence of tropomyosins in prokaryotes.

There are four tropomyosin genes that have been characterized in vertebrates, which appear to have arisen through duplication of an ancestral gene; namely, TPM-1, TPM-2, TPM-3 and TPM-4 (Cuticchia and Pearson, 1993) (Figure 1.2A), although it is not certain if the full complement is found in all vertebrates. Overall, through the use of alternative splicing and alternative promoters these four genes are known to express 23 polypeptide chains that could assemble into 23 different tropomyosin homodimers in vertebrates (Hitchcock-DeGregori et al. 2007). Additional diversity can result from the pairing of the two chains in the coiled-coil as heterodimers and from post translational modifications. TPM-1 and TPM-2 genes correspond to alpha (α) and beta (β) genes that code for alpha and beta tropomyosins found in striated muscle (Helfman et al. 1986, Ruiz-Opazo and Ginard, 1987). The alpha gene is the most complex of all four. It contains 15 exons, only five of which (exons 3, 4, 5, 7 and 8) are common to all nine known isoforms which arise from this particular gene (Ruiz-Opazo and Nadan-Ginard 1987, Wieczorek et al. 1988, Lees-Miller 1990a). Two promoters are associated with exons 1a and 1b coding for high and low molecular weight proteins respectively and the exons 2, 6 and 9 contain alternative splice options. The striated muscle alpha tropomyosin is encoded by exons 1a, 2b, 6b, 9a and 9b in addition to the common exons. One homologue is expressed in the smooth muscle and the rest of the seven isoforms are found in fibroblasts and the brain. Relative to the alpha gene, the beta gene from chicken lacks exons 2a and 9b while that from rat lacks two additional regions; exon 9c and the internal promoter associated with exon 1b (Helfman et al. 1986, Forry-

(A)



(B)



(C)

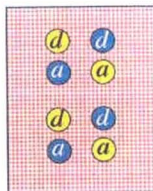


Figure 1.2: The gene organization and structure of tropomyosin

The intron-exon organization of tropomyosin genes (A). Boxes represent the exons and the horizontal lines represent the introns. TPM-1, TPM-2 and TPM-4 are from rat, and TPM-3 is from human. The open boxes depict exons common to all genes. Cross section of the coiled coil showing the amino acid positions, as denoted by the letters from 'a' to 'g', in the pseudoheptapeptide repeat (Perry SV, 2001, Vertebrate tropomyosin: Distribution, properties and function. J Muscle Res Cell Motil, 22, 5-49 with kind permission of Springer Science and Business Media) The interface between the helices derives primarily from hydrophobic residues in core positions *a* and *d* (B). The core interface viewed parallel to the coiled-coil axis shows how residues from one chain occupy the spaces between the corresponding residues from the second chain to give "knobs in holes" packing (C) (Stewart M, 2001, Structural basis for bending tropomyosin around actin in muscle thin filaments. Proc Natl Acad Sci USA, 98, 8165-8166).

Schaudies et al. 1990b, Libri et al. 1989). The TPM-2 gene codes for striated muscle beta, smooth muscle beta and fibroblast TM1 tropomyosin isoforms (Yamawaki-Kotaoka 1985). In chicken, it also codes for a low molecular weight fibroblast TM3 protein. The TPM-3 gene was formerly known as hTMnm (Lin et al. 1997) after human fibroblast TM30nm (Clayton et al. 1988) isoform. Because of its structural similarity with the alpha gene, TM3 has also been referred to as slow-twitch alpha tropomyosin (MacLeod and Gooding 1988, Less-Miller and Helfman 1991, Muthuchamy et al. 1997). TPM-2 also gives rise to a high molecular weight isoform found in slow twitch skeletal muscle (Gunning et al. 1990, Smillie 1996), which is coded by the same combination of exons as in the case of striated alpha tropomyosin. It is uncertain, however, if this gene contains exons 2a and 9c, but it includes the internal promoter at exon 1b and alternative splice choices at exons 6 and 9. The TPM-4 gene encodes a low molecular weight tropomyosin isoform, fibroblast TM4 in rat and fibroblast TM30pl in human (Lees-Miller et al. 1990b, Macleod et al. 1987). In chicken, it gives rise to a high molecular weight isoform specific to cardiac muscle that is homologous to the above two nonmuscle tropomyosins (Forry-Schaudies 1990a).

The tropomyosin from rabbit striated muscle consists mainly of alpha and beta isoforms, products of the TPM-1 and TPM-2 genes respectively (Cummins and Perry 1973). The alpha and beta chains distribute in the dimer mainly as $\alpha\alpha$ and $\alpha\beta$ forms (Eisenberg and Keilley 1974, Lehrer 1975, Bronson and Schachat 1982) with the former being the dominant dimeric form in cardiac and fast twitch skeletal muscles. In slow twitch

muscles, beta is the major isoform. The ratio of alpha to beta is dependent on the developmental stage of the muscle cell (Amplett et al. 1976) and can also vary between different mature muscles of a given type (Heeley et al. 1983, Moore and Schachat 1985). In addition to these two polypeptides, at least two other minor isoforms have been identified in the fast skeletal muscle, namely gamma and delta (Cummins and Perry 1974, Bronson and Schachat 1982, Salviati et al. 1982, Heeley et al. 1983). A similar heterogeneity has been seen with human, cat (Steinbach et al. 1980, Billeter et al. 1982) and chicken as well (Montarass et al. 1981). Although the origin of these isoforms is not defined, at least one is thought to be coded from the TPM-3 gene, which is expressed abundantly in the slow skeletal muscles of mouse and human (~30% of total tropomyosin). It is also expressed in the cardiac muscle of larger mammals such as human, pig and sheep (Pieples and Wieczorek, 1999, 2000). There is no evidence for a TPM-4 gene product in mammalian striated muscles. In contrast to mammals, a cardiac specific isoform is expressed in other classes such as birds, amphibians and fish where it is coded by the TPM-4 gene in the case of chicken (Forry-Schaudies 1990a).

1.2.1.2 Structure

Based on X-ray diffraction studies, Crick showed that tropomyosin has a left-handed coiled-coil structure involving two right-handed alpha helices inclined at an angle of about 20° to each other (Crick, 1953). The sequence of tropomyosin satisfies the requirements of a coiled-coil and can be considered as a repeating heptapeptide in which the amino acid residues are labeled from 'a' to 'g' with non-polar residues at positions 'a'

and 'd' (Figure 1.2A). With 3.6 residues per turn, residues at 'a' and 'd' positions from one chain face those from the other and make a stripe of non-polar residues that runs down the side of each alpha helix. This represents the core or interface of the coiled coil (Figure 1.2B). Since this seam is not parallel to the axis of the helices, the two chains wind round each other with the so-called 'knobs and holes' packing arrangement (Figure 1.2C). Furthermore, a high proportion of positively charged amino acids occur in position 'g' and negatively charged ones in position 'e'. The 'g' position residues of one chain are suitably located spatially to form salt bridges with 'e' position residue of the preceding heptapeptide in the other chain (Figure 1.2B) (McLachlan and Stewart, 1975). These electrostatic interactions between the ionic side chains from the two helices and the hydrophobic interactions between the interfacial non-polar residues stabilize the coiled coil structure of tropomyosin.

Evidence for the parallel, in register, arrangement of the two chains in tropomyosin first came from the observation that complementary Cys 190 residues in the two chains can be cross-linked either by air or disulphide exchange oxidation (Woods 1967, Johnson and Smillie 1975, Lehrer 1975, Stewart 1975 and Phillips et al. 1979). It was confirmed by later studies, which found that the near UV circular dichroism and absorption spectra of tropomyosin tyrosyl residues show ring-ring interaction in complementary strands (Bullard et al. 1976, Nagy 1977), and that the addition of pyrene maleimide labels to the two Cys 190 residues results in the appearance of an excited state dimer (Betcher-Lange and Lehrer 1978, Graceffa and Lehrer 1980).

The fact that tropomyosin makes contact with seven monomeric actin units suggests that some type of equivalent or quasi-equivalent interaction occurs at each of the seven regions of contact. Analysis of the sequence (Hodges et al. 1972, Sodek et al. 1972) by several authors revealed a grouping of acidic residues at non-interface positions repeating fourteen fold through the entire molecule (Parry 1975, Stewart and McLachlan 1975a, McLachlan and Stewart 1976). These regions are spaced 19.7 residues apart, rotated 90 degrees with respect to their neighbors and are arranged in two sets of seven zones, namely alpha and beta. It was therefore speculated that these repeats represent the seven actin binding regions corresponding to seven half turns of the coiled-coil and that they may link to basic sites on actin subunits. Considering the importance of magnesium in actin-tropomyosin complex formation (Yang et al. 1979), magnesium bridges between acidic groups on both molecules are also possible. Later, from tropomyosin crystal structure analysis, Phillips et al. 1986 showed that there are seven dominant acidic zones situated on the outside of the tropomyosin supercoil with high periodicity. They are roughly equivalent to Stewart and McLachlan's alpha sites and therefore, concluded to correspond to seven actin-contacting sites. Studies using deletion mutagenesis and leucine zipper substitutions showed that the contributions of these individual periodic sites, however, are not equal for actin binding (Hitchcock-DeGregori and Varnell 1990, Hitchcock De-Gregori and An 1996, Hammell and Hitchcock-DeGregori 1997 and Hitchcock-DeGregori et al. 2002). Deletion of one internal period, either 2, 3, 4 or 6, weakened actin affinity approximately by 10-30 fold while the deletion of the fifth period eliminated any detectable binding with micromolar amounts of protein. Further, these

deletions showed severe consequences on tropomyosin's regulatory properties as well. For example, thin filaments (Ca^{2+}) containing a mutant that was missing period 4 exhibited impaired myosin activation. Conversely, when period 6 was deleted thin filaments (EGTA) failed to inhibit myosin activity (Landis et al. 1997, Landis et al. 1999, Tobacman and Butters 2000, Hitchcock-DeGregori et al. 2001 and Hitchcock-DeGregori et al. 2002).

In addition, McLachlan and Stewart (McLachlan and Stewart 1976) noted a periodic distribution of small non-polar amino acids (such as Ala) at the interface and suggested that this allowed flexibility and bending of the tropomyosin molecule when binding to actin filament (Brown et al. 2001, Kwok and Hodges 2004). In general, there are seven alanine clusters (or destabilizing clusters) in striated muscle tropomyosin (Brown et al. 2001) where two of them occur within the alpha zones (in period 1 and 5). Replacing alanines in the second and fifth cluster with canonical interface residues (Leu and Val) increased tropomyosin stability and decreased affinity to actin as a result of decreased flexibility to wind around actin (Singh and Hitchcock-DeGregori 2003, Singh and Hitchcock-DeGregori 2006). Overall, using results from various mutation studies, it can be inferred that both the interface stability and the periodic alpha bands are necessary for actin binding and that the periods 1 and 5 contribute more to the overall actin affinity than the others.

The two end regions of tropomyosin are another critical feature for tropomyosin function. While the amino-terminal region is highly conserved: eight of the first nine amino acids are identical and eighteen of the first twenty are conserved in all vertebrate muscle tropomyosins (Basi and Storti, 1986), the carboxy-terminal region is more variable. In addition, the first methionine of tropomyosin is acetylated, a modification that has been postulated to be important for the stability of the amino-terminal end (Greenfield et al. 1994 and Brown et al. 2001). Another post translational modification that occurs in some tropomyosins is phosphorylation at the opposite end, at Serine283. At lower ionic strength conditions (below physiological range), tropomyosin exists in polymeric form and thus the solutions become highly viscous (Astbury et al. 1948). The polymerization involves head-to-tail overlap between eleven residues from the carboxyl and amino termini of individual molecules into long filaments (McLachlan and Stewart 1975). In the 7Å tropomyosin crystal structure the ends are not resolved (Whitby and Phillips 2000) but model peptides of the two termini have been studied using X-ray diffraction and NMR (Greenfield et al. 1998, Brown et al. 2001, Li et al. 2002, Greenfield et al. 2003, Greenfield et al. 2006). The recent NMR work on two model peptides of the ends proposed that, in the overlap, the amino termini fit into a 'jaw' that is created by the opening of the coiled coil at the carboxyl end (Greenfield et al. 2006) (Figure 1.1F). The merger is stabilised, in part, by the amino- and carboxy- terminal regions possessing opposing net charges at physiological pH that explains its depolymerization in the presence of high salt. The amino-terminal chains separate only slightly to interact with the splayed carboxy-terminal chains. Further, according to this model, the planes of the

amino- and carboxy- terminal coiled coils are oriented perpendicular to each other interlocking the chains.

Modification or deletion of residues involved in the overlap has been reported to drastically impair tropomyosin function. The removal of carboxy-terminal residues by carboxypeptidase-A digestion or acetylation of Lys7 reduces tropomyosin polymerization (Johnson and Smillie 1977, Ueno et al. 1976). Exolytic digestion of the last eleven amino acids (Mak and Smillie 1981, Mak et al. 1983, Heeley et al. 1987) as well as deletion of the first nine (Cho et al. 1990, and Moraczewska and Hitchcock-DeGregori 2000), yields shortened products which neither self-associate nor bind to F-actin under conditions where the full-length protein displays the expected property. Troponin restores the binding of carboxy-terminally truncated tropomyosin to actin at micromolar concentrations regardless of the calcium concentration (Mak et al. 1983; Heeley et al. 1987) but this was not observed in the case of the amino-terminally truncated protein (Cho et al. 1990). As compared to the native molecule, the former also displayed reduced affinity to troponin (Pearlstone and Smillie 1981) and myosin-S1-ADP (Pan et al. 1989) as well as reduced Ca^{2+} activated myosin-S1 ATPase (Walsh et al. 1984 and Heeley et al. 1989a). The entire carboxy-terminal region of tropomyosin encoded by exon 9a was required for troponin to induce full tropomyosin binding to F-actin where the first eighteen residues of it are critical (Hammel and Hitchcock-DeGregori 1996). Although phosphorylation at Ser283 did not change tropomyosin-binding properties to F-actin (Heeley et al. 1989b), it strengthened tropomyosin head-to-tail interactions but not in the

presence of N-TnT peptide (the amino-terminal region of troponin T, residues 1-158), and also increased calcium activated myosin-S1 ATPase activity (Heeley 1994). The absence of acetylation on the first methionine reduced head-to-tail association and actin affinity (Hitchcock-DeGregori and Heald 1987, Heald and Hitchcock-DeGregori 1988, Urbancikova and Hitchcock-DeGregori 1994). The effect of non-acetylation can however be overcome by fusing the dipeptide, Ala-Ser, at the beginning of the sequence (Monteiro et al. 1994).

1.2.1.3 Stability

Unfolding of the tropomyosin native structure is a complex process consisting of several discrete steps (Potekhin and Privalov 1982). The molecule is comprised of distinct cooperative blocks having different stabilities, which depend largely on the state of the neighboring blocks. Specifically, neighboring blocks destabilize each other. For the same reason removal of one block can lead to stabilization of neighbouring blocks. One site of local instability in tropomyosin involves the region containing Cys 190 and the stability of the protein is dependent on the state of oxidation (Potekin and Privalov 1978, Lehrer 1978, Krishnan et al. 1978, Williams and Swenson 1981). According to studies using fluorescent (Graceffa and Lehrer 1980, Mihashi 1972) or spin (Chao and Holtzer 1975, Graceffa and Lehrer 1983) labels, under reducing conditions, denaturation of rabbit alpha tropomyosin either by guanidinium chloride or heat, begins with a local unfolding in this region. This loss of structure is then propagated along the molecule in both directions as suggested by intrinsic fluorescence, optical rotation, and $^1\text{H-NMR}$ (Satoh et al. 1972,

Woods 1969, Pont and Woods 1971, Woods 1976). Further, several studies using pyrene maleimide or didansylcysteine labeled protein at Cys 190 showed that tropomyosin equilibrates between two native conformational states: chain closed and chain open (Betcher-Lange and Lehrer 1978, Graceffa and Lehrer 1980, Lehrer et al. 1981, Betteridge and Lehrer 1983). In the closed state the molecule is fully helical and the thiols are further apart and are sterically prevented from forming a disulfide bond. In the open state, the protein is locally unfolded around Cys 190, which allows chain separation to the extent that thiol groups can interact to form a disulfide bond. The presence of a disulfide link destabilizes this low stability block but stabilizes its neighboring blocks. Therefore, under oxidizing conditions, the local unfolding becomes more cooperative and the melting temperature of the stabilized parts of the protein increases. Further, several lines of evidence (Lehrer 1978, Phillips et al. 1980, William and Swenson 1981, Pato et al. 1981b) suggest that the carboxy-terminal half of rabbit tropomyosin is less stable than the amino half and undergoes unfolding more easily.

1.2.2 Actin

Actin is one of the most abundant proteins in eukaryotic cells and is a main component in the thin filament of the muscle cells and the cytoskeleton in the non-muscle cells. It was isolated by Straub in 1942 (Straub 1942) as a water-soluble component of muscle acetone powder. In low salt conditions it exists as a globular protein, called G-actin, with a molecular weight of ~42000 Da (Elzinga et al. 1973). It consists of about 375 residues in which the amino acid sequence is highly conserved throughout evolution. At increased

ionic strength, actin monomers polymerize into F-actin. This polymerization is reversible and is the basis of actin methods of enrichment. Actin binds to one molecule of ATP or ADP (Engel et al. 1977, Wegner 1977) and has a single high affinity metal-binding site (Strzelecka-Golaszewska et al. 1973, Strzelecka-Golaszewska et al. 1978, Frieden et al. 1980), which is usually Mg^{2+} in the cell, and several low affinity metal-binding sites. These metal ions and nucleotide are necessary in G-actin to stabilize its tertiary structure; removal of either can lead to the irreversible denaturation of the protein and the loss of its polymerizability (Frieden et al. 1980, Nagy and Jencks 1962, Lehrer and Kerwar 1972).

The polymerization of actin is initiated by an unfavorable nucleation step and propagated by the addition of subunits to the two ends of the growing filament. The filament formation accompanies hydrolysis of ATP (Straub and Feuer 1950, Mommaerts 1952). ADP remains tightly bound while the phosphate is released. The actin monomers attach and detach at the ends of the filaments at different rates (Wegner and Engel 1975) and the growing filament exhibits polarity as shown by the formation of arrowheads on addition of myosin subfragment 1 or heavy-meromyosin. The two ends are called the 'barbed' and 'pointed' ends. Actin attaches preferentially to the barbed end of the filament, while detachment is favored at the pointed end (Hayashi and Ip 1976, Woodrum et al. 1975, Kondo and Ishiwata 1976). Therefore, at steady state, involving the exchange of ADP-actin units in the filament for ATP-actin units in solution (Pollard and Mooseker 1981, Wegner and Neuhaus 1981, Wegner 1982) the net filament growth becomes zero with one end showing a net positive growth while the other end shows a net negative growth

(Wegner 1976, Coue and Korn 1985, Carlier et al. 1986a, Wegner and Isenberg 1983, Bonder et al. 1983). Polymerization stops when the actin monomer concentration drops below a critical concentration (Hill 1980). Although polymer formation stimulates ATP hydrolysis, the release of phosphate from actin is slower than the formation of the filament so that the growing filament has a cap of ATP-actin at its barbed end, while monomers containing ADP-phosphate-actin accumulate in the rest of the filament. Thus, at steady state, F-actin is made up of ADP-actin except for the terminal ADP-phosphate-actin at the barbed end (Carlier 1991). Further, millimolar concentrations of both Ca^{2+} and Mg^{2+} are required for the fast exchange of monomers and, depending on the divalent metal concentrations, the differences in the addition and dissociation rates at the filament ends can be varied. However MgATP-actin exhibits a higher tendency to form nuclei, a faster elongation rate and faster hydrolysis than CaATP-actin (Cooper et al. 1983, Tobacman and Korn 1983, Gershman et al. 1984, Carlier 1986b, Newman et al. 1985, Mozo-Villarias and Ware 1985). In addition to these cations, several other muscle proteins including myosin, tropomyosin, and actinin can affect the rate or extent of actin polymerization.

The structure of monomeric actin determined using electron microscopy and 3D-reconstruction was first reported in 1983 (Smith et al. 1983). The atomic structure was revealed by a number of subsequent studies, first using crystals of actin complexed with DNase I, which is shown in Figure 1.3 (Kabsch 1990), gelsolin (McLaughlin 1993) and profilin (Schutt 1993) as well as using crystals of uncomplexed actin (Otterbein 2001,

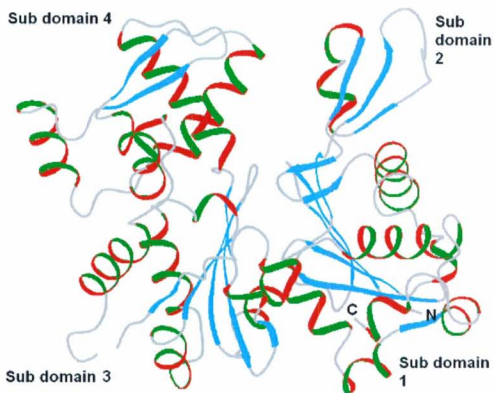


Figure 1.3: Actin structure

A schematic representation of the 3D structure of the actin monomer is shown. A hypothetical vertical line divides the actin molecule into two domains which can be subdivided further into two subdomains each domain being composed of either subdomains 1 and 2 or subdomains 3 and 4. ATP and Ca^{2+} are located between the two domains, in a region called the cleft. Alpha helices are shown in green while beta sheets in blue.

Graceffa and Dominguez 2003, Rould et al. 2006). The actin polypeptide is folded into four subdomains surrounding the nucleotide-binding pocket. The structure can be divided into two similar major domains, each subdivided further into two subdomains (subdomains 1 and 2 in one domain and subdomains 3 and 4 in the other), suggesting that the actin gene was formed by duplication. The protein chain begins and ends in subdomain 1, which is similar to the secondary structural content of subdomain 3. These two contain a central five-stranded beta sheet structure with short alpha helices on each face. Subdomains 2 and 4 are also alike, and are primarily beta sheet but the latter has a small amount of additional alpha helices making it much larger than subdomain 2. This makes the actin molecule polar in the direction from subdomains 1 and 3, called the "barbed end", toward subdomains 2 and 4, called the "pointed end". The apolar cavity in the central cleft binds to the adenine base forming numerous hydrogen bonds with ribose hydroxyls and phosphate groups. The cation is coordinated to oxygens from the nucleotide phosphates and to side chain oxygens from the cleft (Pollard et al. 1994).

Holmes et al. in 1990 described the structure of F-actin as a helix of actin monomers where approximately 13 monomers make 6 left-handed turns with a helix pitch of 59.6 Å. Subsequent studies (Al-Khaya et al. 1995, Lorenz et al. 1993, Oda et al. 1998) agreed more or less with this model and made slight refinements to the structure, but its essential features remain. In the filament, actin monomers orient with subdomains 3 and 4 to the inside of the filament where they interact with the same domains from other monomers.

Subdomains 1 and 2 face to the outside of the filament. The myosin-binding site is also located in subdomain 1 in good agreement with its exterior location.

1.2.3 Troponin

In 1965, troponin was isolated (Ebashi and Kodama 1965) as a new protein from the so-called Ca^{2+} sensitizing factor (or native tropomyosin) (Ebashi 1963, Ebashi and Ebashi 1964) obtained from minced muscle. It is a heterotrimeric complex comprised of troponin C (TnC), troponin I (TnI) and troponin T (TnT) and is only found in striated muscle. Troponin C is the calcium-binding component of the thin filament (Hartshorne and Mueller 1968). Troponin I binds to F-actin in the absence of TnC and inhibits actomyosin ATPase activity (Wilkinson et al. 1972, Eisenberg and Kielley 1974, Eaton et al. 1975). Troponin T binds to tropomyosin and thereby links the troponin complex to the thin filament (Hartshorne 1969, Schaub and Perry 1969, Greaser and Gergely 1973, Ebashi 1972). Troponin is distributed regularly along the entire length of thin filaments with no physical connection between two neighboring molecules (Ohtsuki et al. 1967, Ohtsuki 1974). It consists of a globular head (or core complex) containing TnC, TnI and the carboxy-terminal part of TnT, and a long tail containing the amino-terminal part of TnT (Flicker et al. 1982). This head region binds at the central region of tropomyosin around residues 150-190 and the tail extends away from the core, along the carboxyl half of tropomyosin, past the head-to-tail overlap spanning a short segment of the adjacent tropomyosin molecule (first 10-15 residues) (White et al. 1987). The recent 3-D structure

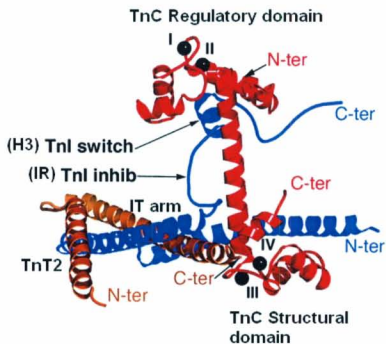


Figure 1.4: Structure of the head region of the skeletal troponin complex.

The troponin subunits are color-coded as follows: brown, TnT2; blue, TnI; and red, TnC. Black spheres indicate Ca²⁺. The termini of subunits are shown and color-coded as described above. The TnC central helix, which links the regulatory and the structural domains, is orientated perpendicular to the plane of TnI and TnT2 coiled coil (IT arm). The TnI inhibitory (IR) and switch segments (H3) are indicated. Roman numerals indicate the Ca²⁺-binding sites (Vinogradova MV, Stone DB, Malanina GG, Karatzaferi C, Cooke R, Mendelson R A, Ca²⁺-regulated structural changes in troponin, Proc Natl Acad Sci USA, 102, 5038-5043).

(Vinogradova et al. 2005) of the head region of skeletal troponin complex using x-ray crystallography (3Å resolution in the presence of Ca^{2+}) is shown in Figure 1.4.

1.2.3.1 Troponin C

Troponin C (TnC), a well-characterized member of the calmodulin superfamily, is a dumbbell shaped molecule with a molecular weight of approximately 18000 Da (Hartshorne and Pyun 1971, Wilkinson et al. 1972, Greaser and Gergely 1971) and a pI of 4.1-4.4 (Hartshorne and Driezen 1972). Its two globular domains, a regulatory amino-terminal domain and a structural carboxy-terminal domain, are separated by a long central α -helix (Figure 1.4). Each domain comprises two α -helix-loop- α -helix motif (EF-hand) (Kretsinger and Nockolds 1973) divalent metal binding sites (Herzberg and James 1985, Sundaralingam et al. 1985, Slupsky and Sykes 1995, Houdusse et al. 1997, Sia et al. 1997). The EF hands are numbered I-IV where sites I and II located in the regulatory domain and sites III and IV located in the structural domain (Figure 1.4). The sites in the regulatory domain have a lower affinity to metal ions and are referred to as Ca^{2+} -specific sites while those in the structural domain are high affinity metal binding sites and are called Ca^{2+} and Mg^{2+} sites (Potter and Gergely 1975, Robertson et al. 1971). In relaxed muscle, the millimolar concentration of free Mg^{2+} would saturate the high affinity sites whereas the low affinity sites would be vacant. In contracting muscle the low affinity sites will be occupied with Ca^{2+} and binding of Ca^{2+} to high affinity sites would be limited by the slow off rate of Mg^{2+} . The binding of Ca^{2+} to sites I and II was shown to open a hydrophobic cleft to which the switch region of TnI binds releasing the TnI

inhibition on actomyosin ATPase (Gagne et al. 1995, McKay et al. 1997). However site I in cardiac TnC is defunct due to several key amino acid substitutions (Van Eard and Takahashi, 1975). Some other properties of TnC are (1) its low A_{280}/A_{260} ratio (Hartshorne and Pyun 1971, Greaser and Gergely 1971), ascribable to the high phenylalanine to tyrosine ratio coupled with the absence of tryptophan; (2) high thermal stability; (3) the ability of the protein to refold after denaturation in 6M guanidine hydrochloride (Hartshorne and Mueller, 1968); and (4) the ability of TnC to solubilize the other troponin subunits in low ionic strength media (Greaser and Gergely 1971).

1.2.3.2 Troponin I

Troponin I (TnI) is an extended molecule with high degree of conformational plasticity, which gives it the ability to switch binding partners, either TnC, TnT, and F-actin (Martins et al., 2002). Cardiac TnI, which has a molecular weight of 24000 Da, is distinguished from skeletal TnI (molecular weight 21000 Da (Wilkinson and Grand 1975)) by an amino-terminal extension of about 27-33 residues. It contains high densities of basic residues and therefore has a pI of about 9.3 (Wilkinson 1974). According to Li et al. 2004, TnI can be divided into six distinct structural segments; the amino-terminal cardiac-specific extension, the amino-terminal region that binds the structural domain of TnC, the TnT binding region that forms a coiled-coil with a part of TnT (IT arm) (Figure 1.4) (Parry 1981, Pearlstone and Smillie 1981, 1985, Stefancsik et al. 1998, Takeda et al. 2003, Vinogradova et al. 2005), the inhibitory region that binds both F-actin and TnC, the switch region that binds the regulatory domain of TnC, and the carboxy-terminal region

that binds F-actin. The inhibitory action of the regulated actomyosin in the absence of Ca^{2+} is exerted by TnI. Troponin I itself can inhibit actomyosin ATPase activity weakly, which is accentuated if tropomyosin is present (Wilkinson et al. 1972, Eaton et al. 1975). This inhibition is neutralized by TnC irrespective of Ca^{2+} concentration when TnT is not present. Troponin T makes the release of TnI inhibition by TnC, sensitive to calcium (Eisenberg and Kielley 1974, Greaser and Gergely 1981).

1.2.3.3 Troponin T

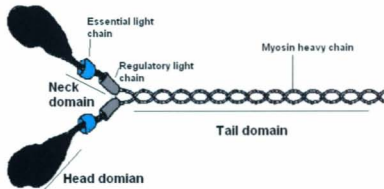
Troponin T (TnT) is a rod shaped molecule (Ohtusuki 1975, Prendergast 1979, Flicker 1982, Byers and Key 1983) with a molecular weight of approximately 31000 Da for skeletal isoforms (Pearlstone 1976) and a pI of 9.1 (Wilkinson 1974). Like TnI, cardiac TnT's are longer than skeletal isoforms at the amino terminus by about 30 amino acids (Anderson et al. 1991; Townsend et al. 1995). Troponin T is a highly charged molecule and is insoluble under physiological low ionic strength conditions. Charged residues are distributed along its entire sequence at the same time the amino-terminal region is rich in negatively charged residues at pH 7 while the carboxy-terminal region is rich in positively charged residues (Pearlstone et al. 1976). Mild treatment with chymotrypsin splits the protein into two long fragments (Ohtusuki 1979), an amino-terminal fragment containing residues 1-158 (N-TnT) and a carboxy-terminal fragment containing residues 159-258 (C-TnT). The C-TnT fragment locates in the head region of the troponin complex and displays Ca^{2+} sensitive interactions with TnI, TnC and tropomyosin (Pato et al. 1981b, Ohtusuki et al. 1981, Tanokura et al. 1982, 1983, Ishi and Lehrer 1991). In the

3Å -resolution crystal structure of the head region of troponin, C-TnT adopts a non-linear V-shape stabilized by the IT coiled-coil, a conformation that is thought to constrain the positions of other components relative to tropomyosin. The N-TnT fragment forms the troponin tail and binds strongly to tropomyosin irrespective of the Ca^{2+} concentration (Jackson et al. 1975, Pearlstone and Smillie 1982). This fragment, rich in helical content, is thought to form a triple stranded coiled-coil structure with the carboxyl one third of tropomyosin at least in some regions. Although the peptide runs towards the amino-terminal region of the adjacent tropomyosin molecule (White et al. 1987), its interactions, if any, around the tropomyosin overlap site are not yet certain. However, this interaction between N-TnT peptide and tropomyosin is thought to stabilize the overall position of troponin head along the actin-tropomyosin filament as well as the tropomyosin overlap structure (Pato and Smillie 1981, Ohtsuki 2007).

1.2 Myosin

Myosin is an enzyme that hydrolyses ATP (Engelhardt and Lyubimova 1939). It is a large family of proteins with 17 types, each of which comprises a number of isoforms (Cheney et al. 1993). The one in the muscle is myosin type II. Myosin II is a large and highly asymmetric hexameric protein with several structural and functional domains (Harrington and Rodgers 1984) (Figure 1.5A). It is composed of two heavy chains (~230,000 Da) (Molina et al. 1987, Maita et al. 1991), two essential light chains and two regulatory light chains (Weeds and Lowey 1971) (16,000-20,000 Da). The carboxyl ends of the two heavy chains form the tail region, which is a long parallel, alpha helical

(A)



(B)

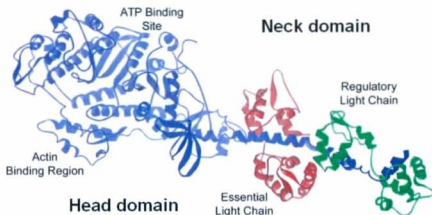


Figure 1.5: Structure of myosin

(A) Schematic representation for myosin molecule structure (Adapted from the website edoc.hu-berlin.de). The myosin heavy chains have a globular "head" with the ATP and actin binding sites at the amino-terminal and a long α -helical "tail" at the carboxy terminal, which forms a coiled-coil. The essential myosin light chain and the regulatory myosin light chain associate at the neck region. (B) The structure of the myosin subfragment I (Rayment et al. 1993) showing the actin binding and nucleotide binding regions.

coiled-coil. The amino-terminal portion of each chain forms the globular head region (Lowey et al. 1969, Elliott and Offer 1978). The ATPase activity of myosin resides in the head region as well as in the actin-binding site therefore it is also called catalytic or motor domain. Linking the heads to the tail are long alpha helical regions, named the neck or the lever arm. An essential light chain and a regulatory light chain are associated with each neck region. Light chains are important for the stability as well as for function of myosin where upon their removal myosin loses its enzymatic properties (Gazith et al. 1970). The myosin head together with the neck can be separated from the rest of the molecule by chymotryptic digestion and is known as myosin-S1. The structure of this molecule as revealed by X-ray crystallography (Rayment et al. 1993) is shown in Figure 1.5B.

Thick filaments are formed by the aggregation of myosin molecules in a bipolar fashion (Huxley 1963). Myosin tails pack in an anti-parallel way in the middle of the filament, while in a parallel fashion towards the outside. This arrangement makes the middle of the thick filament a head free region and either side of the filament to have myosin heads with opposite polarity. Myosin heads protrude from the filament forming so called crossbridges between the thick and thin filaments.

1.3 Muscle contraction

The sliding filament theory to explain the mechanism of muscle contraction was introduced by Huxley and Simmons in 1971. They observed that during muscle

contraction, the sarcomeres become shorter without a change in the lengths of the thin and thick filaments (Huxley and Niedergerke 1954, Huxley and Hanson 1954). In the presence of ligands, Ca^{2+} and rigor myosin, and sufficient ATP, the thin filaments move relative to the thick filaments towards the middle of the sarcomere, resulting in sarcomere shortening, a process that adds up to contraction of the whole muscle. The packing of myosin to make bipolar thick filaments is an important determinant in this regard.

The productive interaction of myosin heads protruding from thick filaments with actin monomers in the thin filaments generates tension (Figure 1.6). In the absence of nucleotide, myosin interacts tightly with actin to form a "rigor" complex. The binding of MgATP to myosin rapidly dissociates the actomyosin complex. This ATP is then hydrolyzed by myosin into ADP and inorganic phosphate, which are stable products in the presence of Mg^{2+} . The reaction primes the crossbridge formation again with actin. Binding to actin accelerates the rate of release of these products (White et al. 1997), phosphate first followed by ADP. Release of phosphate, the rate limiting step of steady-state ATP hydrolysis, causes the myosin crossbridge to change its shape, where the myosin lever arm moves at an approximately 45° angle relative to the thick filament. Because myosin is still attached to the actin filament, the thin filament also moves (Huxley 1969) resulting in sarcomere shortening. This is called the power stroke. At the end of the power stroke, ADP is released allowing a new molecule of ATP to bind to myosin. Actomyosin is thereby dissociated and the process can be repeated. This cycle is called the crossbridge cycle and was first proposed by Lynn and Taylor in 1971.

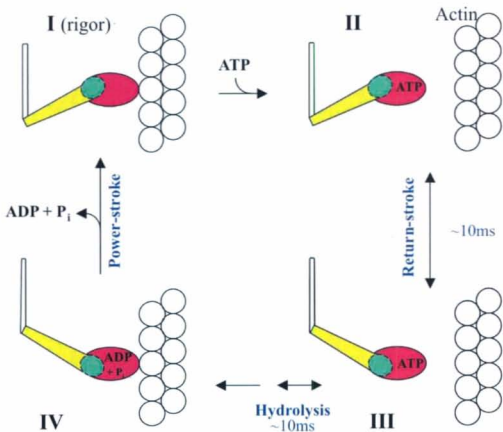


Figure 1.6: The crossbridge cycle (Lynn and Taylor 1971)

The binding of ATP to acto-myosin complex (I) leads to rapid dissociation of the crossbridge from actin (II). The myosin lever arm then undergoes a conformational change followed by ATP hydrolysis (III). Subsequent rebinding to actin (IV) leads to release the products and to change the conformation of the lever arm to the starting conformation (I). Since the crossbridge is still formed, the thin filament also moves along with it. This is the power stroke. (Reprinted from Brown JH and Cohen C, 2005, Regulation of muscle contraction by tropomyosin and troponin: How structure illuminates function, *Adv Protein Chem*, 71, 121-159 with permission from Elsevier)

1.4.1 Regulation of muscle contraction

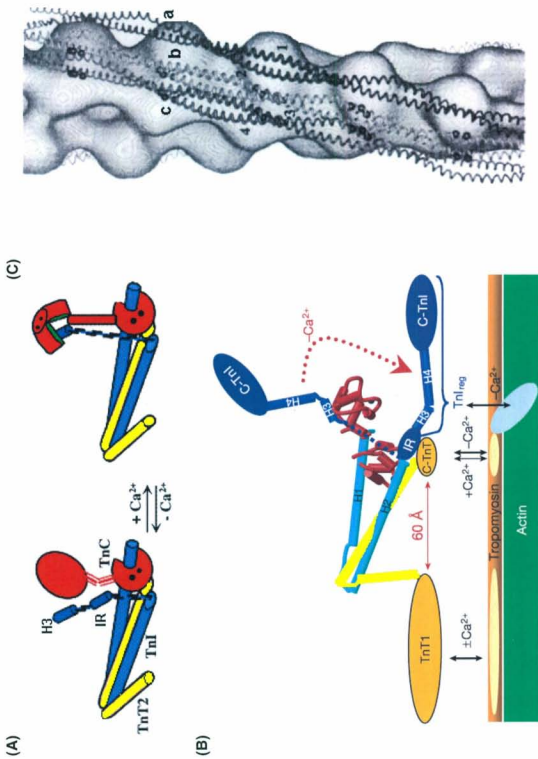
The cyclic interaction of actin-myosin is regulated by changes in troponin-tropomyosin in response to the alterations in the concentration of intracellular Ca^{2+} or rigor myosin. When the action potential spreads over the plasma membrane to the muscle cell (Marshall et al. 1959), Ca^{2+} is released from the sarcoplasmic reticulum and the free Ca^{2+} concentration rises in the cytoplasm. Following this, Ca^{2+} binds to the Ca^{2+} -specific regulatory sites of TnC, inducing a series of conformational changes within the troponin complex, which are then propagated along the complete thin filament.

1.4.1.1 Calcium induced changes in the troponin complex

The changes in the troponin complex as a result of calcium binding to TnC are shown in Figures 1.7A and B. In the resting muscle, TnC is not bound with Ca^{2+} . Therefore the hydrophobic cleft in the regulatory domain is closed and the inter-domain central helix appears to be disordered. In addition, the inhibitory segment and the carboxy-terminal regions of TnI are both bound strongly to F-actin while the C-TnT fragment is bound to the middle region of tropomyosin (Farah et al. 1994, Talbot and Hodges 1981, Takeda et al. 1997, Chong and Hodges 1982, Tanokura et al. 1983, Malnic et al. 1998). In this state, the interactions within and between the troponin subunits are weak, but it displays strong linkages with tropomyosin and actin. The association of calcium with TnC however, reverses these effects. The TnC central linker becomes ordered and the hydrophobic cleft opens (Herzberg et al. 1986, Houdusse et al. 1997, Strynadka et al. 1997). The switch region of TnI now binds to this cleft (Li et al. 1999, Takeda et al. 2003,

Figure 1.7: Regulation of muscle contraction

Representation of the changes occurring (A) in troponin conformation, (B) in troponin and tropomyosin-actin interactions and (C) in tropomyosin position during muscle contraction (A). The troponin subunits are color-coded as follows: yellow, TnT; blue, TnI; and red, TnC. Calcium ions are shown as black dots. The hydrophobic pocket opened in the amino-terminal lobe of TnC, upon binding to Ca^{2+} , is colored in green. The switch segment (H3) and the inhibitory segment (IR) of TnI are also indicated in A and B. In the absence of Ca^{2+} , carboxyl regions of TnT and TnI (including the IR region) interact with tropomyosin-actin (B). In the presence of Ca^{2+} the switch segment is bound to the TnC hydrophobic pocket (A and B) releasing the interactions of the troponin core with tropomyosin-actin (B). Note that the interaction between TnT1 and tropomyosin-actin is unchanged by Ca^{2+} binding. In the absence of Ca^{2+} tropomyosin contacts actin's outer domain (which consists of sub domains 1 and 2) (C-a). In the presence of Ca^{2+} , tropomyosin moves away from the actin's outer domain to the outer edge of the inner domain (C-b). Tropomyosin lies over the inner domain as a result of the subsequent strong binding of myosin (C-c). ((Reprinted from Brown JH and Cohen C, 2005, Regulation of muscle contraction by tropomyosin and troponin: How structure illuminates function, *Adv Protein Chem*, 71, 121-159 with permission from Elsevier and from Vinogradova MV, Stone DB, Malanina GG, Karatzaferi C, Cooke R, Mendelson R A, Ca^{2+} -regulated structural changes in troponin, *Proc Natl Acad Sci USA*, 102, 5038-5043)



Vinogradova et al. 2005) dragging the rest of the carboxyl region of TnI including the inhibitory region away from actin (Li et al. 2001, Luo et al. 2000). The tropomyosin-binding region of C-TnT, which is adjacent to the IT arm, is also affected by the motions of the TnI inhibitory region and therefore weakens the interaction with tropomyosin (Brown and Cohen 2005).

1.4.1.2 Structural changes in the thin filament

How the structure of the thin filament is modified by ligand binding has provided considerable insight into the mechanism of muscle contraction regulation (Figure 1.7C). The steric blocking mechanism of acto-myosin regulation was first put forward after observing a Ca^{2+} -induced movement of tropomyosin strand on the actin filament (Spudich et al. 1972, Haselgrove 1972, Huxley 1972, Parry and Squire 1973), which was later confirmed by a number of other studies (Milligan and Flicker 1987, Milligan et al. 1990, Bivin et al. 1991, Yagi and Matsubara 1989, Lehman et al. 1994b). At low Ca^{2+} , tropomyosin lies toward the periphery of the actin filament in closer association or contact with the outer domain of actin that consists of subdomains 1 and 2. The position of tropomyosin in this state overlaps with part of the myosin binding sites on actin (Moore et al. 1970, DeRosier and Moore 1970), therefore, it was suggested that tropomyosin sterically blocks the interaction between actin and myosin. In response to increased Ca^{2+} , tropomyosin alters its position from the periphery towards the central groove between two actin strands and now lies at the outer edge of actin's inner domain. The movement of tropomyosin exposes myosin-binding sites leading to muscle

contraction. However, several observations from subsequent studies did not satisfactorily fit with this steric blocking model. For example, the change in affinity of myosin subfragment 1 (myosin-S1) to actin during the steady state ATP hydrolysis was small (Chalovich and Eisenberg 1981). In addition, rigor myosin can also activate acto-myosin ATPase even in the presence of tropomyosin and troponin (+EGTA) (Bremel et al. 1972, Bremel and Weber 1972) and tropomyosin alone can inhibit or activate actomyosin ATP hydrolysis depending on the molar ratio of myosin-S1 to thin filaments (Eaton 1976, Williams et al. 1984, Lehrer and Morris 1984).

To address these inconsistencies, the three-state model (Lehrer and Morris 1982, McKillop and Geeves 1993, Lehrer 1994, Lehrer and Geeves 1998, Maytum et al. 1999) and the Hill model (Hill et al. 1980) were proposed. In the three-state model, supported by X-ray diffraction, cryoelectron microscopy and 3D image reconstruction of negatively stained filaments, the thin filament exists in three states not two (Lehman et al. 1994a, 1995, Poole et al. 1995, Homes 1995, Vibert et al. 1997, Xu et al. 1999, Narita et al. 2001, Craig and Lehman, 2002). These correspond to a blocked state, in which the myosin binding sites are completely occluded; a closed state where myosin-binding sites are partly uncovered permitting weak interactions between actin and myosin but cannot proceed to a tightly bound rigor myosin complex; and the open state in which productive interaction between actin and myosin takes place fully activating the ATPase system. The effects of Ca^{2+} and rigor myosin on the positioning of tropomyosin were directly visualized using negative staining, which revealed that there are three positions of

tropomyosin on the filament (Vibert et al. 1997, Lehman et al. 1994a, 1995, Craig and Lehman, 2002). In addition, using FRET (reviewed in Miki 2007) and site directed spin labeled EPR (Arata et al. 2007), three motional states of the troponin complex on the thin filament were detected in response to ligands (Miki 1990, Tao et al. 1990, Miki et al. 1998a, Kobayashi et al. 2001, Hai et al. 2002, Kimura et al. 2002) although the same techniques failed to demonstrate any significant movement in tropomyosin (Miki and Mihashi 1979, Lin and Dowben 1983, Tao et al. 1983, Miki 1990, Miki et al. 1998b, Miki et al. 2004). The three-state model suggests that in the absence of Ca^{2+} and rigor myosin troponin holds tropomyosin in the blocked state. With increasing Ca^{2+} , conformational changes in troponin release tropomyosin, which now moves to the closed state. These blocked and closed states correspond to the two positions of tropomyosin observed in the steric blocking model. A further movement of tropomyosin occurs with subsequent binding of myosin, to the open state. It is also suggested that in the absence of calcium, TnI and myosin compete for actin but, if rigor myosin is present, its strong binding to actin can displace tropomyosin-troponin from the blocked to the open state. Tropomyosin is more evenly spread on actin in the open conformation where myosin and tropomyosin cooperatively enhance each others binding to F-actin and the muscle is in the fully activated state, called potentiated (Weber and Murray, 1973).

The role of tropomyosin in regulation, whether it is active or passive, is a question that is currently under debate (Chalovich 2002, Perry 2003). The states of tropomyosin on F-actin in the absence of the troponin complex are thought to be the closed and the open

states, depending on the myosin concentration (Lehman et al. 1995, Vibert et al. 1997). Therefore, only a partial inhibition of acto-myosin ATPase is observed in the system with tropomyosin and high F-actin to myosin-S1 ratios. Full inhibition is achieved upon the addition of troponin (EGTA), particularly TnI, therefore the blocked state requires TnI (Eaton et al. 1975). TnI alone in the absence of tropomyosin can inhibit both myosin binding to F-actin and ATPase activity but requires one TnI per actin monomer for the full effect. Instead, only one seventh of TnI per actin molecule is required in the presence of tropomyosin, which is consistent with the fact that one TnI molecule can block only one actin monomer in the filament (Eisenberg and Kielley 1974). In addition, tropomyosin is essential for the cooperative ATPase activation by myosin binding (Lehrer and Morris 1982). It is more likely therefore that the role of tropomyosin is to transmit the conformational changes in the actin monomer that binds the TnI molecule or myosin, to neighbouring actin monomers which are not in direct contact with the ligands. This leads to the possibility that tropomyosin does not exert a direct blocking role on myosin binding to actin, but rather moves as a consequence of adapting to the conformational changes occurring in the actin filament as a result of troponin (Ca^{2+} /EGTA) and myosin binding (Rosol et al. 2000, Lehman et al. 2000b, Perry 2001, Levine et al. 1999).

In the alternate model, the Hill model (Hill et al. 1980), thin filament exists in two states; the active state and the inactive state. Myosin binds to the inactive state only weakly whereas it binds to the active state strongly. The equilibrium between the two states is

determined by the concentration of the ligands, calcium, or rigor myosin. Myosin binding weakly to actin exists in relaxed muscle but cannot generate force, whereas myosin binding strongly to actin produces force and therefore occurs in contracting muscle. Some recent studies of ATPase measurements using a stop flow apparatus supported this model (Heeley et al. 2002, Heeley et al. 2006). They showed that the predominant mechanism of regulation is the acceleration of product release, which is about 200 fold higher in the presence of both ligands as compared to the inhibited state (no ligands). Regulation by a change in myosin affinity to actin was only minor as would have expected for an active role of tropomyosin by blocking myosin-binding sites on F-actin. They also demonstrated that the binding of rigor myosin-S1 alone was insufficient to fully activate ATPase, an observation that was inconsistent with the three-state model of McKillop and Geeves. The results suggested that binding of either Ca^{2+} or myosin shifts the equilibrium between thin filament states in favor of the active state and both ligands are required for the full effect.

1.4.1.3 Thin filament cooperativity

Tropomyosin is essential for cooperative regulation of the thin filament. Tropomyosin bound to actin induces cooperative binding of myosin-S1 to actin as well as cooperative activation of acto-myosin ATPase. The flexibility of the tropomyosin molecule is thought to be a principal determinant of the degree of cooperativity and the cooperative unit size, n , the number of actin monomers activated by binding of a single myosin-S1. Tropomyosin-tropomyosin interactions, specifically the head-to-tail overlap, play an

important role in this regard. Tropomyosin isoforms with stronger head-to-tail interactions show higher values for n , which can be greater than 7, the structural unit size of actin monomers (Lehrer et al. 1997, Geeves and Lehrer 1994). Troponin, in particular the N-TnT fragment, which bridges the overlap making it stronger, has been shown to increase the n value (Schaert et al. 1995). When the head-to-tail interaction between tropomyosin molecules is strong, tropomyosin filament can be considered as a semi-flexible strand capable of transmitting signals in response to ligand binding not only within one structural unit but also to the neighboring units (Lehrer et al. 1997, Geeves and Lehrer 1994, Smith and Geeves 2003, Boussouf and Geeves 2007).

Another model of cooperativity, which was developed by Tobacman (Butters et al. 1993, Tobacman and Butters 2000), is actin-actin cooperativity. Like tropomyosins, actins are also in contact with each other. The fact that nonpolymerizable tropomyosins with missing residues in the overlap bind to actin with only slightly reduced cooperativity (Mak et al. 1983, Heeley et al. 1987, Butters et al. 1993) as compared to the native form, suggested long distance propagation of conformational changes through the actin filament itself. This model suggests that binding of either tropomyosin or myosin generate changes in the actin filament, which influence each other's binding to the filament in a cooperative manner.

1.5 Objectives of the study

The properties of tropomyosin were described in various sections of Chapter 1. To summarise, tropomyosin is an alpha-helical coiled coil protein that participates in interactions with: itself, seven actin monomers and at least two regions of troponin T. By way of these interactions it responds to the association of ligand (either Ca^{2+} or myosin) with the thin filament and thereby regulates the enzymatic activity of striated muscle myosin.

The physical connection between adjoining molecules of tropomyosin has long been recognized as being vital to this regulatory function. (Figure 1.1F). The continuity of the thin filament depends, in part, upon this end-to-end overlap of contiguous tropomyosins, involving the amino-, and carboxy-terminal, ten or so amino acids in the sequence. Further, given the proximity of troponin T binding, this overlap is situated at a convergence point in the thin filament (Figure 1.1F). A major focus of this thesis is the portion of tropomyosin that shows a high degree of sequence conservation and constitutes the amino-terminal half of this overlap.

The end regions of tropomyosin have been investigated biochemically by subtraction of the primary structure with a view to understanding their roles in muscle contraction regulation. One example is the exolytic digestion of eleven carboxy-terminal amino acids (Mak and Smillie 1981, Mak et al. 1983, Heeley et al. 1987). Despite having weak affinity for F-actin, the shortened tropomyosin (residues 1 - 273) could be incorporated

back into thin filaments under typical experimental conditions (Mak and Smillie 1981, Mak et al. 1983, Walsh et al. 1984, Heeley et al. 1987, Heeley et al. 1989a, Pan et al. 1989), a feature that allowed the carboxy-terminal region to be well explored.

If tropomyosin is made shorter at its amino-terminal end by nine amino acids, the consequences are drastic and the shortened molecule (residue 10 – 284), which did not reassemble into thin filaments (Cho et al. 1990, and Moraczewska and Hitchcock-DeGregori 2000), could not be deployed in actomyosin ATPase assays and was, therefore, of limited use. As a result, currently, information regarding the amino-terminal region is scarce. However, an earlier observation encouraged us to return to this problem. In 1996 Jackman et al. reported the unexpected cleavage of a muscle tropomyosin expressed in *Escherichia coli* JM109 cells. Truncation was attributed to the action of outer membrane protease T (Omp T), since it did not occur with *E. coli* strain BL21 DE3s, which is deficient in this protease. Chain hydrolysis was shown to occur between residues Lys6 and Lys 7 (Kluwe et al. 1995, Jackman et al. 1996). Preliminary experiments, carried out at the beginning of the research term, suggested that the unique digestion product, encompassing residues 7 – 284, was potentially very useful. Since Omp T-digested tropomyosin is missing only the first six residues, rather than the first nine, we reasoned that it might behave differently to those prepared previously. And this proved indeed to be the case. Specifically, Omp T digested tropomyosin was observed to bind F-actin to saturation in the presence of troponin, at low and high Ca^{2+} concentration. This finding allowed a biochemical examination of the role of tropomyosin's amino-

terminal region. Chapters 3, 4 and 5 pertain to this new proteolytic cleavage and its application:

(i) Chapter 3 describes the proof of method, the digestion of several different muscle tropomyosins (from mammal, bird and fish) by Omp T, as well as a method to prepare hundred milligram quantities of product.

(ii) Chapter 4 comprises the characterisation of the binding properties of the shortened tropomyosin (residues 7-284), under different buffer conditions. Compared to the full-length protein, Omp T digested tropomyosin shows weakened binding to the asymmetric portion of troponin T. This is of interest because there is uncertainty as to the precise docking position of this portion of troponin T on tropomyosin, whether it stops short of the overlap site or extends into the next tropomyosin molecule in the filament. The findings in this chapter are consistent with troponin T linking two tropomyosins.

(iii) Chapter 5 examines the regulatory consequences of removing the amino-terminal hexapeptide. It is evident that thin filaments (pCa 4) composed of Omp T digested tropomyosin activate myosin to a greater extent than those which are fully integral. Interestingly, this result is the reverse of what was observed with thin filaments containing tropomyosin shortened at the carboxy-terminal end (Walsh et al. 1984, Heeley et al. 1989a).

The final Results Chapter (Chapter 6) is different, but not entirely unrelated, from the other three. The focus is naturally occurring substitutions within tropomyosin, substitutions, which correlate with a particular type of striated muscle. Protein isoforms are of interest because they provide information on 'plasticity' – how a protein may be altered to suit a particular structural and functional demand. Chapter 6 examines the conformational stability of tropomyosins from Atlantic salmon, a cold water fish. One isoform, which contains a substitution within the fifth alanine cluster (Ala179Thr), undergoes a low temperature structural transition (T_m , $\sim 25^\circ\text{C}$; pH 7; 0.1M salt). The results in this chapter provide insight into the adaptation of the coiled coil to cold.

Chapter 2. Materials and methods

2.1 Extraction of muscle proteins

Fresh muscle samples were used for most preparations. Wild type tropomyosin, actin and troponin were extracted from dried muscle fibres (acetone powder) prepared by dehydrating muscle samples with cold ethanol and acetone. All procedures were carried out at 4°C unless otherwise noted. The pH of the buffers (and every buffer featured in this thesis) was set, at the appropriate temperature, using a pH meter (Beckman PHI ϕ 32 pH meter; electrode, Beckman Futura™ Plus) which had been calibrated with the pH 4 and 7 standards (Fisher Scientific) having a same temperature as the buffer.

2.1.1 Tropomyosin

Tropomyosins were isolated from fast and slow trunk (myotomal) muscles of Atlantic salmon (*Salmo salar*), cardiac muscle of rainbow trout (*Salmo gairdneri*) and back muscle of New Zealand white rabbits according to the method described by Stone and Smillie 1978 and described in more detail below.

2.1.1.1. Acetone powder preparation

In a typical preparation, 500g of muscle tissue was minced in a precooled stainless steel grinder and then stirred in 500ml of distilled water (dH₂O) for 2-3 min. After standing for 20 min, the liquid was strained through two layers of cheesecloth. The collected residue

was then stirred for 2-3 min in 500ml of 95% ethanol and the liquid was again separated through cheesecloth. This procedure was repeated three times with 2L of 50% ethanol, twice with 2L of 95% ethanol and twice with 2L of cold acetone (T, -20°C). The final residue, acetone powder, was then air dried in a fume hood at room temperature. A yield of approximately 50g was obtained. The dried powder was stored at 4°C till required.

2.1.1.2 Tropomyosin isolation.

30g of acetone powder was continuously stirred in 500ml of extraction buffer (1M KCl, 25mM Tris, 0.5 mM dithiothreitol (DTT), pH 8) for 2hr. To prevent unwanted proteolysis, phenylmethylsulphonyl fluoride (PMSF) was added to a final concentration of ~1mM at 1/2hr intervals. The extract was centrifuged at 4200rpm (Beckman J6HC centrifuge) for 20min, the supernatant retained and the residue re-extracted with another 300ml of the buffer for 1hr. After adjusting the concentration of combined supernatants to 1mg/ml (ϵ_{280} 1mg/ml = 1), crude tropomyosin was isoelectrically precipitated by lowering the pH to 4.6 with 5M HCl. The solution was gently stirred for 30min and then centrifuged at 8000rpm (Sorvall RC3 centrifuge; rotor, GS-3) for 30min. The pellet was redissolved in 1L of the extraction buffer, adjusted to pH 8, and clarified by centrifugation at 8000rpm for 20min. Tropomyosin was then enriched by salting out between 40% and 70% $(\text{NH}_4)_2\text{SO}_4$. The 70% pellet was dissolved in dH_2O (~250ml), dialyzed against 4-5 changes of 10-15L dH_2O in the presence of ~5mM $(\text{NH}_4)\text{HCO}_3$ and ~2mM mercaptoethanol, and lyophilized.

Lyophilized powder (300 mg) was dissolved in Q-Sepharose Fast Flow chromatography start buffer (50mM NaCl, 30mM Tris, 1mM DTT, pH 8.00). The solution was clarified by centrifugation at 8000rpm for 20 min before loading onto the column (2.5 cm x 15 cm), which had been equilibrated with two column volumes of the start buffer. Tropomyosin was then eluted with a linear gradient of 50-500 mM NaCl. Protein containing fractions were analyzed by measuring absorbance at 280nm and sodium dodecyl sulfate polyacrylamide gel electrophoresis (SDS PAGE). Tropomyosin containing fractions were pooled and loaded directly onto a hydroxylapatite column (BioRad) (2.5 cm x 15 cm) equilibrated in 1M NaCl, 50 mM sodium phosphate, 1 mM DTT, 0.1 % (w/v) NaN_3 , pH 7.0 at room temperature. Tropomyosin was eluted with a linear gradient of phosphate (50-250 mM). The fractions were analyzed by absorbance at 280nm and SDS PAGE. Fractions containing tropomyosin were pooled, dialyzed against 4-5 changes of 10-15L dH_2O in the presence of $\sim 5\text{mM}$ $(\text{NH}_4)\text{HCO}_3$ and $\sim 2\text{mM}$ mercaptoethanol and then lyophilized. The yield of pure tropomyosin was approximately 200mg.

2.1.2 Troponin

Troponin was prepared from New Zealand rabbit skeletal muscle dissected from back and hind legs following the protocol of Potter 1982 with a few modifications as described below.

2.1.2.1 Acetone powder preparation

Minced muscle (500g) was stirred in 3 x volume of Guba Straub buffer (0.3M KCl, 0.10M KH_2PO_4 , 0.05M K_2HPO_4) for 15 min and then centrifuged at 4200rpm for 10min. This step was repeated. The resulting residue was then resuspended in 1 x volume of 0.4% NaHCO_3 , following added 3 x volume of 0.05M Na_2CO_3 , stirred gently for 20 min and then centrifuged for 15min. After resuspending the residue in 1 x volume of 0.05M NaHCO_3 /0.05M Na_2CO_3 , 8L of 0.5mM CaCl_2 was added, stirred for 5min and strained through two layers of cheesecloth. The drained residue was then added to 2L of acetone (T, -20°C), stirred and strained through cheesecloth three times. The final acetone powder was air dried overnight in a fume hood. A yield of approximately 45g was obtained.

2.1.2.2 Troponin isolation

Troponin acetone powder (20g) was continuously stirred in 300ml extraction buffer (1M KCl, 25mM Tris, 0.1mM CaCl_2 , 0.1mM DTT, pH 8) for 2hr. After centrifugation at 4200rpm (Beckman J6HC centrifuge) for 30min, the supernatant was saved and the pellet reextracted with 150ml of 1M KCl for 60min followed by centrifugation. The two supernatants were combined and the pH of the mixture lowered to 4.6 with 5M HCl to isoelectrically precipitate out tropomyosin. After 30min stirring, the solution was centrifuged at 4200rpm (Beckman J6HC centrifuge) for 20min and the pH of the supernatant raised to 8.0 with 1M KOH. The solution was then subjected to three salt cuts; 0-40%, 40-50% and 50-60% with $(\text{NH}_4)_2\text{SO}_4$ (w/v). The pellets (4200rpm for 10min) obtained at 50% and 60% salt were dissolved in the buffer (10mM imidazole,

50mM KCl, 0.1mM CaCl₂, 0.02% NaN₃, pH 7.0), dialyzed against 2-3 changes of 10-15L of dH₂O in the presence of ~5mM (NH₄)HCO₃ and ~2mM mercaptoethanol. The dialysates were clarified by centrifugation and lyophilized.

2.1.2.3 Separation of troponin subunits

Troponin subunits were separated using Q-Sepharose Fast Flow chromatography under denaturing conditions. Isolated whole troponin (~740mg) dissolved in the start buffer (6M urea, 50mM Tris, 1mM EGTA, 1mM DTT, pH 8) was applied to the column (2.5 cm x 15 cm), which had been equilibrated with two column volumes of the same buffer. Troponin I eluted in the flow through while TnT and TnC eluted, after a NaCl gradient (0.0 – 750mM) was applied to the column, with peaks centered at NaCl concentrations of approximately 150mM and 230mM respectively. Fractions were analyzed by absorbance measurements at 280nm as well as by SDS PAGE. Those fractions containing subunits were pooled separately, dialyzed against dH₂O and lyophilized.

2.1.3 Actin

Actin was prepared from skeletal muscle dissected from back and hind legs of New Zealand rabbit according to Spudich and Watt 1971.

2.1.3.1 Acetone powder preparation

Minced muscle (500g) was stirred in 12 x volume of dH₂O for 30 min and then allowed to settle for an additional 30 min. After centrifugation for 10min at 4200rpm (Beckman

J6HC centrifuge) the residue was resuspended in 3 x volumes of 0.4% (w/v) NaHCO_3 and stirred for 15min. The step was repeated with 0.05M Na_2CO_3 / 0.05M NaHCO_3 and centrifuged at 4200rpm for 10min. The residue was then stirred in 3 x volume of 0.2mM CaCl_2 and centrifuged as before. The resultant residue was stirred in 3 x volume of cold 95% ethanol (T, 4°C) for 2min and then strained through two layers of cheesecloth. This step was repeated three times with 3 x volume of cold acetone (T, -20°C) and then the final acetone powder air-dried in a fume hood. Typically a yield of 30g of powder was obtained.

2.1.3.2 Actin isolation

Acetone powder (5g) was gently stirred in 50mL of extraction buffer (2mM Tris, 0.2mM CaCl_2 , 0.2mM ATP, 0.1mM DTT, pH 8) for 30 min with solid DTT added to a final concentration of 0.5mM. The mince was centrifuged at 4200rpm (Beckman J6HC centrifuge) for 15min and the residue washed with another 50ml of buffer. The supernatant and the soaked residue were strained through two layers of cheesecloth. The resultant filtrate was further filtered through 8.0um, 0.45um and 0.22um Millipore filters sequentially. Extracted actin was then isolated by polymerization and depolymerization. Polymerization was initiated by the addition of 0.05M KCl and 0.002M MgCl_2 with stirring for one hour. Solid KCl was added to a final concentration of 0.8M and stirring continued for another 1.5hr (These two steps were carried out at room temperature). Polymerized actin was sedimented at 45,000rpm (Beckman L-90K ultracentrifuge; rotor, 70 Ti) for 1.5hr, the pellet redissolved in 3-4ml of extraction buffer and dialyzed against

4L of the same buffer with 2-3 changes. After dialysis depolymerized actin was clarified by centrifugation at 45,000rpm for 1.5hr. The resulting G-actin was stored at 4°C in the presence of 0.01% NaN₃.

2.2 Expression of tropomyosin in bacteria

A cDNA encoding full-length salmon fast muscle tropomyosin (Heeley et al. 1995), previously cloned into the expression vector pTrc 99A (Pharmacia 27-5007-01) and then transformed into *Escherichia coli* BL21 DE3 (Jackman et al. 1996), was used to prepare unacetylated full-length tropomyosin (residues 1-284). Typically, 3L (4 x 750 ml aliquots) of Luria broth (LB) (Sigma) containing 50µg/ml ampicillin (Fisher) and 25µg/ml chloramphenicol (Fisher) was inoculated with a starter culture of *E. coli* BL21 DE3 at 37°C. When the absorbance of the culture at 600nm had reached 0.6-0.8, 1mM isopropyl β-D-thiogalactopyranoside (IPTG) was added to induce expression. After an overnight incubation, the cells were pelleted at 4200 rpm for 25 min, redissolved in buffer containing 0.1 M NaCl, 20mM imidazole pH 7 (3ml/g wet weight of cells) and passed through a French pressure cell, at 12000 psi. An additional 10ml of the same buffer and 0.1 mM PMSF was added to the lysate before centrifugation at 8000 rpm (Sorvall RC3 centrifuge; rotor, GS-3) for 25 min. The supernatant was then heated to 80°C in a water bath for 5 min, left to cool down to room temperature and then cooled on ice for 15 min. Bacterial proteins were removed by centrifugation at 8000 rpm for 25 min, and then tropomyosin in the supernatant was isoelectrically precipitated at pH 4.6.

The resultant tropomyosin pellet (8000rpm for 30 min) was then subjected to Q-Sepharose Fast Flow and hydroxylapatite column chromatography as described in section 2.1.1. Alternatively, to avoid the heating step, tropomyosin in the cell lysate was directly isoelectrically precipitated at pH 4.6 and further enriched by salting out between 50 - 70% $(\text{NH}_4)_2\text{SO}_4$. The final pellet was dialyzed against dH_2O , lyophilized, and passed through Q-Sepharose Fast Flow and hydroxylapatite columns. The yield of recombinant (unacetylated) tropomyosin was approximately 100mg.

2.3 Preparation of amino-terminally truncated tropomyosin

Truncated tropomyosin (residues 7-284) was generated by an enzymatic cleavage of the sixth peptide bond using the bacterial protease Omp T. Two methods were employed: by inducing expression from a tropomyosin cDNA clone in *E. coli* JM109 or by incubating previously isolated tropomyosin with a cell suspension of *E. coli* JM109.

2.3.1 Expression of tropomyosin in *E. coli* JM109

In order to express tropomyosin in *E. coli* JM109, total plasmid DNA was isolated from *E. coli* BL21 DE3 cells. This preparation contained two plasmids, one was the salmon fast muscle cDNA cloned in pTrc 99A (Jackman et al. 1996), the other was pLys S. In order to separate the two, plasmid DNA was digested, individual bands were excised and purified, and those corresponding to the salmon fast tropomyosin cDNA and pTrc 99A were religated, and then transformed into *E. coli* JM109 cells.

2.3.1.1 Cloning tropomyosin cDNA into the expression vector

Total plasmid DNA (pTrc 99A cloned with salmon fast muscle tropomyosin cDNA and pLys) was isolated from a 50ml overnight culture of *E. coli* BL21 DE3. Briefly, the cells were centrifuged at 5000rpm (Sorvell RC2-B centrifuge) for 25min and resuspended in 2ml of 50mM glucose, 25mM Tris, 10mM EDTA, pH 8. To the suspension was added 4ml of 0.2N NaOH, 1% SDS followed by 3ml of 3M potassium acetate, 88% formic acid. After mixing and centrifugation at 10,000rpm (Eppendorf 5415 Microfuge) for 10min, the supernatant was removed to a new tube and 0.6 x volume of isopropanol was added. After mixing the centrifugation step was repeated. The DNA pellet was washed with 70% ethanol, resuspended in 70ul of Tris/EDTA (TE) buffer (10mM Tris, 1mM EDTA, pH 8), extracted with phenol/chloroform and then precipitated with 0.5 x volume of 7.5 M ammonium acetate/ 0.6 x volume of isopropanol. The DNA pellet was washed with 70% ethanol, air-dried and resuspended in 100ul of TE. Then, 25ul of plasmid DNA was digested with Hind III and Nco I in the reaction buffer, 10mM Tris pH 8, 10mM MgCl₂, 100mM NaCl, 10mM 2-mercaptoethanol at 37 °C overnight. The whole digest was electrophoresed in 0.8% agarose, the gel bands with the DNA corresponding to pTrc 99A vector (~4200bp) and salmon fast muscle tropomyosin cDNA (1100bp) were excised, the DNA electroeluted, extracted with phenol/chloroform, concentrated (to 10ul) by ethanol precipitation and then religated using T4 ligase as described in Sambrook et al. 1989. All the restriction enzymes and ligase were purchased from either Promega or Pharmacia.

2.3.1.2 Transformation and induction

Ligated DNA was then transformed into *E. coli* JM109 cells, as described below. A 2ul aliquot of ligated DNA was mixed with 100ul of competent *E. coli* JM109 cells (prepared by Donna M. Jackman) and left on ice for 30min. Following a brief heat shock (90sec at 42°C and 2-3min on ice), 1ml of LB medium was added and the sample was incubated at 37°C for 1hr. After centrifuging at 5,000rpm for 2min (Eppendorf 5415 Microfuge) and discarding most of the supernatant, leaving only approximately 100ul, the pelleted cells were redispersed and plated on LB Agar medium containing the antibiotic (Bacto Agar (DIFCO laboratories), 15g/L; ampicillin, 50ug/ml). Following an overnight incubation at 37°C, a number of colonies on the plates were picked and grown in 5ml LB media in the presence of 50µg/ml ampicillin. When the absorbance of the cultures at 600nm had reached 0.6-0.8 (typically after 4-5hr of growth), 1mM IPTG was added. After an overnight growth, cultures were tested for the induction of salmon fast muscle tropomyosin using SDS PAGE. The cultures that expressed the protein were used to inoculate 50ml starter culture for a large-scale tropomyosin preparation as described in section 2.2. In this case, amino terminal truncation of tropomyosin is commensurate with cell lysis (Jackman et al. 1996).

2.3.2 Cleavage of isolated tropomyosin with a suspension of *E. coli* JM109 cells

2.3.2.1 Analytical-scale digestion

The digestion conditions were established by performing small-scale experiments. A 10mL overnight culture of *E. coli* JM109 was harvested by centrifuging at 5,000 rpm

(Sorvall RC2-B) for 25 min and the cells resuspended in 1mL of digestion buffer (0.1 M NaCl, 5mM EDTA, 1mM DTT, 50mM sodium phosphate, pH 7) after washing the cell pellet with the same buffer. A small volume of substrate (~0.5mg of previously isolated tropomyosin) was added and continuously agitated at either room temperature or 37°C. Aliquots of reaction mixture were withdrawn at different time intervals, centrifuged at 10,000rpm (Eppendorf 5415 Microfuge) for 2min to remove the cells, and analyzed by SDS PAGE.

2.3.2.2 Large-scale digestion

Large-scale processing of rabbit skeletal tropomyosin (100mg) was carried out as follows. Three liters of overnight culture were sedimented by centrifuging at 4200 rpm (Beckman J6HC centrifuge) for 25 min. The cells were washed once in digestion buffer and resuspended in 300 ml of the same buffer. Tropomyosin (10mL of 10mg/mL, in the same buffer) was then added to the suspension. The reaction mixture was incubated at 37°C with continuous agitation. When digestion was complete (~4h), as determined electrophoretically, the cells were removed by sedimentation and the truncated tropomyosin-containing supernatant was subjected to tropomyosin enrichment procedures as described in section 2.1.1.

2.4. Electrophoretic methods

SDS PAGE and isoelectric focusing were performed on a Bio-Rad mini-Protean II apparatus (BioRad, Richmond, CA) with 0.75mm thick electropherograms. Polymerization of acrylamide was initiated by the addition of N, N, N, N-tetramethylethylenediamine (TEMED) followed by ammonium persulfate. Agarose gel electrophoresis was carried out on a Bio-Rad DNA Sub Cell apparatus.

2.4.1 Sodium dodecyl sulfate polyacrylamide gel electrophoresis (SDS PAGE)

SDS PAGE was carried out according to the method of Laemmli (1970) using either 12% or 15% (w/v) polyacrylamide slabs (thickness, 0.75mm) consisting of an acrylamide/N,N-methylene-bis-acrylamide (BioRad) (w/v) ratio of 37.5:1. All samples were dissolved in SDS sample buffer (a trace of Bromophenol blue, 13% (v/v) glycerol, 1.3% (w/v) SDS, 0.02% (w/v) NaN_3 and 0.79% (w/v) Tris-HCl, pH 6.8 and ~1mM DTT) to a final dilution as noted in the figure legends. Electrophoresis was carried out at 180V until the bromophenol blue dye ran off the gel. The gels were stained using 0.2% (w/v) Coomassie Brilliant Blue R-250 (Bio-Rad) in 50% (v/v) ethanol, 10 % (v/v) acetic acid and then destained in 20% (v/v) ethanol, 10% (v/v) acetic acid.

2.4.2 Isoelectric focusing gel electrophoresis

Isoelectric focusing was performed on slab gels consisting of 9M urea, 2% (w/v) ampholines (pH 4-6), 4% (w/v) acrylamide, 0.24% (w/v) N,N-methylene-bis-acrylamide

and 0.022% (v/v) NP40. The samples were dissolved in saturated urea containing ~1mM DTT and a trace of bromophenol blue, and loaded onto the gels which had been briefly pre-run. The inner tank was filled with 4mM NaOH and the outer tank with 15mM H₃PO₄. After electrophoresing for 1000Vhr, gels were incubated first in 15% trichloroacetic acid for 30 min and then in 20% (v/v) ethanol / 10% (v/v) acetic acid until the gel became transparent. Finally gels were stained as described in section 2.4.1.

2.4.3 Agarose gel electrophoresis

The gels were composed of 0.8% agarose dissolved in Tris/Borate/EDTA (TBE) buffer (0.01%(w/v) NaOH, 1.08%(w/v) Tris-base, 0.55%(w/v) boric acid, 0.074%(w/v) EDTA). The samples were mixed with 2-4ul of loading dye (0.25% bromophenol blue, 0.25% xylene cyanol, 50% sucrose, 10mM Tris pH 8) and electrophoresed at 100 V until the bromophenol blue tracking dye was near the end of the gel. The gels were stained with ethidium bromide (1ug/ml) and destained with dH₂O.

2.5 Spectroscopic methods

2.5.1 UV-Visible absorbance

Protein concentration determinations were carried out using near UV absorbance measurements in a Beckman DU-64 Spectrophotometer. Proteins were dialyzed overnight at 4°C against a given buffer and then clarified by centrifugation at 12,000rpm (Eppendorf 5415 Microfuge) for 2 min. First, the instrument was calibrated with dH₂O and then the absorbances of both the dialysis buffer and the protein sample were

measured at the relevant wavelength. Measurements were between 0.1-1.0 absorbance units. The following extinction coefficients, ϵ_{280} 1mg/ml, were used: tropomyosin, 0.25; troponin, 0.47; TnI, 0.4; N-TnT, 0.143; and myosin-S1, 0.71, after correction for light scattering by subtracting $1.5 \times A_{320}$. F-actin was determined using ϵ_{290} 1mg/ml, 0.694 and correcting for scatter by subtracting $1.34 \times A_{320}$ (Johnson and Taylor 1978). The molar masses (g/mole) of proteins were taken as: tropomyosin, 66,000; troponin, 70,500; G-actin, 42,000; myosin-S1, 115,000; TnI, 21,000; N-TnT, 18,600.

2.5.2 Matrix Assisted Laser Desorption Ionization – time of flight (MALDI-tof) Mass spectrometry.

The mass spectra were taken using a Matrix Assisted Laser Desorption Ionization, linear time-of-flight (MALDI-tof) mass spectrometer (Voyager-DETMTMPRO) at the CREAT facility, Memorial University, Newfoundland. Protein samples were dissolved in 70% (by vol) aqueous acetonitrile, 0.1% (by vol) trifluoroacetic acid and mixed 1:1 with the matrix 3,5-dimethoxy-4-hydroxy-cinnamic acid. Approximately 1-4pmol of protein was present in each sample spot. All spectra were the summation of 100 laser shots.

2.5.3 Circular Dichroism

Spectra were recorded using a Jasco-J-810 spectropolarimeter. Proteins were dissolved and dialyzed against the buffer indicated in the respective figure legend. Thermal melting of the protein was determined by heating the protein from 5-65°C and measuring the ellipticity change at 222 nm (far UV) or 280nm (near UV). Temperature was controlled

by a circulating thermostatted water bath. The percentage of each transition (Table 3.1) was estimated by expressing the change in ellipticity within each transition as a percentage of the total ellipticity change from 5-65°C.

Far UV spectra at a given temperature were recorded from 198-300nm. A water-jacketed cell of 0.05 cm path length and a protein concentration of 1mg/ml were used. The mean residue ellipticity at 222nm ($[\theta]$) and the fractional helix (f_H) of the protein at 5°C were calculated using the following equations.

$$[\theta] = \frac{\theta \cdot m \text{ (g/mol)}}{10 \cdot L \text{ (cm)} \cdot C \text{ (mg/ml)}}$$

θ - observed ellipticity at 222nm

m - mean residue weight

L - path length

C - concentration

$$f_H = \frac{[\theta] - [\theta]_R}{[\theta]_H - [\theta]_R}$$

Following parameters are from Chen et al. (1994).

$$[\theta]_R = 1580 \text{ at } 222\text{nm}$$

$$[\theta]_H = 39500 \text{ at } 222\text{nm}$$

Near UV spectra were recorded from 250-340nm. A water-jacketed cell of 0.2 cm pathlength and a protein concentration of 10mg/ml were used.

2.6 Protein blotting

Protein bands electrophoretically separated by SDS PAGE were transferred to PVDF membranes (GelmanSciences) as follows. The gel and the membrane were soaked in transfer buffer (10mM CAPS, 10% methanol, pH 11) for 30min, assembled into the apparatus (Bio-Rad mini-Protean II) and electrophoresed for 2 hrs at 60V. The membrane was stained in 0.025%(w/v) Coomassie Brilliant Blue R250 and 40%methanol, destained in 50% methanol, air-dried and submitted to the Advanced Protein Technology Centre – Peptide Sequencing Facility (The Hospital for Sick Children, Toronto) for automated Edman degradation.

2.7 Affinity chromatography

Predialyzed samples of whole troponin (20mg) or tropomyosin (10mg) were coupled to CNBr activated Sepharose 4B (Pharmacia) following the manufacturer's instructions.

Briefly, 5g of freeze dried CNBr-activated Sepharose 4B was suspended in 1mM HCl. The swollen gel was washed for 15min with 1mM HCl (200ml/g of powder) and the ligand dissolved in 10ml of coupling buffer (0.1M NaHCO₃, 0.5M NaCl, pH 8.3) was mixed with the gel and rotated overnight at 4°C. The medium was washed with coupling buffer and any remaining active groups were blocked with 0.1M Tris-HCl, pH 8 for overnight at 4°C. Coupling was >95% as judged by the A₂₈₀ of the filtrate. The product was washed with three cycles of alternating pH, each consisting of a wash with 0.5M NaCl, 0.1M acetate, pH 4 buffer followed by a wash with 0.5M NaCl, 0.1M Tris, pH 8 buffer. The final material was stored at 4°C in the presence of 0.01% NaN₃ until packed into columns.

Samples (either tropomyosin or the amino-terminal chymotryptic fragment of rabbit skeletal troponin T, N-TnT, residues 1 - 158) were applied to columns (0.9cm x 8cm) containing the appropriate ligand equilibrated in 10mM imidazole, 0.5mM EGTA, 0.25 mM DTT, 0.01% NaN₃, pH 7, at 4°C. Elution was effected by a linear gradient of 0 to 500mM NaCl. Fractions were analyzed electrophoretically, by absorbance measurements at 230nm and by the Bradford assay (Bradford 1976). The NaCl concentrations of fractions were obtained by measuring the conductivity (Radiometer Copenhagen, CDM 80 conductivity meter and CDC 114 electrode) and then converting into molarity using a standard curve generated for conductivity vs. NaCl concentration.

2.7.1 Bradford assay

To 100ul samples of affinity chromatography column fractions was added 700ul of H₂O and 200ul of Bradford reagent and the tubes were gently mixed by inversion. Following 10min incubation for colour development, absorbance at 595nm was read in the Beckman DU-64 Spectrophotometer.

2.8 Tropomyosin binding to Actin

Binding was investigated by sedimentation in an airfuge (Beckman) at room temperature (Eaton et al. 1975) or in an ultracentrifuge (TLA 100.2; rotor, TLA 100) at 4°C. For qualitative analysis (gel electrophoresis) of binding, unlabeled tropomyosin was used whereas ¹⁴C labeled protein was used for quantification.

2.8.1 Labeling tropomyosin with Iodo[1-¹⁴C]acetamide

Tropomyosin was labeled at cysteine 190 with Iodo[1-¹⁴C]acetamide (Amersham Biosciences) as described in Allen 1989 with a few modifications. Tropomyosin was dissolved at 10mg/ml solution in buffer containing 0.1 M Tris, 1mM EDTA, 2mM DTT, pH 8.3. Protein reduction was carried out for 1h at room temperature in a sealed container and then excess DTT was dialyzed out at 4°C overnight against the same buffer (degassed) with no added DTT. Finally, Iodo[1-¹⁴C]acetamide was added to give a 2-3 fold molar excess over thiol groups and reactions were incubated at room temperature overnight. Labeled protein was dialyzed extensively against 2-3 changes of actin binding

buffer to remove excess reagent until the dialysate showed no radioactive counts above background. The labeled tropomyosins yielded specific radioactivities of 5.25×10^4 cpm / nmol (for rabbit skeletal truncated tropomyosin), 1.1×10^4 cpm / nmol (for salmon fast muscle unacetylated tropomyosin) and 3×10^3 cpm / nmol (for salmon fast muscle truncated tropomyosin, residues 7-284).

2.8.2 Actin binding assay

Stock solutions of various tropomyosins were prepared in binding buffers of varying ionic strength (as indicated in the respective figure legend), dialyzed overnight and stored at 4°C. Whole troponin was dissolved in the same buffer and was used for 1-2 days after the overnight dialysis. G-actin was polymerized by overnight dialysis against the above buffer. Proteins were combined, by adding them in the order F-actin, tropomyosin and troponin (or TnI +/- N-TnT), at final concentrations of 7 uM, 0.25- 9 uM and 2uM respectively. The total volume of the mixture was 100ul. Solutions were carefully mixed by using a Gilson Pipetman with a cut off tip and set at $2/3^{rd}$ of the volume, incubated for 45 min at 4°C and then centrifuged in the Airfuge (Beckman) or ultracentrifuge (Beckman TLA 100; rotor, TLA 100.2) for 30 min at 150,000 x g. Samples taken before and after centrifugation were analyzed on SDS PAGE. Alternatively, two 10ul aliquots were removed before and after centrifugation for radioactivity counting. The difference was attributed to the amount of tropomyosin bound. Correction for aggregation of tropomyosin was obtained by sedimentation in the absence of actin.

2.9 ATPase activity measurements

The assay was carried out in buffer 10mM MOPS, 4.5mM MgCl₂, 1 mM DTT, pH 7.0 (ionic strength, 18.5mM). The actomyosin-S1 Mg-ATPase activity was measured as a function of tropomyosin concentration, myosin-S1 concentration or thin filament concentration. F-actin, tropomyosin and troponin (if present), and S1 were combined at final concentrations as described in the figure legends. Protein mixtures (total volume, 300ul) were then incubated at 4 °C for 45 mins. The assay was initiated by adding 2mM Mg-ATP at 25 °C in a thermostatted water bath. Samples were collected between 0-16 min depending on the concentration of myosin-S1 or thin filaments. The reaction was terminated by transferring 50ul of the reaction mixture into a test tube containing 100 ul of stop solution (13.3% (w/v) SDS, 0.12M EDTA). The inorganic phosphate released was determined colorimetrically according to White 1982. For each reaction, five time points were taken in order to determine the rate of reaction. Then 850ul of a developing solution (0.5% (w/v) ferrous sulfate, 0.5% (w/v) ammonium molybdate, 0.5 M sulfuric acid) was added, and after 10min, absorbance was read at 550nm.

2.10 Myosin binding assay

Myosin-S1 binding to actin was determined according to Chalovich and Eisenberg 1981. Thin filaments containing either truncated or full length tropomyosin were mixed with varying concentrations of myosin-S1 in a buffer composed of 5.5 mM MgCl₂, 50mM

KCl, 10mM imidazole, 3mM MgADP, 0.5mM EGTA/Ca²⁺, 1mM DTT, 20uM myokinase inhibitor (Sigma), pH7 (ionic strength 71.5mM). The final mixtures (total volume, 100ul) contained 4.0uM actin, 2.28uM tropomyosin, 2.28uM troponin and 0-5uM myosin-S1. The samples were incubated at 4°C for 1hr and centrifuged in the Airfuge (Beckman) for 30min at 150,000 x g. Free myosin-S1 in the supernatant was determined by NH₄/EDTA ATPase assay of free S1 (Pan et al 1989). The supernatant (30ul) was first mixed with 255ul of buffer 0.44M NH₄Cl, 30mM EDTA, 28mM Tris, pH 8.0 and then 15ul of 100mM ATP (to a final concentration of 5mM) was added to start the reaction. The reaction was carried out at 25°C in a thermostatted waterbath. The reaction was quenched at five time points with SDS/EDTA stop solution and the inorganic phosphate was determined colorimetrically as described in the section 2.9. The free myosin-S1 concentration in the sample was obtained from a standard curve, which was constructed by assaying known quantities of myosin-S1 for NH₄/EDTA ATPase activity.

2.11 Data fitting

All the binding and ATPase plots were fitted using the GraphPad Prism software. One of the following equations were used to obtain the best fit curve.

1. Sigmoidal dose-response (variable slope)

$$Y = B_{\max} / (1 + 10^{-(\log Kd - \log X) * n})$$

2. One site binding (hyperbola)

$$Y = B_{\max} * X / (Kd + X)$$

Chapter 3. Preparation and analysis of amino-terminally truncated tropomyosin

3.1 Introduction

The bacterial outer membrane protease T, Omp T, produces a cleavage at the amino-terminal end of tropomyosin resulting in a product which is six residues shorter than the intact tropomyosin. The observation has been reported previously (Kluwe et al. 1995, Jackman et al. 1996), when tropomyosin cDNA expression was attempted in *Escherichia coli* cells that contain a functional Omp T gene. The tropomyosin product from Omp T digestion retains more amino acids at its amino-terminal end as compared to two previous amino-terminally truncated tropomyosins lacking the first nine residues (Cho et al. 1990, and Moraczewska and Hitchcock-DeGregori 2000), a feature that prompted us to use the Omp T cleaved protein as a model to revisit the problem of evaluating the functional significance of the tropomyosin amino-terminal end. This chapter describes a method to prepare hundreds of milligrams of tropomyosins lacking the first six residues, from various muscle sources, utilizing this bacterial outer membrane bound protease. This proteolytic enzyme specifically cleaves between two consecutive positively charged residues of the substrate [Sugimura and Nishihara 1988, Dekker et al. 2001, McCarter et al. 2004]. The source of the enzyme was simply whole cells of the bacterial strain, *E. coli* JM109. Truncation was implemented in two different ways: by inducing tropomyosin cDNA expression in *E. coli* JM109 or by treating previously isolated full-length protein

with a cell suspension of the same strain. The final product was then characterized in terms of its purity, sequence, stability and ability to incorporate into thin filaments.

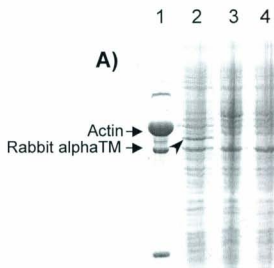
3.2 Results

3.2.1 Induction of tropomyosin expression in *E. coli* JM109

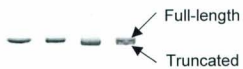
The expression of cDNA encoding full-length salmon fast muscle tropomyosin was induced in *E. coli* JM109 and was monitored by SDS gel electrophoresis (Figure 3.1). There was no detectable tropomyosin in uninduced cells (Figure 3.1A, lanes 3 and 4) whereas a distinct band in the tropomyosin region of the gel was observed in induced cultures (Figure 3.1A, lane 2). It should be noted that although salmon 'fast' tropomyosin is an alpha-type isoform by sequence, it exhibits a slower mobility in the presence of SDS than rabbit alpha-isoform (molecular weight marker; Figure 3.1A, lane 1) (Heeley et al. 1995). Induction of three liters of culture yielded approximately 100 mg of tropomyosin. SDS PAGE analysis of this protein showed it to possess a slightly higher mobility than the full-length counterpart indicative of its shorter length (Figure 3.1B, lane 3). Further, no traces of the undigested, intact protein molecule were observed in this sample. The difference in migration between the product and intact protein is illustrated by co-electrophoresis (Figure 3.1B, lane 4). Since Omp T is an extracellularly bound protease the cleavage is effective only after cellular disruption in the French pressure cell. In agreement with a previous report from this lab (Jackman et al. 1996) chain cleavage is complete and virtually instantaneous upon cell lysis. By comparison expression in *E. coli*

Figure 3.1 : SDS PAGE analysis of salmon fast muscle tropomyosin expressed in *E. coli* JM109.

- A) Induction of salmon fast muscle tropomyosin cDNA expression in *E. coli* JM109 cells. 5ml LB (containing 50ug/ml ampicillin) was inoculated with a colony of *E. coli* JM109 containing pTrc 99A cloned with salmon fast muscle tropomyosin cDNA. After about 4-5 hr of growth at 37°C (absorbance at 600nm had reached 0.6-0.8) protein expression was induced by the addition of 1mM IPTG. Following overnight incubation at 37°C a 1ml sample was mixed 1:1 with SDS sample buffer and 20ul loaded per lane for electrophoresis. Lanes: 1, molecular weight marker (actin and rabbit alpha tropomyosin are indicated by arrows); 2, induced culture (expressed salmon TM is indicated by an arrow); 3 & 4, uninduced culture.
- B) A 12% SDS PAGE of purified tropomyosin isolated from muscle and prepared by expressing in *E. coli* JM109 (truncated tropomyosin) or *E. coli* BL21 DE3 (unacetylated tropomyosin). Lanes: 1, unacetylated; 2, wild type; 3, truncated, 4, mixture of wild type + truncated (indicated by arrows). 1-2 ug of protein was loaded per lane.



B)



BL21 DE3, an *E. coli* strain lacking Omp T, yields a tropomyosin that migrated with identical mobility as the wild type protein (Figure 3.1B, lane1) indicating that the truncation is specific to *E. coli* strains such as JM109 that contain a functional Omp T gene.

3.2.2. Treatment of tropomyosin with *E. coli* JM109 cell suspension.

The amino-terminal truncation can be implemented in different ways. One, by inducing the expression of protein in an appropriate bacterium (eg., *E. coli* JM109) as described above. As an alternative method, cleavage was also attempted by exposing previously isolated tropomyosin to a suspension of *E. coli* JM109 cells. Formation of amino-terminally cleaved tropomyosin was again monitored electrophoretically. Once more the removal of a small peptide resulted in an increase in mobility in SDS gels.

3.2.2.1 Time course and temperature.

The conditions for cleavage were optimized by carrying out small-scale digestions of salmon fast and rabbit skeletal tropomyosins. The cleavage was not instantaneous as in the earlier case; therefore digestion was carried out at varying temperatures and monitored over time till completion. This is shown for rabbit skeletal tropomyosin in Figure 3.2A. At room temperature, the protein is largely intact after 4 hrs of incubation (Figure 3.2A lanes 1-4). Conversely, at 37 °C (0.1M salt at pH7), processing of mammalian tropomyosin is complete after 4 hours (Figure 3.2A, lane 8). No intact protein is detected after this time, as determined by gel analysis. (It should be noted that

Figure 3.2 : Truncation of rabbit and salmonid tropomyosin with a *E. coli* JM109 cell suspension.

10mL of an overnight culture was centrifuged, the sedimented cells were dispersed in 1mL of buffer (0.1 M NaCl, 5mM EDTA, 1mM dithiothreitol, 50mM phosphate, pH 7) and mixed with 100 μ L of 5mg/mL rabbit skeletal wild type tropomyosin dissolved in the same buffer and incubated at room temperature (lanes 1-4) or 37 $^{\circ}$ C (lanes 5-8). Reaction was terminated at times specified below by pelleting the cells, resuspending the supernatant in an equal volume of SDS sample buffer and boiling. 1-2 μ g of protein was loaded per lane and electrophoresed in a 12 % SDS polyacrylamide gel. A) Rabbit skeletal tropomyosin. Lanes: 1 & 5, at zero time; 2 & 6, after 60min; 3 & 7, after 120min; 4 & 8, 240 min incubation. B) Salmon fast muscle tropomyosin. Lanes: 1 & 8, at zero time; 2 & 5, after 30min incubation; 3 & 6, after 60min, 4 & 7 after 120min incubation.



the tropomyosin used in this experiment consists of a preponderance of the alpha isoform and a small fraction of beta tropomyosin, which is observed as a faint upper band, Cummins and Perry 1973; Cummins and Perry 1974). The truncation is evident with the beta isoform as well (Figure 3.2A lanes 7 and 8). Longer times were required to achieve complete reaction at temperatures below 37 °C; room temperature (24 hrs) or 4 °C (longer than 48 hrs) (data not shown).

However, in the case of salmonid fast muscle tropomyosin, complete digestion was achieved within 2 to 4 hours at room temperature. Only a marginal increase in the rate of reaction was observed if it was performed at 37 °C. (Figure 3.2B, compare lanes 2 and 5). The non-identical rates of digestion of the Atlantic salmon and mammalian wild type tropomyosins can be attributed to their having distinct conformational stabilities at the two temperatures (William and Swenson 1981, Jackman et al. 1996).

3.2.2.2 Effect of pH, divalent cations and cell lysate over cell suspension

Although the Omp T protease is reported to be optimally active slightly below neutrality (pH 6) (Sugimura and Nishihara 1988), decreasing pH from 7 to 6.5 did not bring about a noticeable change in reaction rate (data not shown). In addition, it has been reported that the protease is inhibited by bivalent cations, Zn²⁺, Cu²⁺, Fe²⁺ (Sugimura and Nishihara 1988). Therefore 5mM EDTA was routinely included in the assay buffers. However, no detectable change was observed when the chelating agent was omitted. Further, in accordance with the extracellular location of Omp T, no added advantage in terms of

reaction rate was observed by mixing wild type protein with a *E. coli* JM109 cell lysate rather than a cell suspension, at either room temperature or 4 °C. Using a cell suspension is of practical significance because a lysate introduces bacterial proteins into the sample.

3.2.2.3 Digestion of other tropomyosins

The same principle, that of incubating enriched protein with a cell suspension, can be employed to effect cleavage of a variety of muscle tropomyosins from a variety of classes. The electrophoretic analysis in Figure 3.3 shows fully truncated tropomyosins produced from various muscle tropomyosins after 4hr of digestion with Omp T showing its broad range applicability; bovine heart (lanes 1 and 2), shark skeletal trunk muscle (lanes 3 and 4), bovine uterus (lanes 5 and 6), chicken breast (lanes 7 and 8) and chicken gizzard (lanes 9 and 10). A similar result was obtained with rabbit cardiac muscle tropomyosin (data not shown).

3.2.2.4 Effect of acetylation on digestion.

The experiment was repeated with unacetylated full-length salmon fast muscle tropomyosin obtained via expression of tropomyosin cDNA in the Omp T minus strain, *E. coli* BL21 DE3. The earliest time points obtained in these experiments were at 30 min and interestingly, cleavage was complete within this time period at both room temperature and 37 °C. One of these experiments performed at room temperature is shown in Figure 3.4 (see lane 2). By contrast, the wild type counterpart is largely intact after 30min of incubation at either room temperature (Figure 3.4, lane 4) or 37 °C. It is



Figure 3.3 : Digestion of various vertebrate muscle tropomyosins

Reaction and electrophoresis conditions are as described in the legend to figure 3.2. Lanes: 1 & 2, bovine cardiac; 3 & 4, Blue shark skeletal (trunk); 5 & 6, bovine uterus; 7 & 8, chicken breast and 9 & 10, chicken gizzard. Odd-numbered lanes, full-length (wild type) proteins (at zero time); even-numbered lanes, truncated proteins (after 240min reaction). T, room temperature. Note, an identical result was obtained with Mako shark skeletal tropomyosin as Blue shark (not shown).

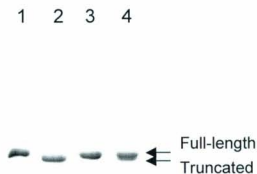


Figure 3.4 : The effect of acetylation on Omp T digestion.

Reaction conditions are as described in the legend to figure 3.2. Lanes: 1 & 2, unacetylated salmon fast muscle tropomyosin at zero and 30 min incubation, respectively; 3 & 4, wild type (acetylated), at zero and 30 min incubation, respectively. T, room temperature. Arrows show the positions on the gel of full-length and truncated tropomyosins. The results of this experiment infer that the unacetylated tropomyosin is fully truncated after 30 min reaction whereas the acetylated protein is mostly in the intact form after the same incubation time.

evident, therefore, that the blocking group has a bearing on the susceptibility of the protein to hydrolysis by the bacterial enzyme. The scissile bond is more labile when Met1 is unacetylated. The rapid cleavage observed in the first method, that is expressing the protein in *E. coli* JM109, even at low temperatures (-4°C) can also be attributed to the same reason, as tropomyosin expressed in the bacterium is unacetylated. This result is compatible with the claim that the acetyl group stabilizes the structure of the amino-terminal region of tropomyosin (Greenfield et al. 1994 and Brown et al. 2001).

3.2.2.5 Preparative scale digestion

Digestion was successfully stepped up to a preparative scale for the truncation of hundred milligram quantities of rabbit skeletal, rabbit cardiac, salmon fast and Mako shark tropomyosins. A preparative scale digestion carried out with rabbit skeletal tropomyosin is shown in Figure 3.5A. Truncation was complete after 4hrs of incubation with a *E. coli* JM109 cell culture at 37°C (lane 2). The difference in mobility is again demonstrated by electrophoresing proteolysed and intact protein in the same lane (see lane 3).

It also has to be noted that sometimes, when loaded in large quantities, the electrophoretic analysis provided evidence of fragmentation at secondary sites. Such breakdown of rabbit skeletal tropomyosin leads to production of two minor fragments; the more slowly migrating one corresponding in length to roughly half of the molecule (Figure 3.5B, lane 2). At short incubation times these fragments are present in low amounts, as evidenced from its faint staining. The unwanted products can be removed by subsequent enrichment

Figure 3.5 : Preparative scale truncation of rabbit skeletal tropomyosin.

3L of an overnight culture was centrifuged, the sedimented cells were dispersed in 300ml of buffer (0.1 M NaCl, 5mM EDTA, 1mM dithiothreitol, 50mM phosphate, pH 7) and mixed with 10ml of 10mg/mL rabbit skeletal wild type tropomyosin dissolved in the same buffer and incubated at 37 °C. Aliquots of samples were removed, mixed 1:1 with SDS sample buffer, and run on SDS 12% polyacrylamide gels. 1-2 ug of protein was loaded per lane. A). Lanes; 1, wild type; 2, truncated after 240min incubation; 3, mixture of wild type + truncated (indicated by arrows). B) Truncated product was enriched by pI precipitation and chromatography. Lanes 1, wild type; 2, truncated after 240min; 3, chromatographically enriched truncated protein. The arrows in lane 2 show low molecular weight tropomyosin fragments resulting from Omp T cleavage at secondary sites, which are not present after the truncated tropomyosin has been subjected to enrichment. Loading ~6ug per lane.



(isoelectric precipitation and chromatography) of the main cleavage product (Figure 3.5B, lane 3). It should be further noted that the hydroxylapatite column chromatography during the protein enrichment process separates the alpha isoform from the beta in rabbit skeletal tropomyosin (Eisenberg and Keilley 1974), which can be seen in lane 3 having lesser amounts of beta in the purified truncated sample than the other two.

3.2.3. Analysis of truncated tropomyosins.

3.2.3.1. Edman-based sequencing

Truncated tropomyosins were blotted onto PVDF membranes and subjected to amino-terminal sequencing using the Edman degradation method. Five cycles of Edman-based sequencing of purified truncated samples from salmon fast muscle tropomyosin (expressed in *E. coli* JM109) and rabbit skeletal tropomyosin yielded the sequence: Lys-Met-Gln-Leu-Lys (Table 3.1). Since this matches residues 7 - 11 of the known sequence of salmon fast (Heeley et al. 1995) and rabbit skeletal (Stone and Smillie 1978) muscle tropomyosins, the site of Omp T cleavage of the main product is described as Lys6 and Lys7, in agreement with previous studies (Kluwe et al. 1995, Jackman et al. 1996).

3.2.3.2 Mass analysis

In order to confirm that the truncated products are intact at the carboxyl end, accurate analysis of their masses was necessary. Some of the truncated products were therefore analyzed by Matrix Assisted Laser Desorption Ionization- time of flight (MALDI-tof) mass spectrometry. A major peak corresponding to a m/z of 31800 Da (Figure 3.6) was

Table 3.1: The amino-terminal sequences of various tropomyosins

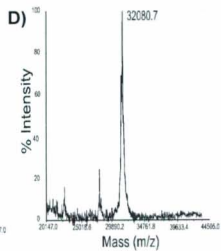
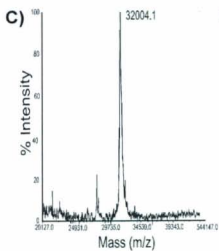
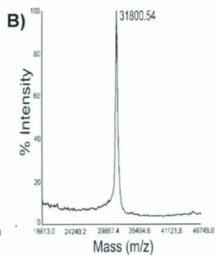
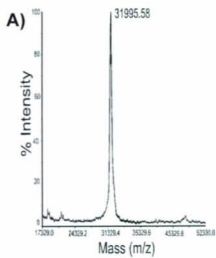
	Amino terminal sequence
Acetylated full-length	Ac- ¹ Met-Asp-Ala-Ile-Lys-Lys- ⁷ Lys-Met-Gln-Leu-Lys
Unacetylated full-length	¹ Met-Asp-Ala-Ile-Lys-Lys- ⁷ Lys-Met-Gln-Leu-Lys
Truncated tropomyosin	¹ Lys-Met-Gln-Leu-Lys

obtained for truncated salmon fast muscle tropomyosin. The sequence predicted value for the protein with the above cleavage is 31805 Da, only 5 Da higher than the measured value. The mass value obtained for the truncated rabbit skeletal tropomyosin was 31995 Da (Figure 3.6), which is only 1 Da higher than the sequence-based value. In addition, truncated bovine cardiac and truncated chicken breast tropomyosins showed mass values of 32004 Da (sequence based value, 32007 Da) and 32080 Da (sequence based value, 32077 Da) respectively. In all cases, no intact protein was observed indicating a complete digestion with the protease. Further, in the case of rabbit skeletal and bovine cardiac tropomyosins, the detected signals corresponded to alpha isoforms but those corresponding to beta forms were not detected, presumably due to their low abundance. These results from mass analysis confirm that the main cleavage site is between Lys6 and Lys7 and in turn suggest that the truncated protein is intact at the carboxy-terminal end.

Mass measurements of Omp T digested rabbit skeletal tropomyosin before and after protein enrichment were also analyzed in the low molecular weight range to emphasize the detection of fragments resulting from Omp T digestion at secondary cleavage sites. Two prominent peaks with m/z values of 18460.5 Da and 13517.0 Da were evident in the unpurified sample, in addition to the ones corresponding to the main Omp T cleavage product (31994.8 Da) and its doubly charged molecule (15994.6 Da) (data not shown). Their masses are in agreement with the relative mobilities of the two minor peptides detected on the SDS gel (Figure 3.5B, lanes 1 and 2) and can be thought to have originated from Omp T cleavage at a secondary site. Further, consistent with SDS PAGE

Figure 3.6 : Matrix Assisted Laser Desorption Ionization, linear time-of-flight mass spectral analysis of truncated tropomyosins.

A) Rabbit skeletal (mass of the main peak, 31995 Da); B) salmon fast (mass of main peak, 31800 Da); C) bovine cardiac (mass of the main peak, 32004.1 Da) and D) chicken breast (mass of the main peak, 32080.7 Da). Salmon fast was prepared by expressing in *E. coli* JM109 while the other three proteins were prepared by treating with a *E. coli* JM109 cell suspension. X axis, mass (m/z); Y axis, % intensity of the peak. Samples were dissolved in 70% (by vol) aqueous acetonitrile, 0.1% (by vol) trifluoroacetic acid and mixed with matrix 3,5-Dimethoxy-4-hydroxy-cinnamic acid.



analysis these two peaks are remarkably diminished following the enrichment procedure (Figure 3.5B, lane 3).

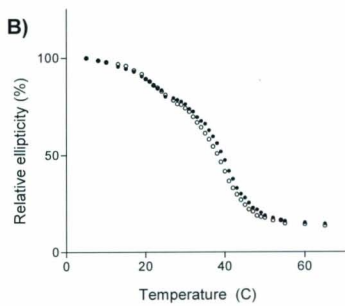
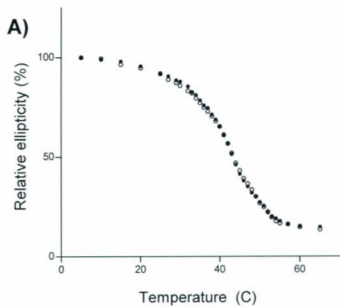
3.2.3.3. Circular Dichroism spectrometry of truncated tropomyosins.

The secondary structure and melting profiles of truncated proteins were assessed by far UV Circular Dichroism spectrometry (Figure 3.7) as detailed below, to determine if the proteins are properly folded. Thermostabilities of truncated salmon fast muscle tropomyosin and truncated rabbit skeletal tropomyosin were compared with the corresponding native proteins.

Mean residue ellipticity values of 34896.8 ± 3407.6 mdeg.mol⁻¹.cm⁻¹ and 35040.9 ± 3769.5 mdeg.mol⁻¹.cm⁻¹ were obtained at 5°C for truncated salmon fast and truncated rabbit skeletal tropomyosins respectively, indicating that the truncated proteins possess a high degree of helical content. The average ellipticity values calculated for the wild type proteins were slightly higher (38035 ± 1993 mdeg.mol⁻¹.cm⁻¹ for salmon and 35260.3 ± 1811.9 mdeg.mol⁻¹.cm⁻¹ for rabbit) but the difference was within experimental error. One reason for the variability in mean residual ellipticity is attributable to small variations in protein concentration determination. The thermal melting profiles of the proteins were obtained by measuring ellipticity at 222nm between 5-65°C. The buffer was 20mM Phosphate, 0.1 M KCl, 1mM DTT, pH 7. Two transitions, a minor transition at 24.5 ± 1.4 °C and a major transition at 38.6 ± 2.2 °C, both of which are characteristic of the full-

Figure 3.7 : Circular Dichroism spectrometry of truncated tropomyosins.

Relative ellipticities for A) rabbit skeletal tropomyosins, B) salmon fast muscle tropomyosins are plotted as a function of temperature. Open symbols, wild type tropomyosins; closed symbols, truncated tropomyosins. Buffer, 20mM HEPES, 0.1M KCl, 1mM DTT, pH 7; heating rate, 30°C/hr; wavelength, 222nm; scan speed, 100nm/min; protein concentration, ~0.5-1mg/ml; light path, 0.05cm. Rabbit skeletal truncated: T_m, 43.5 ± 0.5°C; [θ], 35040.9 ± 3769.5mdeg.mol⁻¹.cm⁻¹. Rabbit skeletal wild type: T_m, 44.1 ± 1.7°C; [θ], 35260.3 ± 1811.9mdeg.mol⁻¹.cm⁻¹. Salmon fast truncated: T_ms, 24.5 ± 1.4°C and 38.6 ± 2.2°C; [θ], 34896.8 ± 3407.6 mdeg.mol⁻¹.cm⁻¹. Salmon fast wild type: T_ms, 24.2 ± 1.06°C and 38.1 ± 1.3°C; [θ], 38035 ± 1993mdeg.mol⁻¹.cm⁻¹.



length protein were seen in the melting profile of the truncated salmon fast muscle tropomyosin.

Observed melting temperatures for full-length proteins were $24.2 \pm 1.1^\circ\text{C}$ and $38.1 \pm 1.3^\circ\text{C}$ (Figure 3.7). For rabbit truncated protein, a melting temperature of $43.5 \pm 0.5^\circ\text{C}$ was observed. The full-length counterpart showed a major transition with a melting temperature of $44.1 \pm 1.7^\circ\text{C}$. In both cases, the melting temperatures are in agreement with previous reports (Jackman et al. 1996, Lehrer 1978, Krishnan et al. 1987, Graceffa and Lehrer 1980, Graceffa and Lehrer 1984, Betteridge and Lehrer 1983) on the thermal unfolding of corresponding intact proteins.

3.2.3.4. Ability to form thin filaments

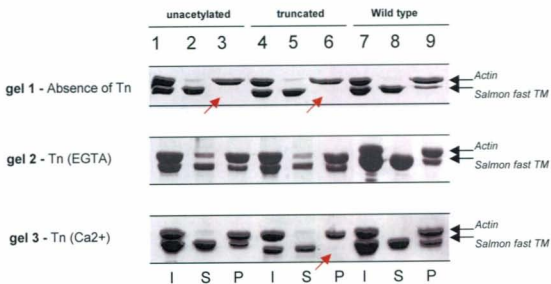
Finally, the ability to reconstitute thin filaments with the Omp T-digested tropomyosins was assessed by actin binding experiments. To optimize the binding, moderate ionic strength conditions were employed (5.5mM Mg^{2+} , 50mM KCl ; ionic strength, 71.5mM). For these experiments, truncated and full-length tropomyosins from two sources, salmon fast and rabbit skeletal muscles were selected. Regulatory proteins (tropomyosin and, when present, troponin) were mixed with F-actin in the assay buffer and were sedimented following a 45min incubation period. Fractions before and after sedimentation were analyzed by SDS PAGE. The sections of the stained gels containing tropomyosin, troponin T and actin, are presented in Figure 3.8. It should be noted that TnT is separately visualized only when rabbit skeletal tropomyosins are used, because salmon

Figure 3.8 : Binding of tropomyosins to actin in the presence and absence of troponin.

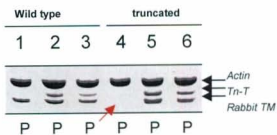
Actin, tropomyosin and troponin (if present) were mixed at a 7uM : 4uM : 4uM ratio of which 70ul was cosedimented at 150,000 x g at 4°C for 45 min. Buffer: 10 mM MOPS, 50 mM KCl, 5.5 mM MgCl₂, 1 mM DTT, pH 7, and either 0.5 mM EGTA or 0.5 mM Ca²⁺. The samples before (l) and after (p, pellet and s, supernatant) were mixed with SDS sample buffer and loaded 10uL per lane, onto a 12% SDS polyacrylamide gel. The section of the stained gel containing tropomyosin, troponin T and actin, is presented. The absence of tropomyosin in the pellet fractions are indicated by red arrows.

- A) Binding of salmon fast muscle tropomyosins to actin at 4°C. The three gels are respectively: in the absence of troponin, in the presence of troponin (EGTA) and in the presence of troponin (Ca²⁺). Lanes: 1-3, unacetylated; 4-6, truncated; 7-9, wild type.
- B) Binding of rabbit skeletal tropomyosins to actin at room temperature. The molar ratio of regulatory proteins to actin was 4:7. Lanes: 1, wild type tropomyosin + actin; 2, wild type tropomyosin + actin + troponin (EGTA); 3, wild type tropomyosin + actin + troponin (Ca²⁺); 4, truncated tropomyosin + actin; 5, truncated tropomyosin + actin + troponin (EGTA) and 6, truncated tropomyosin + actin + troponin (Ca²⁺). In the second gel: molar ratio of regulatory proteins to actin was 2:7. Lanes: 1-3, truncated; 4-6, wild type.

A)



B)



fast muscle tropomyosin migrates with TnT on the gel. In the case of rabbit skeletal tropomyosins, only the pellets after sedimentation are shown (Figure 3.8B). Binding to F-actin was confirmed by the presence or absence of tropomyosin in the pellet fraction.

As anticipated given the ionic conditions, wild type tropomyosin complexes with actin in the absence of troponin (Figure 3.8A (gel-1, lane 9); Figure 3.8B (gel-1, lane 1)) but the unacetylated and the truncated tropomyosins do not. (Figure 3.8A, (gel-1, lanes 3 and 6); Figure 3.8B, (gel-1, lane 4)). Although not explicitly determined, the latter result can be interpreted as an indication of the non-polymerisable nature of the unacetylated and truncated proteins. Although unacetylated tropomyosin does not bind to F-actin, it has previously been reported that troponin induces its binding to actin in the presence or absence of Ca^{2+} (Hitchcock-DeGregori and Heald 1987, Heald and Hitchcock-DeGregori 1988), which is also seen in Figure 3.8A (gel-2 and -3, lanes 3). Interestingly, in the presence of troponin, rabbit truncated tropomyosin also co-sedimented with F-actin (Figure 3.8B, (gel-1, lanes 5 and 6)) at both high and low calcium concentrations, indicating its binding to F-actin. (Close inspection of the stained gel verifies the presence of the shortened tropomyosin in the actin pellet, since the separation between it and troponin T (in Figure 3.8B, lanes 5 and 6) is slightly wider than that of the intact (Figure 3.8B, lanes 2 and 3). With added Ca^{2+} , however, sedimentation needed to be carried out at high molar ratio of regulatory proteins to F-actin, 4/7ths, rather than 2/7ths. At lower molar ratios saturation is observed at low Ca^{2+} , but not high (data not shown), suggesting that troponin's ability to induce binding is Ca^{2+} sensitive. In the case of salmon truncated

tropomyosin, under the protein concentrations used in the study (tropomyosin, 4 μ M; F-actin, 7 μ M), troponin induction of binding to F-actin was only detected at low Ca²⁺ (Figure 3.8A (gel-2 and -3, lanes 6)). The result again illustrates the Ca²⁺ dependency of tropomyosin binding to F-actin. It may also imply that in the presence of high Ca²⁺, actin affinity of salmon truncated tropomyosin is weaker such that the binding cannot be induced at micromolar range of tropomyosin. Nonetheless, these results suggest that, at moderate ionic strength, it is feasible to reconstitute thin filaments with some of the Omp T-digested tropomyosins irrespective of Ca²⁺ concentration.

3.3. Discussion

This chapter describes a method for the preparation of a truncated tropomyosin, in which six residues from the conserved amino-terminal end have been enzymatically removed. The extracellular membrane bound bacterial protease Omp T is responsible for the cleavage. This proteolytic enzyme is an endopeptidase that specifically cleaves between two consecutive basic residues [Sugimura and Nishihara 1988, Dekker et al. 2001, McCarter et al. 2004]. Although vertebrate muscle tropomyosin contains several such sequences, remarkably, hydrolysis occurs predominantly at one peptide bond, namely between residues 6 and 7 as confirmed by Edman based sequencing and mass analysis.

According to Dekker et al. 2001, Omp T shows a preference for cleavage of different positively charged sequence combinations in the order of; Lys-Lys > Lys/Arg -

Lys/Arg/His > Arg-Arg. If the residues immediately prior to and following the scissile bond are termed P1 and P1' (see Table 3.2), their flanking residues, P2 and P2' also have an impact on the proteolytic activity. For example negatively charged residues at either P2 or P2' diminish all activity of Omp T towards any of the above positively charged cleavage sites. Certain amino acids, such as Ala, Phe, Ile, Val, Lys at these positions favor high reactivity however. In addition, McCarter et al. 2004 showed that residues at P3/P3' and P4/P4' are also of importance in determining protease activity. Arginine or tryptophan are preferred residues at these positions.

Analysis of rabbit alpha and salmon fast muscle tropomyosin sequences, respectively, revealed 8 and 7 sequences comprising two consecutive positively charged residues (at neutral pH) including the main cleavage site, Lys6-Lys7 (Figure 3.9). These sites with their flanking residues are tabulated in Table 3.1. Using a synthetic hexapeptide containing the Omp T recognition sequence, Ala-Arg-Arg-Ala, and varying each position in the recognition sequence one at a time, Dekker et al. 2001 reported varying levels of preference by Omp T towards each of the 20 amino acids at P2, P1, P1' and P2' positions. Based on their results, these Omp T preferences for each residue in tropomyosin recognition sites are indicated with highlights in Table 3.2.

Three sites in rabbit alpha tropomyosin (Lys29-Lys30, Lys76-Lys77, Arg160-Arg161) and two in salmon fast muscle (Lys29-Lys30, Arg160-Arg161) contain an acidic residue in the P2 position (Table 3.2) making those sites resistant to cleavage. Both the Lys5-Lys6 and Lys6-Lys7 sites appear

```

m d a i k k k m q m l k l d k e n a l d r a e q a e a d 28
m d a i k k k m q m l k l d k e n a l d r a e g a e g d

k k a a e d r s k q l e d e l v s l q k k l k g t e d e 56
k k a a e d k s k q l e d d l v a l q k k l k g t e d e

l d k y s e a l k d a q e k l e l a e k k a t d a e a d 84
l d k y s e s l k d a q e k l e v a e k t a t d a e a d

v a s l n r r i q l v e e e l d r a q e r l a t a l q k 112
v a s l n r i q l v e e e l d r a q e r l a t a l t k

l e e a e k a a d e s e r g m k v i e s r a q k d e e k 140
l e e a e k a a d e s e r g m k v i e n r a s k d e e k

m e i q e i q l k e a k h i a e d a d r k y e e v a r k 168
m e l q d i q l k e a k h i a e e a d r k y e e v a r k

l v i i e s d l e r a e e r a e l s e g k c a e l e e e 196
l v i i e s d l e r t e e r a e l s e g k c s e l e e e

l k t v t n n l k s l e a q a e k y s q k e d k y e e e 224
l k t v t n n l k s l e a q a e k y s q k e d k y e e e

i k v l s d k l k e a e t r a e f a e r s v t k l e k s 252
i k v l t d k l k e a e t r a e f a e r s v a k l e k t

i d d l e d e l y a q k l k y k a i s e e l d h a l n d 280
i d d l e d e l y a q k l k y k a i s e e l d n a l n d

m t s i 284
m t s i

```

Figure 3.9 : Sequences of salmon fast muscle and rabbit alpha tropomyosins.

Sequences are from NCBI gene bank with the accession numbers of AAB34957 (rabbit, upper sequence) and AAB36559 (salmon, lower sequence). Consecutive positively charged residues with Lys/ Arg at P1 and Lys/Arg/His at P1' positions are highlighted.

Table 3.2 : Omp T susceptible sequences in rabbit skeletal alpha and salmon fast muscle tropomyosins showing P4,P3,P2,P1,P1',P2',P3',P4' positions.

cleavage site
↓

	P4	P3	P2	P1	P1'	P2'	P3'	P4'
Lys5-Lys6	Asp	Ala	Leu	Leu	Leu	Lys	Met	Asp
Lys6-Lys7	Ala	Ile	Leu	Leu	Leu	Met	Asp	Met
Lys29-Lys30	Ala/ Gly	Ala	Asp	Leu	Lys	Leu	Ala	Glu
Lys48-Lys49	Ser/ Ala	Leu	Gln	Leu	Leu	Leu	Lys	Gly
Lys76-Lys77	Leu	Ala	Glu	Leu	Leu	Leu	Leu	Asp
Arg90-Arg91	Ser	Leu	Asn	Leu	Leu	Leu	Gln	Leu
Lys152-His153	Lys	Glu	Leu	Leu	Leu	Leu	Ala	Glu
Arg160-Lys161	Asp/ Glu	Ala	Glu	Leu	Leu	Tyr	Glu	Glu
Arg167-Lys168	Glu	Val	Leu	Leu	Leu	Leu	Leu	Val

Possible Omp T cleavage sites on rabbit skeletal and salmon fast muscle tropomyosin sequences are shown with their flanking sequences (Dekker et al. 2001). Green colour indicates residues giving ~100% susceptibility at the corresponding position, while blue, yellow and red colors indicate respectively ~50%, ~30% and <5% susceptibility.

highly susceptible to the enzyme by having the most favored positively charged residue combination and highly favored P2 residues (isoleucine and lysine respectively) with the former being the highest if the residue at P2' is considered. In the latter case, although a methionine at P2' position is an unfavorable scenario, the effect should be compensated by the rest of its favored factors. One or more of the remaining four sequences can be expected to be responsible for the minor cleavages that were detected during the digestion procedure (Figure 3.5B). Possible explanations for their low reactivity as compared to the main site can be given as follows (Dekker et al. 2001): Lys48-Lys49 constitute glutamine and leucine at P2 and P2', which are less favored (Table 3.2); the Arg90-Arg91 combination is only ~50% susceptible for cleavage and also asparagine at P2 position is a less favored residue at that position (Table 3.1); Lys152-His153, although containing residues at P1, P2 and P2' that are highly preferred by the enzyme, may not be as susceptible as it appears because of the uncertainty of the fractional charge of histidine (which ionizes in the neutral pH range); Arg167-Lys168 has highly favored residues at the P1 and P2 positions, but moderately and less favored residues at the P1' and P2' positions, respectively (Table 3.2). It should also be appreciated that any influence by the residues at P3/P4/P3'/P4' also has a bearing on rendering some of these four sites more susceptible than the others.

Attention was also given to the position of the cleavage site in the heptad repeat. This revealed that five of the above positively charged sequences occupy 'f' and 'g' positions (Lys6-Lys7, Lys29-Lys30, Lys48-Lys49, Arg90-Arg91, Arg160-Lys161

Table 3.3: Omp T cleavage sites showing their positions in the heptad-repeat of the tropomyosin coiled-coil.

	Heptad-repeat position
Lys5-Lys6	<i>e - f</i>
Lys6-Lys7	<i>f - g</i>
Lys29-Lys30	<i>a - b</i>
Lys48-Lys49	<i>f - g</i>
Lys76-Lys77	<i>f - g</i>
Arg90-Arg91	<i>f - g</i>
Lys152-His153	<i>e - f</i>
Arg160-Lys161	<i>f - g</i>
Arg167-Lys167	<i>f - g</i>

The Omp T cleavage sites in tropomyosin were identified according to their position in the tropomyosin coiled-coil heptapeptide repeat. The residues at *c*, *f* and *g* are the most exposed being at the outer phase of the coiled-coil. Therefore the peptide bond between *f* and *g* position residues is the most susceptible bond to enzymatic hydrolysis.

and Arg167-Lys168) in the repeat. This is shown in Table 3.3. The 'f', 'c' and 'g' sites are the most exposed sites in the coiled-coil structure and as a result the peptide bond between 'f' and 'g' positions is the most exposed. When this information is combined with the earlier analyses, from the two cleavage sites most susceptible to Omp T, the preference of Lys6-Lys7 over Lys5-Lys6 as the main site can be rationalized, by the former being a well-exposed 'f'-'g' site while the latter is a less exposed 'e'-'f' site.

Now the next question is: 'what is the secondary Omp T cleavage site?' There are five more sites at 'f'- 'g' positions, out of which, two are resistant by virtue of their having an adjacent negative charge. Although it is not overt evidence, taking into account the Omp T preferences for different positively charged and flanking residues at the remaining three cleavage sites, then Arg167-Lys168 is the most likely secondary site. The secondary Omp T cleavage at Arg167-Lys168 is also in agreement with the mass analysis data. Cleavage at this site yields an amino-terminal fragment with a mass value of 18498.52 (residues 7-167) and a carboxy-terminal fragment (residues 168-284) with a mass of 13513.06 for rabbit skeletal tropomyosin. These are very close to the observed mass spectrometry values (m/z 18460.22 and 13517.01 respectively) of the minor fragments detected after four hours incubation of wild type rabbit skeletal tropomyosin with Omp T before the chromatographic enrichment step (data not shown).

The amino-terminal truncation can also be undertaken by expressing tropomyosin within a bacterium that contains a functional Omp T gene, such as *E. coli* JM109, but the real

strength of the method was found in the processing of hundred milligram quantities of protein obtained from a natural source (tropomyosin extracted from a muscle). In accordance with the extracellular location of Omp T, whole cells from the *E. coli* strain JM109 provide a convenient enzyme source and the proteolysis proceeds to completion in a timely fashion thereby limiting unwanted breakdown. The method of truncation by expressing tropomyosin in *E. coli* JM109 resulted in an instantaneous digestion, which is attributed to the lack of an amino-terminal acetyl group in tropomyosins expressed in bacteria. Likewise, a faster truncation was observed with unacetylated salmon fast muscle tropomyosin digested with a cell suspension of *E. coli* JM109. The same observation has previously been reported by Kluwe et al. 1995, with unacetylated rabbit skeletal tropomyosin. Therefore the above results strengthen the claim that the acetylation stabilizes the secondary structure of the first few residues at the tropomyosin amino terminus (Greenfield et al. 1994, Brown et al. 2001). Truncation by the second method, that of treating wild type (acetylated) tropomyosins with a *E. coli* JM109 cell suspension, while slower, can be taken to completion within 4 hours of reaction at 37°C. Several lines of evidence confirmed that the main product arises from cleavage of the sixth peptide bond. In addition, the slower rate of cleavage supports the protective role of the acetyl group. The second method is of greater practical significance because: (i) the product can be directly compared to the full-length protein, from which it originated and (ii) the protein is expressed and folded in a eukaryotic muscle cell rather than in a bacterial cell. Further, the ability to digest tropomyosins from a range of species including mammals,

birds and fish, by this bacterial protease Omp T, strengthens the applicability of the method.

The ability of Omp T cleaved truncated tropomyosin to form thin filaments under both high and low Ca^{2+} conditions (with rabbit) is a promising result. The result may reflect the effect of three extra residues at the amino-terminal end of Omp T-digested tropomyosin as compared to the previously truncated proteins (Cho et al. 1990, and Moraczewska and Hitchcock-DeGregori 2000). On the other hand, it may be the effect of moderate ionic strength condition used in this study as opposed to the high ionic strength conditions used in previous studies. In terms of secondary structure and thermostability, Omp T-digested tropomyosins are highly helical indicating that any functional change that would be observed with these proteins can be attributed to the sequence modification.

In conclusion, the cleavage of tropomyosin by Omp T protease is a useful one. Its ability to incorporate into thin filaments at salt concentrations, which are compatible with functional assays, permits further evaluation of the role of the conserved amino-terminal region.

Chapter 4. Binding of Omp T-digested tropomyosin to other thin filament proteins

4.1 Introduction

The goal in this section of the thesis is to investigate, in greater detail, the troponin induced binding of Omp T-digested tropomyosin to F-actin that was observed in the previous chapter (Figure 3.8). As outlined in the introduction, troponin possesses a finger-shaped domain, the amino-terminal fragment of troponin T, N-TnT, that extends all of the way from the core of the complex towards the tropomyosin overlap region. However, there is no consensus as to how much of tropomyosin is in physical contact with this section of troponin T. Some, but not all, findings are consistent with this troponin T tail making contact with the next tropomyosin in the filament (White et al. 1987, Brisson et al. 1986). In this chapter, we have addressed this question by studying the interaction of troponin and N-TnT with the Omp T-cleaved tropomyosin. As discussed in the previous chapter, binding of Omp T-digested tropomyosin to F-actin can be induced by troponin at an ionic strength of ~ 70 mM. This chapter describes the quantification of the affinity of truncated tropomyosin for F-actin under various ionic strength, salt and $[Ca^{2+}]$ conditions and in the presence of different components of the troponin complex. These experiments were carried out again with various tropomyosins from only two selected sources, rabbit skeletal and salmon fast skeletal muscles.

4.2 Results

4.2.1 Binding of truncated tropomyosin to troponin or its constituents

The interaction between tropomyosin (full-length and truncated) and troponin was initially investigated by affinity chromatography. Firstly, different tropomyosins were chromatographed over troponin-Sepharose. Secondly, the amino-terminal fragment of troponin T, N-TnT, was chromatographed over various tropomyosin-Sepharose. Proteins applied to the respective columns were eluted by a linear gradient of NaCl from 0-500mM. The conductivity values of column fractions were converted to molarity using a standard curve generated for conductivity (ms/cm) against NaCl concentration (M). The NaCl concentration of the fraction of maximal protein concentration was taken as an indication of the strength of binding to the affinity medium.

4.2.1.1 Binding to whole troponin

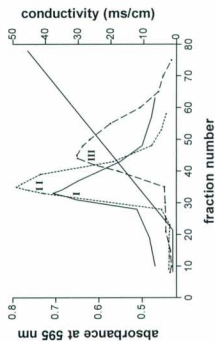
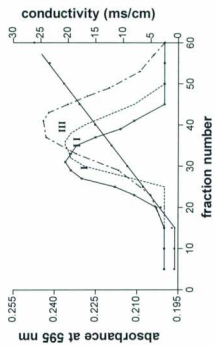
It was a consistent observation that removal of the first six amino acids of rabbit skeletal tropomyosin weakened its interaction with immobilised troponin. This was demonstrated by chromatographing a mixture comprising equal amounts of truncated and full-length proteins on the same column, followed by electrophoretic analysis of the eluant. Fractions are ordered across the gel presented in Figure 4.1A such that the salt gradient increases from left to right. The shortened-derivative of alpha-tropomyosin (lower band) is clearly seen to elute ahead of the full-length counterpart.

The availability of unacetylated tropomyosin allowed assessment of any contribution

Figure 4.1: Affinity chromatography.

Chromatography was performed in the cold (4°C). Buffer, 10mM imidazole, 0.25mM DTT, 0.01% NaN₃, pH 7; salt gradient, zero to 0.5M NaCl (total volume, 100ml); fraction volume, 1.2ml; flow rate, 0.24ml/min; amount of protein loaded, tropomyosin, 1mg and N-TnT, 0.4mg; protein detection was by Coomassie R-250 staining of electrophoresed protein and Bradford assay of the eluant. Conductivity values were converted to molarity using a standard curve of conductivity (ms/cm) vs. NaCl (M) concentration. The mean NaCl concentrations at peak elution are averages of between two and four determinations. Fractions are ordered across the gels such that the salt gradient increases from left to right.

- A) Binding of wild type and truncated rabbit skeletal tropomyosin to troponin-Sepharose. A mixture of wild type and truncated proteins was applied to the column and fractions were analyzed by 12% SDS PAGE. Column fractions were diluted 1:1 (by vol) with sample buffer and 20ul per lane was loaded: lane 1, starting sample; lanes 2-7, column fractions 32, 36, 38, 40, 42, 44 respectively (profile not shown). The arrows indicate the elution of truncated tropomyosin in earlier fractions than the wild type tropomyosin.
- B) Elution profiles of different salmon tropomyosins from troponin-Sepharose. The profiles are for separate experiments, which have been superimposed for purpose of comparison. The NaCl concentrations at peak elution: truncated tropomyosin, 0.10 ±0.002 M (I); unacetylated tropomyosin, 0.11 ±0.002 M (II) and wild type tropomyosin, 0.19 ±0.004 M (III).
- C) A mixture of wild type and unacetylated salmon tropomyosins was applied to troponin-Sepharose and fractions were analyzed by isoelectric focusing, pH gradient 4 - 6. The gel is oriented with the alkaline end as the upside (acid end, down). Column fractions were diluted 1:1 (by vol) with sample buffer and 12ul per lane was loaded: lanes 1 & 8; starting sample, lanes 2-7; column fractions 30, 34, 38, 42, 46, 50 respectively. Arrows indicate the elution of unacetylated tropomyosin (upper band) in earlier fractions as compared to the wild type tropomyosin (lower band).
- D) A mixture of unacetylated and truncated salmon tropomyosins was applied to troponin-Sepharose and fractions were analyzed by 12% SDS PAGE after diluting 1:1 (by vol) with sample buffer. 20ul per lane was loaded: lanes 1-8; column fractions 40, 42, 43, 44, 45, 46, 47, 48 respectively. Arrows indicate the elution of truncated protein (lower band) in earlier fractions than the unacetylated one (upper band).
- E) Elution profiles of N-TnT peptide from tropomyosin-Sepharose. Profiles from separate experiments have been superimposed for purpose of comparison. The NaCl concentrations at peak elution are: truncated tropomyosin, 0.10 ±0.001 M (I); unacetylated tropomyosin, 0.13 ±0.001 M (II) and wild type tropomyosin, 0.15 ±0.001 M (III).

A)**C)****D)****B)****E)**

arising from the amino-terminal acetyl group. Towards this end, various salmon fast muscle tropomyosins; full-length acetylated (wild type), full-length unacetylated (recombinant) and truncated were passed, separately, over troponin-Sepharose. The respective elution profiles appear together superimposed in Figure 4.1B for ease of comparison. Wild type protein was the most strongly bound. The chromatography profile of this tropomyosin peaked at a salt concentration of 0.19 M. The profiles of both unacetylated and truncated tropomyosins were shifted towards lower NaCl concentrations by comparison. The former eluted at 0.11 M NaCl and the latter at 0.1 M. It is evident, therefore, that the free alpha-amino group causes a significant decrease in affinity. This can be explained by the charge on the terminal group inducing the local disruption of a region (Greenfield et al. 1994 and Brown et al. 2001) containing a troponin-binding site. Comparison of the binding affinities of wild type and unacetylated tropomyosins was again attempted by co-chromatography. In this instance, the column fractions were analyzed by isoelectric focusing (Figure 4.1C). It is apparent that the unacetylated protein, which has a slightly lower pI, elutes ahead of wild type (compare Figure 4.1C, lanes 3 - 6). Further, when these two tropomyosins are loaded together in the presence of 0.12 M salt, the unacetylated protein elutes in the flow through whereas the wild type is retained (data not shown). The absence of residues 1 - 6 produces a further, but marginal, decrease in affinity. This is more evident when the unacetylated and the truncated were chromatographed together (Figure 4.1 D). As monitored by SDS PAGE analysis the truncated protein eluted before the unacetylated counterpart.

4.2.1.2 Binding to N-troponin T

Interpretation of the findings from troponin-Sepharose chromatography is complicated by the fact that tropomyosin is expected to bind to multiple sites on troponin. It was also a concern that the above results may merely be reflecting differential polymerization of wild type tropomyosin versus unacetylated and truncated tropomyosins. With these considerations in mind, the experiment was repeated but with tropomyosin as the immobilised ligand and the N-TnT fragment (residues 1 – 158 of rabbit skeletal troponin T) as the test sample. This fragment constitutes one of the major sites of tropomyosin binding in the troponin complex. In addition, in this instance, it is assumed that the immobilized tropomyosin is in the unpolymerized form as the coupling to Sepharose is carried out in the presence of 0.5M salt. The N-TnT peptide was applied to a separate affinity medium prepared using a given form of tropomyosin from salmon and eluted with a NaCl gradient as before. The superimposed profiles for separate elutions show that affinity increases in the order: truncated < unacetylated < wild type (Figure 4.1E). The peptide eluted from each column containing either wild type, unacetylated or truncated at NaCl concentrations of 0.15, 0.13 and 0.1M respectively. Thus, a contextual requirement for the first six amino acids as well as the blocking group has been demonstrated.

4.2.2 Binding of truncated tropomyosin to F-actin

4.2.2.1 Effect of whole troponin

The induction of binding of amino-terminally shortened tropomyosin to actin was investigated by sedimentation with a view to measuring the affinity of the interaction.

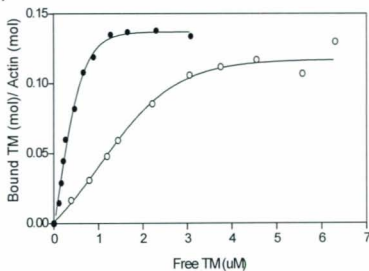
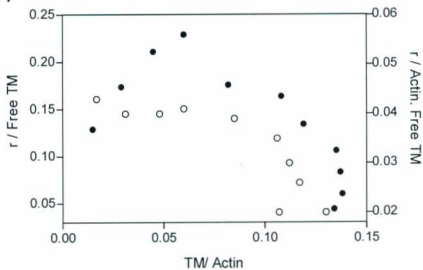
Proteins were dispersed in buffers of various ionic compositions. Binding curves were constructed by increasing the concentration of tropomyosin between 0-10 μ M, while maintaining troponin (or constituents) and F-actin concentrations constant at 2 μ M and 7 μ M, respectively. The apparent constant for the binding of tropomyosin to actin, K_a , is expressed as the reciprocal of the free tropomyosin at half saturation of the actin filaments. The following tropomyosins were included in the study: full length unacetylated salmon fast muscle tropomyosin (residues 1-284), Omp T digested salmon fast muscle tropomyosin (residues 7-284), Omp T digested rabbit skeletal tropomyosin (residues 7-284). The wild type tropomyosins were excluded due to their strong binding to actin in the presence of troponin. In the case of salmonid proteins, the sedimentation steps were performed at 4°C due to the observed temperature dependency of their binding to actin.

The F-actin binding curves of truncated tropomyosin depicted in Figure 4.2A are for experiments performed with truncated rabbit skeletal tropomyosin at an intermediate ionic strength (50 mM KCl, 5.5mM MgCl₂) in the presence of troponin and EGTA or Ca²⁺. In control experiments, (in the absence of troponin) truncated tropomyosin did not co-sediment with F-actin to any measurable extent. These data clearly show the ability of the troponin complex to restore stoichiometric binding of truncated tropomyosin to actin at both Ca²⁺ concentrations. Binding in the presence of EGTA was stronger than that with added Ca²⁺, which is reflected in the corresponding apparent binding constants of 3.9 x 10⁶ M⁻¹ and 6.2 x 10⁵ M⁻¹. The difference in binding is approximately six fold. The

Figure 4.2: The induction of binding of truncated rabbit skeletal tropomyosin to F-actin by troponin (in the presence or absence of Ca^{2+}) at 70mM ionic strength.

Buffer: 10 mM MOPS, 50 mM KCl, 5.5 mM MgCl_2 , 1 mM DTT, pH 7, and either 0.5 mM EGTA or 0.5 mM Ca^{2+} . Actin and troponin concentrations in each experiment were kept constant at 7 μM and 2 μM respectively, while tropomyosin concentration was varied. Sedimentation was performed in the Airfuge at 150,000 g for 30 min, room temperature. The sedimentation of F-actin was taken as 100% as there were no significant amounts of F-actin left in the supernatant (Figure 3.8). Curves were fit using the equation, Sigmoidal dose-response (variable slope) $Y = Y_{\text{max}} / (1 + 10^{-(\log Kd - \log X)^n})$, GraphPad Prism software (section 2.11).

- A) Binding of truncated rabbit skeletal tropomyosin (residues 7-284) in the presence of troponin (EGTA or Ca^{2+}). Filled circles, EGTA; Open circles, Ca^{2+} .
- B) Scatchard plot of data calculated directly from 'A'. Symbols used are the same as in 'A'. Left y axis denotes data with EGTA while right y axis denotes data with Ca^{2+} .
 r = bound tropomyosin / total actin.

A)**B)**

sigmoidal nature of the binding curves illustrates the presence of residual cooperativity. This is also demonstrated in the Scatchard analysis of the same data (Figure 4.2B).

The isotherms of various salmon fast muscle tropomyosins under the same ionic conditions are presented in Figure 4.3. The weakened affinity for actin when the first six residues of tropomyosin are removed is clearly evident. Unacetylated tropomyosin showed a stronger affinity to actin than the truncated tropomyosin, which is reflected by their K_a values of $2.9 \times 10^7 \text{ M}^{-1}$ and $5.0 \times 10^6 \text{ M}^{-1}$ respectively in the presence of EGTA (Figure 4.3A). The actin affinities of the two truncated proteins appeared not significantly different from each other. At high Ca^{2+} concentrations, the calcium sensitivity of tropomyosin binding to actin was again evident but only the full-length protein showed saturated binding to actin (K_a , $1.0 \times 10^7 \text{ M}^{-1}$) at least under the tested tropomyosin concentration range (Figure 4.3B). These results suggest that the F-actin affinity of truncated tropomyosin from salmon is weaker than that from rabbit.

To test the effect of ionic strength, experiments were performed using buffers of differing composition. Binding carried out using a lower ionic strength buffer, 5.5 mM MgCl_2 and 5mM KCl (ionic strength, 26.5 mM), with the rabbit protein, showed apparent binding constants of $5.3 \times 10^6 \text{ M}^{-1}$ and $1.3 \times 10^6 \text{ M}^{-1}$ in the presence of EGTA and Ca^{2+} , respectively (Figure 4.4A) which is twice as strong as the binding at 70 mM ionic strength (Figure 4.2A). The experiments were repeated in a higher salt buffer, 140 mM

Figure 4.3: The induction of binding of various salmon fast muscle tropomyosins to F-actin by troponin (in the presence or absence of Ca^{2+}) at 70mM ionic strength.

Buffer: 10 mM MOPS, 50 mM KCl, 5.5 mM MgCl_2 , 1 mM DTT, pH 7, and either 0.5 mM EGTA or 0.5 mM Ca^{2+} . Actin and troponin concentrations in each experiment were kept constant at 7 μM and 2 μM respectively, while tropomyosin concentration was varied. Sedimentation was performed in a TLA 100.2 (Beckman) ultracentrifuge at 150,000 g for 45 min, 4°C. Curves were fit as in Figure 4.2.

- A) Binding of salmon fast muscle tropomyosins in the presence of Tn (EGTA). Squares, unacetylated; circles, truncated (residues 7-284).
- B) Binding of salmon fast muscle tropomyosins in the presence of Tn (Ca^{2+}). squares, unacetylated; circles, truncated (residues 7-284).

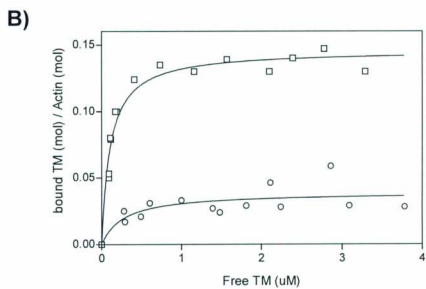
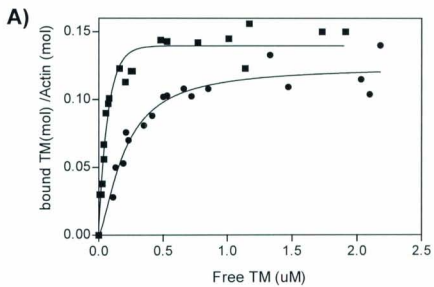
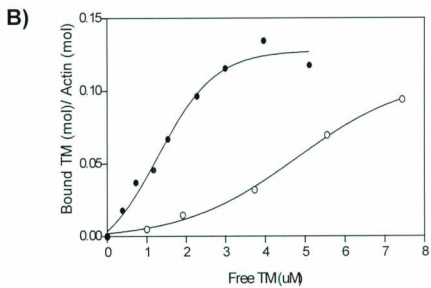
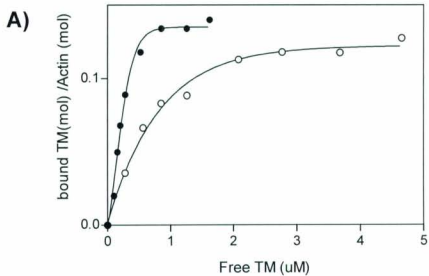


Figure 4.4: The effect of ionic strength on the induction of binding of rabbit truncated tropomyosin to F-actin by troponin (in the presence or absence of Ca^{2+}).

Buffer: 10 mM MOPS, 5mM/ 140mM KCl, 5.5 mM MgCl_2 , 1 mM DTT, pH 7, and either 0.5 mM EGTA or 0.5 mM Ca^{2+} . Actin and troponin concentrations in each experiment were kept constant at 7 μM and 2 μM respectively, while tropomyosin concentration was varied. Sedimentation was performed in TLA 100.2 (Beckman) ultracentrifuge at 150,000 g for 45 min, 4°C for salmon tropomyosins and in the airfuge at 150,000 g for 30 min, room temperature for rabbit skeletal tropomyosin. Curves were fit as in Figure 4.2.

- A) Binding in the presence of 5mM KCl and Tn (EGTA or Ca^{2+}). Filled circles, EGTA; Open circles, Ca^{2+} .
- B) Binding in the presence of 140mM KCl and Tn (EGTA or Ca^{2+}). Filled circles, EGTA; Open circles, Ca^{2+} .



KCl, 5.5 mM MgCl₂, 10mM MOPS pH 7 (ionic strength, 163 mM) (Figure 4.4B). This is equivalent to the ionic conditions used in a previous study involving chicken and rat skeletal muscle tropomyosin lacking the first nine residues (Cho et al. 1990, and Moraczewska and Hitchcock-DeGregori 2000). Raising the concentration of neutral salt also weakened induction in our system. With added EGTA, the apparent binding constant was approximately five fold reduced to a value of $7.6 \times 10^5 \text{ M}^{-1}$, compared to an ionic strength of 70mM. With added Ca²⁺, binding was too weak and saturation was not attained within the tropomyosin concentration range used in the study.

Interestingly, when neutral salt is replaced with an equivalent amount of potassium acetate (140mM), the isotherms shifted leftward and stoichiometric binding is achieved under both Ca²⁺ conditions (Figure 4.5). In the presence of EGTA, the K_a was $3.1 \times 10^6 \text{ M}^{-1}$, which is four times stronger than that observed in the presence of KCl. With added Ca²⁺ binding was observed to saturation with an apparent K_a of $3.6 \times 10^5 \text{ M}^{-1}$ confirming that the binding is now stronger. The sigmoidal binding curves further reflected the fact that the binding was cooperative.

4.2.2.2 Effect of troponin sub-components troponin I and N-troponin T

Next we investigated whether or not sub-components of troponin could restore binding of OmpT digested tropomyosin to F-actin (Figure 4.6). Proteins were dispersed in 70 mM ionic strength buffer as per Figure 4.2. Two experiments were performed: in the presence of troponin I, TnI, alone; and in the presence of TnI and N-TnT. The unacetylated

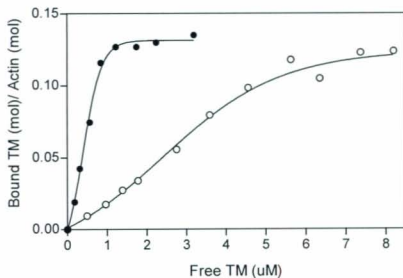
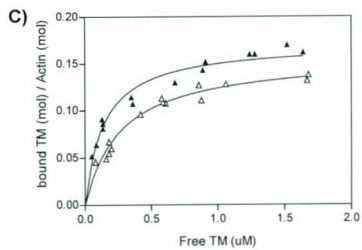
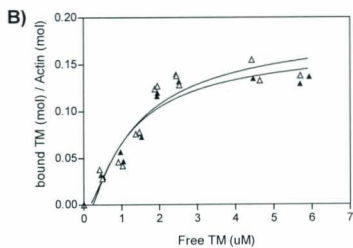
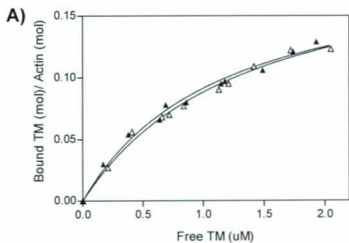


Figure 4.5: The effect of potassium acetate on the induction of binding of truncated rabbit skeletal tropomyosin to F-actin by troponin (in the presence or absence of Ca^{2+}).

Buffer: 10 mM MOPS, 140 mM KAc, 5.5 mM MgCl_2 , 1 mM DTT, pH 7, and either 0.5 mM EGTA or 0.5 mM Ca^{2+} . Actin and troponin concentrations in each experiment were kept constant at 7 μM and 2 μM respectively, while tropomyosin concentration was varied. Sedimentation was performed in the Airfuge at 150,000 g for 30 min, room. Filled circles, EGTA; Open circles, Ca^{2+} . Curves were fit as in Figure 4.2.

Figure 4.6. The effects of troponin I and N-troponin T on binding of truncated tropomyosin to F-actin.

Buffer: 10 mM MOPS, 50 mM KCl, 5.5 mM MgCl₂, 1 mM DTT, pH 7. Actin and troponin subcomponents were kept constant at 7 uM and 2uM respectively, while tropomyosin concentration was varied. Sedimentation was performed in TLA 100.2 (Beckman) ultracentrifuge at 150,000 g for 45 min, 4°C for salmon tropomyosins and in the airfuge at 150,000 g for 30 min, room temperature for rabbit skeletal tropomyosin. Actin, tropomyosin and troponin I (filled triangles), Actin, tropomyosin, troponin I and amino-terminal fragment of rabbit skeletal troponin T (N-TnT, residues 1-158) (open triangles). A), truncated rabbit skeletal tropomyosin; B), truncated salmon tropomyosin; C), unacetylated salmon tropomyosin. Curves were fit using the equation, One site binding (hyperbola) $Y = B_{max} * X / (K_d + X)$, GraphPad Prism software.



salmon fast muscle tropomyosin here served as the control. As was noted in a parallel set of experiments performed with carboxy-terminally shortened tropomyosin, which had been digested with carboxypeptidase-A to remove eleven residues (Heeley et al. 1987), troponin I by itself can restore interaction of Omp T digested rabbit skeletal tropomyosin with F-actin (K_a , $1.07 \times 10^6 \text{ M}^{-1}$) (Figure 4.6A). When the soluble amino-terminal chymotryptic peptide of troponin T, N-TnT, is included in the assay mixture (ie F-actin + tropomyosin res. 7-284 + troponin I + N-TnT, 70mM ionic strength) the isotherm is virtually superimposable to the one generated with troponin I alone (Figure 4.6A). A similar result was observed for truncated (7-284) salmon tropomyosin as well (Figure 4.6B). The measured apparent binding constants in the presence of TnI alone and TnI + N-TnT were $\sim 0.8 \times 10^6 \text{ M}^{-1}$. This is an interesting result because the peptide enhanced the effect of troponin I for inducing tropomyosin binding to F-actin in the case of carboxy-terminally shortened tropomyosin, which is intact at the amino-terminal end (Heeley et al. 1987). Like the carboxypeptidase-treated tropomyosin, the control experiment also showed stronger binding to F-actin when TnI and the N-TnT peptide were present together (K_a , $1 \times 10^7 \text{ M}^{-1}$) than if TnI was present alone (K_a , $4.2 \times 10^6 \text{ M}^{-1}$) (Figure 4.6C). This observation therefore implies that in the case of truncated tropomyosin, the interaction between N-TnT and the tropomyosin overlap has been weakened such that it does not accentuate the interaction.

4.3 Discussion

In two previous studies to elucidate the significance of the tropomyosin amino-terminal region for F-actin binding, two mutants lacking the first nine amino acids were prepared respectively using chicken and rat striated muscle tropomyosin cDNA (Cho et al. 1990, and Moraczewska and Hitchcock-DeGregori 2000). With the former protein, F-actin binding was not observed under any tested condition (Cho et al. 1990) while with the latter one binding was observed in the presence of whole troponin and added EGTA but not added Ca^{2+} (Moraczewska and Hitchcock-DeGregori 2000). The presence of extra amino acids in the tropomyosin product prepared by Omp T cleavage, therefore, prompted us to revisit the problem of preparing thin filaments with amino-terminally shortened muscle tropomyosin. Working with solutions of moderate ionic strength ($\sim 70\text{mM}$) and micromolar amounts of protein, we observed full incorporation of tropomyosin (res 7-284) into thin filaments, both in the presence of added Ca^{2+} , as well as added EGTA (Figure 4.2). This finding has also permitted evaluation of the functional consequence of removing this half of the overlap as will be discussed in chapter 5.

To reconcile our results with the previously published work (Cho et al. 1990, and Moraczewska and Hitchcock-DeGregori 2000), we repeated the sedimentation experiments in a compatible buffer having the same ionic strength, 163mM , as in those studies. Under these conditions (and micromolar protein), thin filament reconstitution is successful only at low $[\text{Ca}^{2+}]$ (Figure 4.4B). The apparent binding constant obtained at

low $[Ca^{2+}]$, $\sim 7.6 \times 10^5 M^{-1}$, is also in agreement with what was reported for the slightly shorter tropomyosin product (Moraczewska and Hitchcock-DeGregori 2000) (rabbit, $7.6 \times 10^5 M^{-1}$; rat, $7.1 \times 10^5 M^{-1}$). Interestingly, the ionic strength dependency can be managed by manipulation of the buffer composition. By replacing chloride with acetate it is feasible to prepare thin filaments in a buffer of 'physiological' ionic strength containing millimolar Ca^{2+} (Figure 4.4C). A possible explanation for the differential effect of these two ions comes from their positioning in the Hofmeister series, where acetate exists more towards the end of protein stabilizing ions than chloride (Kunz et al. 2004). Therefore, at a concentration of 140mM, chloride may be acting as a chaotrope while acetate as a kosmotrope, thereby yielding respectively unfavourable and favourable effects on thin filament protein interactions. Collectively, these findings indicate that the concentration and nature of the salt employed in the binding buffer is more important than the number of subtracted amino-terminal residues.

One approach to working out the details of the association between tropomyosin and troponin T has been the use of large fragments in conjunction with chromatographic methods [Mak and Smillie 1981b, Pato et al. 1981 and Pearlstone and Smillie 1982]. These experiments shed considerable light on the respective surfaces of interaction. It was demonstrated that whereas the carboxy-terminal half of troponin T docks near to the center of tropomyosin, the remainder of the molecule, the so-called 'tail', runs along the carboxy-terminal one third of tropomyosin. The question of how far the 'tail' extends along tropomyosin is not precisely known. However, there is reason to assume that it

spans the overlap site and attaches to the next tropomyosin in the filament, in effect forming a bridge (Pato et al. 1981a; Brisson et al. 1986; White et al. 1987). One line of supporting evidence is provided by the study of White et al. 1987 in which N-TnT was observed by X-ray diffraction to cover the first 10-15 amino acids of glutaraldehyde-fixed crystals of tropomyosin. The ability to remove the first six amino acids from tropomyosin afforded an opportunity to repeat some of the earlier chromatography experiments. Affinity chromatography was performed two ways. Firstly, by chromatographing tropomyosin on troponin-Sepharose (Figure 4.2B) and secondly, by chromatographing a soluble fragment of troponin T that comprises most of the tail on tropomyosin-Sepharose (Figure 4.2D). In both instances, we observed that any change in the amino-terminal region of tropomyosin, whether it be the loss of the acetyl group or the hexapeptide, weakened the affinity of interaction. These findings add to the body of evidence, which suggests that this part of tropomyosin, which requires the blocking group to stabilize it conformationally, 'participates' in troponin T binding.

This proposal also fits nicely with the results of the F-actin binding studies of Omp T-digested tropomyosin in the presence of troponin subunits. The shortened tropomyosin associated with F-actin in the presence solely of troponin I (Fig. 4.6). Troponin I has a substantial effect in inducing tropomyosin binding to actin by having interactions with both actin and tropomyosin (Mak et al. 1983, Heeley et al. 1987). However, whereas the N-TnT fragment enhanced the effect of sub-saturating amounts of troponin I in the case of carboxypeptidase-treated tropomyosin (Heeley et al. 1987), it is ineffectual in the case

of the product of Omp T digestion (Figure 4.6). As mentioned above, there is reasonable evidence to assume that the troponin T subunit bridges the overlap making contact with the next tropomyosin in the filament. If it does, the attachment at the amino-terminal region of tropomyosin would contribute only a fraction of the total binding surface. Therefore one can expect that the disruption of this end of the protein would have a greater impact on forming this tertiary complex than deleting the opposite end. If the first six amino-terminal residues have a significant contribution for the interaction between tropomyosin amino terminus and the N-TnT peptide, then the lack of potentiation effect of N-TnT can be accounted for by the inability to form the tertiary overlap structure at the ends of Omp T-digested tropomyosin molecules. In the case of carboxypeptidase-treated tropomyosin, therefore, the bridge can still be formed by N-TnT binding to its residual binding sites at the intact amino terminus and shortened carboxy terminus. Overall, the data strongly agree with the idea that the conserved tropomyosin amino terminus constitutes a binding surface for N-TnT peptide.

F-actin binding of amino-terminally truncated tropomyosin from rabbit also bears comparison with that of carboxypeptidase-treated protein (Heeley et al. 1987). First, both shortened tropomyosins bind to actin with similar affinity in the presence of troponin (EGTA), K_a 4.6×10^6 M^{-1} . Second, calcium weakens the binding in both instances, but more so for the product which has been processed at the amino-terminal end (K_a : Carboxypeptidase-treated, 3.0×10^6 M^{-1} ; Omp T-digested, 6.2×10^5 M^{-1}). This is an interesting result in view of the fact that the number of subtracted amino acids from the

amino end is only half of that from the carboxyl end (six and eleven respectively). In addition, at an ionic strength of 163 mM, the F-actin affinity of tropomyosins lacking the last nine or eleven residues was higher than that of the protein lacking residues from the opposite end (Moraczewska and Hitchcock-DeGregori 2000; Mak et al. 1983). These results support the idea that the amino-terminal end has a greater influence on the affinity of tropomyosin to F-actin than the carboxyl end (Moraczewska and Hitchcock-DeGregori 2000). A clue to understanding this distinction is obtained when induction of tropomyosin binding to F-actin is attempted with individual components of troponin (Figure 4.6 and Heeley et al. 1987). The troponin T tail has no induction towards the Omp T-digested tropomyosin binding to F-actin. The greater difference between the two tropomyosins with whole troponin (Ca^{2+}) can be explained by the tighter binding of troponin I and troponin T to troponin C and the weaker binding of these subunits to actin and tropomyosin: therefore the induction of tropomyosin binding to F-actin by the head region of troponin is reduced.

With regard to truncated salmon tropomyosin, it appears this particular variant has a weaker affinity to F-actin in the presence of high Ca^{2+} concentrations (Figures 4.3B) as compared to rabbit skeletal tropomyosin. We also observed weaker binding of this protein to F-actin when the experiments were performed at room temperature even under 70mM ionic strength and with troponin (EGTA). This can be rationalized on the basis of its having a local unfolding transition occurring at $\sim 24^{\circ}\text{C}$, in a region within the fifth actin binding period (see Chapter 6), which has been found to have the greatest influence

on F-actin affinity out of the five internal actin binding periods. Further, this particular isoform has destabilized regions in both halves of its sequence as compared to the rabbit skeletal tropomyosin (see Chapter 6). The differences in the F-actin binding between these truncated molecules can be attributed to the different conformational stabilities of native rabbit skeletal and salmon fast skeletal tropomyosins as reflected by isomorphisms at key positions of their sequence (discussed in Chapter 6).

Chapter 5. Effects of removal of the amino-terminal six amino acids of tropomyosin on the regulatory properties and myosin binding of the striated muscle thin filament

5.1 Introduction

The ability to prepare thin filaments with Omp T-digested tropomyosin as a constituent, as demonstrated in the previous chapter, has permitted examination of the functional role of the amino-terminal region of tropomyosin. As discussed earlier, full binding of this tropomyosin to F-actin can be obtained under both low and high calcium concentrations. In this chapter, we have evaluated the myosin ATPase regulatory properties of amino-terminally truncated tropomyosin as compared to native tropomyosin. The affinity of myosin-S1 to thin filaments containing each tropomyosin was also investigated.

5.2 Results

5.2.1 Activation of myosin subfragment 1.

The steady state activation of myosin-S1 MgATPase activity by thin filaments containing Omp T digested truncated tropomyosins was performed as a function of tropomyosin, myosin-S1 and thin filament concentration. Thin filaments comprised of wild type protein served as the control. Each comparison between the two tropomyosins was performed on the same day with the same proteins. The experiments were carried out in a low ionic strength buffer containing 4.5 mM MgCl₂ and zero salt at which protein

interactions would be much stronger. In addition, only the rabbit skeletal tropomyosins were used in the study since truncated tropomyosin from salmon fast could not be incorporated into thin filaments under high Ca^{2+} concentrations and micromolar protein concentrations (Figure 4.3B).

5.2.1.1 Effect of varying tropomyosin concentration

In Figure 5.1, relative ATPase activity is plotted as a function of the concentration of tropomyosin (either truncated or full-length). In this experiment, troponin, actin and myosin-S1A1 concentrations were kept constant at a molar ratio of 1.5: 5: 1 μM while the tropomyosin concentration was varied from 0-6 μM . This molar ratio of S1: actin is such that the association of regulatory proteins with actin brings about a net inhibition of the steady-state MgATP hydrolysis rate (Eaton 1976, Williams et al. 1984, Lehrer and Morris 1984). Relative ATPase activities were calculated by normalizing ATPase activities (nmol/s) at varying protein combinations to the ATPase activity of actin-S1 alone.

Troponin is known to inhibit the ATPase rate by itself in the absence of tropomyosin (Eaton et al. 1975). It has a greater effect at high pCa than at low (~50% inhibition with EGTA and ~20% inhibition with Ca^{2+} , i.e. 80% acto-S1 activity). Gradually raising the concentration of tropomyosin (either wild type or truncated) is seen to enhance the effect

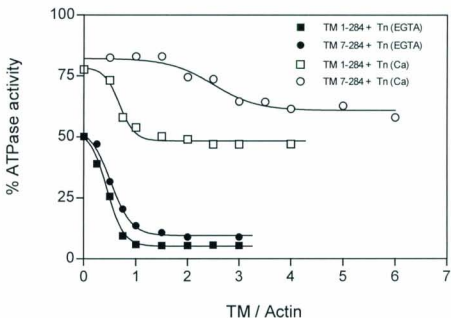


Figure 5.1. Comparison of regulatory properties of thin filaments containing either truncated or wild type rabbit skeletal tropomyosin.

Buffer: 10 mM MOPS, 4.5 mM $MgCl_2$, 1 mM DTT, pH 7, an either 0.5 mM Ca^{2+} or 0.5mM EGTA (ionic strength, 63mM); T, 25°C. Myosin-S1, actin and troponin were employed at 1 μ M, 5 μ M and 1.5 μ M respectively, while tropomyosin was varied in concentration. All rates are expressed relative to the MgATPase activity of actin-S1 alone (100% = .042 nmol/s). Activities were corrected for the rate of S1 alone. Filled circles and squares, EGTA; open circles and squares, Ca^{2+} ; squares, wild type tropomyosin; circles, truncated tropomyosin. Curves were fit using the equation, Sigmoidal dose-response (variable slope) $Y = B_{max} / (1 + 10^{(\log Kd - \log X) * n})$, GraphPad Prism software (section 2.11).

of troponin in the presence of EGTA. At saturation, this inhibition was approximately 95 % with wild type tropomyosin and approximately 90 % with truncated tropomyosin (Figure 5.1). In both instances, maximum inhibition was achieved at roughly stoichiometric concentrations of tropomyosin to actin (1 μ M: 7 μ M). Slightly less inhibition was observed for the thin filament containing truncated tropomyosin than for those containing the full-length counterpart. When Ca^{2+} was added to the assay buffer, inhibition is released but to different extents. Titration with wild type tropomyosin yielded a final percentage inhibition of approximately 50 % (Figure 5.1). Interestingly, maximum inhibition attained with truncated tropomyosin was only 35 % (Figure 5.1). Also apparent is the fact that more of the truncated protein (approximately 4/7ths of actin concentration) is required to reach the end point of the titration. This is presumably due to the weaker induction by troponin (Ca^{2+}) as shown in Chapter 4 (Figures 4.2 and 4.4).

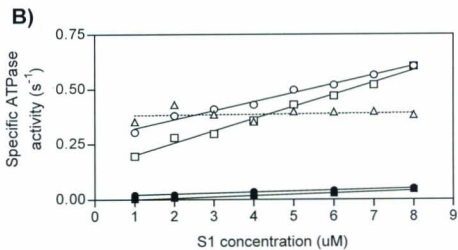
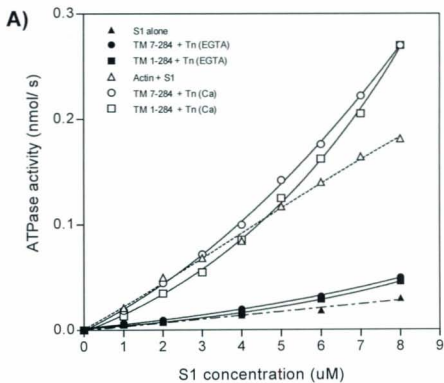
5.2.1.2 Effect of varying myosin-S1 concentration

At low concentrations of regulated actin, activation of myosin-S1 MgATPase shows cooperative dependence on the myosin-S1 concentration, for which tropomyosin is essential (Murray et al. 1982; Bremel et al. 1972; Lehrer and Morris 1982). Specifically, at low S1: actin ratios tropomyosin inhibits the actomyosin ATPase activity while at high S1: actin ratios it potentiates the ATPase activity. To study the importance of the amino-terminal region in this phenomenon, the same experiment was performed with thin filaments containing Omp T-digested tropomyosin. Again, wild type tropomyosin served as a control.

The experiment was performed with myosin-S1 concentrations increasing from 1 to 8 μM while actin, tropomyosin and troponin were kept at 4 μM , 2.3 μM and 1.15 μM respectively. A tropomyosin concentration of 4/7 that of actin (4 μM) was used in order to ensure full binding of truncated tropomyosin to F-actin in the presence of high Ca^{2+} , because under these conditions the induction by troponin is weaker (as is reflected in Figure 5.1 and F-actin binding in 5.5 mM MgCl_2 and 5mM KCl buffer (Figure 4.4A)). The results for this ATPase experiment are shown in Figure 5.2A. In the presence of troponin and tropomyosin (wild type or truncated) and added EGTA, inhibition was observed at all concentrations of S1 tested (0-8 μM). In the presence of Ca^{2+} , both tropomyosins inhibited myosin-S1 MgATPase activity at low S1: actin molar ratios and potentiated it at high S1: actin molar ratios (Figure 5.2A). As reflected by the myosin-S1 concentration at which the regulated activity intersects the unregulated activity, filaments containing truncated tropomyosin commence potentiation at a lower myosin-S1 (2 μM) concentration than the filaments containing the full-length protein (4.5 μM). With truncated tropomyosin, the ATPase activity remained higher than that of wild type tropomyosin up to a S1 concentration of 8 μM , at which activations by both systems were equal (Figure 5.2A). This observation suggests that the cooperativity in the system in response to increasing S1 concentration is reduced, when truncated tropomyosin replaces the full-length molecule. The less pronounced curvature evident in Fig 5.2A and the line with a shallower gradient in Figure 5.2B for truncated tropomyosin as compared to the wild type, also reflect the same idea.

Figure 5.2. Activation of myosin-S1 by different thin filaments as a function of myosin-S1 concentration.

Buffer: 10 mM MOPS, 4.5 mM $MgCl_2$, 1 mM DTT, pH 7, and either 0.5 mM Ca^{2+} or 0.5 mM EGTA; T, 25°C. Actin, tropomyosin and troponin concentrations in each experiment were kept constant at 4 μ M and 2.3 μ M and 1.15 μ M, respectively, while myosin-S1 concentration was varied. A) MgATPase activity as a function of myosin-S1 concentration. B) Data shown in 'A' are expressed as specific activity and corrected for the rate of S1 alone. Filled circles and squares: EGTA; open circles and squares: Ca^{2+} ; squares, wild type tropomyosin; circles, truncated tropomyosin; open triangles, unregulated actin; closed triangles, myosin-S1 alone. Curves in 'A' were fit as in Figure 5.1



5.2.1.3 Effect of varying thin filament concentration

Regulation was investigated further by determining the thin filament concentration-dependence of the steady-state rate of ATP hydrolysis (Figure 5.3). In this case, the myosin-S1 concentration was kept constant at 0.25 μM and the concentration of thin filaments reconstituted with either wild type or truncated tropomyosin was increased from zero to 70 μM (by the concentration of actin). The consequence of trimming the amino-terminal region is clearly evident in this experiment (Figure 5.3). Over this concentration range, thin filaments (Ca^{2+}) containing the shortened tropomyosin produce about two-fold greater myosin activation than the control. Extrapolation of the curves demonstrates that the effect is primarily on V_{max} ; 6.8 s^{-1} (control), 16 s^{-1} (tropomyosin 7 – 284) with little, if any, change in myosin binding affinity ($\sim 5 \times 10^4 \text{ M}^{-1}$). It should be noted that comparison of the two types of thin filaments was performed on the same day. In addition, sedimentation analysis showed that F-actin remains saturated with regulatory proteins in the presence of myosin-S1, MgATP and added Ca^{2+} (data not shown). Thus, the difference in activation can not be attributed to dissociation. In the presence of EGTA, the two systems produced an equivalent level of inhibition.

5.2.2 Myosin-S1 binding to thin filaments containing truncated or full-length tropomyosin.

Binding of S1-ADP to thin filaments involved first separating actin-S1 from unbound S1 by sedimentation and then measuring the free S1 concentration in the supernatant using

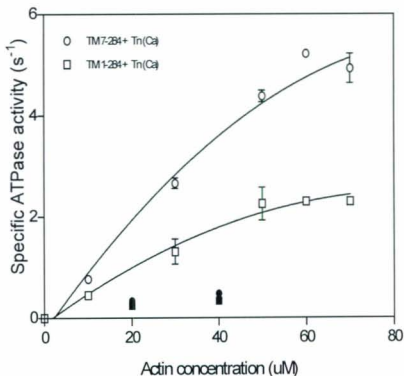


Figure 5.3. Dependence of the actomyosin MgATPase activity on the concentration of thin filaments containing either truncated or intact tropomyosin.

Buffer: 10 mM MOPS, 4.5 mM MgCl₂, 1 mM DTT, pH 7, and either 0.5 mM Ca²⁺ or 0.5 mM EGTA; T, 25°C. Myosin-S1 concentrations in each experiment were kept constant at 0.5 μM. Actin, troponin and tropomyosin concentrations were varied. At each actin concentration, the molar ratio of actin: troponin: tropomyosin was maintained at 7: 2: 4. Activities were corrected for the rate of S1 alone. Filled circles and squares: EGTA; open circles and squares: Ca²⁺; squares, wild type tropomyosin; circles, truncated tropomyosin. Curves were fit using the equation, One site binding (hyperbola) $Y = B_{max} * X / (K_d + X)$, GraphPad Prism software.

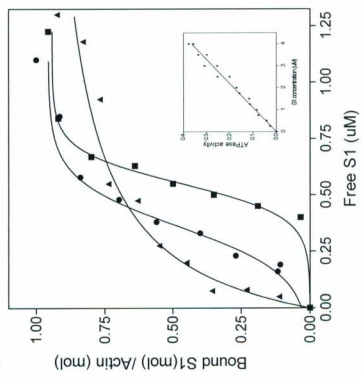
the ammonium ATPase activity of myosin-S1 (see inset to Figure 5.4A). Again, only rabbit proteins were used since thin filaments could not be formed with truncated salmon fast muscle tropomyosin at high Ca^{2+} and micromolar amounts of protein. Binding was measured in the presence of both high and low Ca^{2+} . The results are shown in Figure 5.4.

Binding of S1-ADP to unregulated F-actin was non-cooperative as indicated by the hyperbolic binding curve with a binding constant of $4 \times 10^6 \text{ M}^{-1}$. In the presence of EGTA, the sigmoidal curves show that the interaction of the ligand to each type of thin filament is cooperative (Figure 5.4A). However, as judged by the steepness of the binding curves, it appears binding to the filaments containing full-length protein is more cooperative than the binding to the ones containing truncated protein (Hill coefficients; 3.8 and 3.1 respectively). The apparent binding constants to the two types of filaments were; $2.7 \times 10^6 \text{ M}^{-1}$ (control) and $3.7 \times 10^6 \text{ M}^{-1}$ (truncated). It was a consistent observation that S1-ADP showed slightly stronger affinity towards the thin filaments containing truncated tropomyosin as compared to the full-length counterpart. However, in the presence of added Ca^{2+} no detectable differences in cooperativity or apparent binding constants were evidenced in the two isotherms (Figure 5.4B) (K_a : Full-length, $6.33 \times 10^6 \text{ M}^{-1}$; truncated, $6.25 \times 10^6 \text{ M}^{-1}$), indicating that the substitution of truncated tropomyosin for wild type did not significantly affect S1-ADP binding to regulated F-actin.

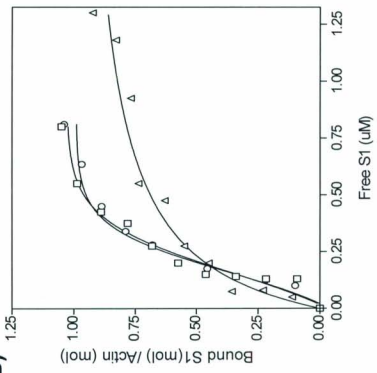
Figure 5.4: Binding of myosin-S1 to thin filaments containing truncated or full-length rabbit skeletal tropomyosins.

Buffer 5.5 mM MgCl₂, 50mM KCl, 10mM Imidazole, 3mM MgADP, 20mM myokinase inhibitor, 1mM DTT, pH7, and either 0.5mM EGTA or 0.5 mM Ca²⁺. Actin, tropomyosin and troponin were kept constant at 4.0uM, 2.28uM and 2.28uM while myosin-S1 varied from 0 to 5uM. The samples were incubated at 4°C for 1hr and centrifuged in the Airfuge for 30min at 150,000 x g. The supernatant was subjected to NH₄/EDTA ATPase activity of free S1 at 25°C. A), EGTA; B), Ca²⁺; squares, wild type tropomyosin; circles, truncated tropomyosin; triangles, unregulated actin. Free myosin-S1 concentration was obtained using a standard curve generated for NH₄/EDTA ATPase activity of myosin-S1 against S1 concentration (inset in A). The 'bound S1/Actin' values for the plots in the presence of EGTA have been normalized to one. Curves for regulatory actin were fit as in Figure 5.1, and curves for unregulatory actin were fit as in Figure 5.3.

A)



B)



5.3 Discussion

Elucidating the functional properties of an amino-terminally shortened tropomyosin has not been previously possible as a consequence of the inability to incorporate such a protein into thin filaments at low pCa. As outlined in the previous chapter, we have been able to devise conditions to reconstitute thin filaments with amino-terminally truncated tropomyosin at both high and low Ca^{2+} concentrations. Thus, we have been able to characterize how truncated tropomyosin molecules, lacking the amino-terminal ends can function in a thin filament complex in the presence or absence of Ca^{2+} .

On the issue of regulation, results obtained for the ATPase activity measured as a function of tropomyosin concentration (Figure 5.1) with the wild type protein were similar to those described by other workers on the basis of percentage maximal inhibition and stoichiometries of the proteins required to achieve maximal inhibition (Bremel et al. 1972; Lehrer and Morris 1982; Murray et al. 1981; Eaton et al. 1975; Williams et al. 1985; Heeley et al. 1989). When wild type tropomyosin was replaced with truncated tropomyosin, at low Ca^{2+} , very little difference between the two proteins was observed in their abilities to accentuate inhibition by troponin. A similar result was observed over a range of S1 concentrations or thin filament concentrations. However, at high Ca^{2+} the ATPase activity of the system with truncated tropomyosin was significantly above that of the system with wild type protein. This is a very interesting result. It is the opposite of what was seen with carboxypeptidase-treated tropomyosin, which showed reduced

ATPase activity as compared to the wild type counterpart (Heeley et al. 1989a). Opposite effects on the regulatory properties by removing the two ends may reflect their having different roles in thin filament assembly and function.

The Omp T-digested tropomyosin showed higher activation than the native protein at molar ratios of S1: actin below 8 μ M: 4 μ M (Figure 5.2). At molar ratios above that, ATPase activity with wild type tropomyosin appeared to exceed that of truncated tropomyosin. This can be explained in terms of the reduced cooperativity in the potentiation effect with increasing S1 concentrations by truncated tropomyosin as compared to the wild type tropomyosin. The result that reduced cooperativity occurred with truncated tropomyosin containing systems was expected, since Omp T digestion may have interrupted a line of continuity within the thin filament, which is involved in long-range communication between functional units (Edwards and Sykes 1978; 1980; 1981; Graceffa and Lehrer 1980). Despite this fact, the regulated actin filaments containing truncated tropomyosin were able to potentiate actomyosin ATPase with some degree of retained cooperativity either because of the communication that can still occur through tropomyosin within one thin filament unit or because of the communication that occurs through actin filaments (Butters et al. 1993, Tobacman and Butters 2000).

The effect of amino-terminal truncation on Ca²⁺ induced myosin-S1 ATPase activity was more pronounced in the thin filament titrations (Figure 5.3). Thin filaments (Ca²⁺) composed of tropomyosin missing the amino-terminal hexapeptide, produced twice as

much myosin activation than the control. The primary effect was a change in the V_{max} of the ATPase reaction with no significant change in apparent binding constant. This suggests, that at high Ca^{2+} , the absence of first six residues in tropomyosin causes an equilibrium shift in the regulatory units more towards the turned-on (open) state. A simple explanation to rationalize the results would be: since N-TnT has been shown to exert a tropomyosin-dependent inhibition of actomyosin MgATPase, by stabilizing the turned-off (blocked) state of thin filament (Nakamura et al. 1981; Onoyama and Ohtsuki 1986; Heeley 1994; Tobacman et al. 2002), it follows that it would be less effective in this capacity when the first six amino acids of tropomyosin are absent because the interaction between N-TnT and Omp T-digested tropomyosin has been disrupted (discussed in Chapter 4). This lesser inhibition observed in the system constituted with truncated tropomyosin therefore yields a greater activation than the system with wild type protein. In this regard, tropomyosin phosphorylated at Serine₂₈₃, bears some degree of resemblance to the Omp T-digested tropomyosin. The phosphorylated molecule also showed higher activation when reconstituted in to thin filaments, as well as lesser inhibition with N-TnT peptide than if the modification was absent (Heeley 1994, Heeley et al. 1989). However, in this case, the latter effect cannot be attributed to the same explanation mentioned above, that is to the weakened affinity of phosphorylated tropomyosin to N-TnT, since both phosphorylated and unphosphorylated proteins showed equal affinities to N-TnT fragment (Heeley et al. 1989). The alternative (or an additional) explanation is therefore, that the amino-terminal region of tropomyosin could itself be

inhibitory: thus, removal of this element fully or partly causes reduced amounts of inhibition.

A result that is opposite to that of carboxypeptidase-treated tropomyosin was observed with Omp T-digested tropomyosin in S1-ADP binding experiments to thin filaments (Figure 5.4 and Pan et al. 1988). Myosin-S1 showed higher affinity to filaments with tropomyosin lacking amino-terminal residues than ones lacking carboxy-terminal residues (Pan et al. 1988). In addition, it is consistent with the suggestion that the removal of the first six residues causes the regulatory thin filaments to shift more towards the open state in correlation with the ATPase experiment results. The effect of troponin to keep tropomyosin filaments in the turned-off (blocked) state, in other words the amount of inhibition, seems to be reduced in the case of Omp T-digested tropomyosin-containing system. Therefore, binding of S1-ADP is more favored. However, it should also be mentioned that the results from these two lines of experiments might not be directly linked with each other, due to the fact that myosin-S1-ADP is not the true substrate in the ATPase experimental system. It is either myosin-S1-ATP or myosin-S1-ADP-Pi. Binding of myosin-S1 carrying these different nucleotides is not the same: myosin-S1-ADP is in the rigor form and binds tighter to actin turning-on the system than either myosin-S1-ATP or myosin-S1-ADP-Pi. Nonetheless, decreased cooperativity of S1-ADP binding to the system with truncated tropomyosin can be rationalized again on the basis of the missing part of the overlap: a corollary would be that the residual cooperativity observed

in the isotherms in the presence of EGTA stems either via tropomyosin within one unit or from changes occurring within actin.

In agreement with Moraczewska and Hitchcock-DeGregori (2000), collectively these results suggest that the amino and carboxyl ends of tropomyosin have independent functions. The amino-terminal region of tropomyosin through its interaction with troponin T, in particular the N-TnT region, can be suggested to facilitate the turned-off (blocked) state of the thin filament. Thus the disruption of this interaction, as in the case with Omp T-digested tropomyosin, favors switching the thin filaments from the turned-off (blocked) to the turned-on (open) state. Knowledge of the atomic structure of the overlap complex would facilitate a fuller understanding of these results.

Chapter 6. Sequence diversity and the conformational stability of salmon tropomyosins.

6.1 Introduction

The cold-water fish, Atlantic salmon (*Salmo salar*) possesses different tropomyosin isoforms in each type of striated muscle: single and distinct proteins in fast trunk and cardiac muscles, and two distinct isoforms in slow trunk muscle (Heeley and Hong 1994, Heeley et al. 1995). One of the slow isoforms, however, constitutes only about 10% of the total tropomyosin (Heeley et al. 1995). The amino acid sequence comparisons of the three major salmonid isoforms with each other show: 15% difference (8% nonconservative) between slow and cardiac, 13% difference (7% nonconservative) between fast and cardiac and 11% differences (6% nonconservative) between fast and slow (Jackman et al. 1996). Differences in the conformational stabilities and the primary sequences between these isoforms as well as between salmonid and mammalian tropomyosins provide insight into adaptation to cold.

The temperature-dependent unfolding of the three salmonid muscle tropomyosin isoforms and the recombinant form of the fast isoform was analyzed using Circular Dichroism (CD) (Greenfield et al. 1967, Greenfield and Fasman 1969, Saxena and Wetlaufer 1971, Lehrer 1978, Brahm and Brahm 1980, Hennessey and Johnson 1981) under various solvent conditions (varying pH, salt (KCl), osmolyte (trimethyl N-amino oxide, TMAO), and added divalent cations). Coiled-coil alpha-helical secondary structure

has a characteristic far UV CD spectrum consisting of a maxima at 190nm and double minima at 208 and 222nm due to differential absorbance by the peptide bond, with the minima at 222nm being more negative than that at 208nm (Cooper and Woody 1990). The magnitude of the minima at 222nm is used to estimate mean residue ellipticity and fractional helix values of tropomyosin at 5°C. Further, near UV CD can be used as a probe for aromatic residues (Chao and Holtzer 1975, Bullard et al. 1976, Lehrer 1978, Holtzer et al. 1989). The melting temperatures (T_m) were obtained by recording ellipticity (at 222nm or 280nm) with increasing temperature and by plotting the first differential of the ellipticity change due to loss of protein secondary structure as a function of temperature.

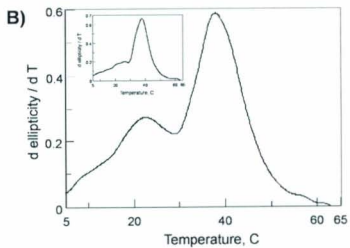
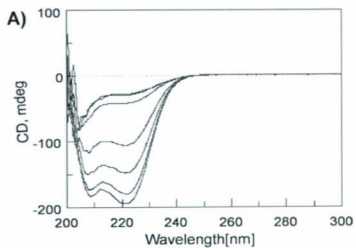
6.2 Results

6.2.1 Characterization of the thermostabilities of wild type and recombinant salmon fast muscle tropomyosins

Figure 6.1A shows CD spectra of wild type salmon fast muscle tropomyosin in the far UV range as the temperature is increased in intervals of 10°C. As anticipated, the magnitude of the double minima becomes less pronounced as the temperature is raised. At low temperatures (<25°C) the spectrum was indicative of predominately coiled-coil alpha helix. The mean residue ellipticity value at 5°C was 38035 ± 1993 mdeg.cm².mol⁻¹ corresponding to a fractional helical content value of 0.97 ± 0.05 , indicating the presence of high alpha helical content in this isoform as has been previously reported for other

Figure 6.1 : Thermostability of wild type salmon fast muscle tropomyosin

- A) Circular dichroism UV spectra from 198-300nm at different temperatures. Buffer, 20mM potassium phosphate, 0.1M KCl, 1mM DTT, pH 7; heating rate, 30°C/hr; scan speed, 100nm/min; protein concentration, ~1mg/ml; light path, 0.5mm.
- B) First derivative of the ellipticity change at 222nm as a function of temperature. Experimental conditions are the same as in A). The protein heated to 65°C was slowly cooled back to 5°C with the same rate as the heating step (30°C/hr). The sample was then reheated to 65°C. Main figure, first run; inset, second run.



tropomyosins (Oikawa et al. 1968, Pato et al. 1981a, Heeley and Hong 1995). Above 50°C it is evident that the protein has undergone thermal denaturation and is a random coil (Figure 6.1A). An unfolding profile was obtained by continuously monitoring the ellipticity change at 222nm as a function of temperature (Figure 6.1B). At 0.1M KCl, 1mM DTT, pH 7 the thermal melting profile consists of two asymmetric transitions: a prominent minor transition with a T_m value of 24.2°C preceding a major transition with a T_m value of 38.1°C. This asymmetry suggests the existence of more than one cooperative unfolding step.

When the thermally unfolded protein (at 65°C) is slowly cooled to 5°C over 2hrs, it attains a mean residue ellipticity value similar to the native protein indicating a return to complete helical content. However upon reheating, the minor transition becomes significantly diminished or unobserved and the amplitude of the major transition is increased (Figure 6.1B, inset). The results show that the low temperature transition observed in native salmon fast muscle tropomyosin is not completely reversible within the time frame the protein was allowed to refold as monitored by CD spectrometry.

Interestingly, under the same buffer conditions, the recombinant form of the same protein, prepared by cDNA expression in *E. coli* BL21 DE3, lacks a pronounced minor transition as well (Figure 6.2A). The bacterially expressed protein is identical to the wild type in terms of the sequence except for the absence of an amino-terminal acetylation (Jackman et al. 1996). Therefore we investigated whether the disappearance of the minor

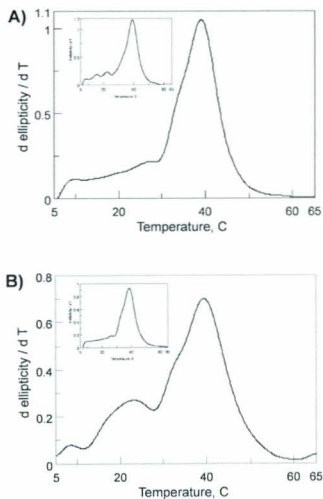


Figure 6.2 : Thermostability of recombinant salmon fast muscle tropomyosin

First derivative of the ellipticity change at 222nm as a function of temperature for recombinant fast tropomyosin prepared with (A) and without (B) a heating step are shown in main figures. Insets, second run. Buffer, 20mM potassium phosphate, 0.1M KCl, 1mM DTT, pH 7; heating rate, 30°C/hr; scan speed, 100nm/min; protein concentration, ~1mg/ml; light path, 0.5mm.

transition could be due to the heating step (to -80°C) included in the isolation protocol of recombinant tropomyosin to remove bacterial proteins. When the protein was isolated omitting the heating step, a prominent minor transition (T_m , 23.2°C) was observed as in the case with the wild type counterpart (Figure 6.2B). Like the wild type tropomyosin, when this material was heated to 65°C , cooled and reheated the minor transition was lost (Figure 6.2B, inset). In addition, either method of isolation yielded a product displaying a major transition not significantly different from the wild type (with and without heating, 38°C and 38.7°C respectively). The calculated mean residue ellipticity and the fractional helical content for heat-treated recombinant salmon fast muscle tropomyosin were $36431 \pm 3455 \text{ mdeg.cm}^2.\text{mol}^{-1}$ and 0.93 ± 0.08 ($n, >5$). The same protein isolated without a heat treatment showed a mean residue ellipticity value of $36675 \pm 2368 \text{ mdeg.cm}^2.\text{mol}^{-1}$ ($n, >5$) corresponding to a fractional helical value of 0.94 ± 0.06 . Part of the variability in mean residual ellipticity values can be attributed to small errors in protein concentrations.

In Table 6.1, the change in ellipticity within each transition is expressed as a percentage of total ellipticity change from 5 - 65°C . For wild type and non heat-treated recombinant fast tropomyosins, the minor transition accounts for 16.4% and 16.9%, while the major transition accounts for 71.7% and 73.3% of the original helix, respectively. When the proteins have been heated once, the minor transitions decrease to 11% and 8.9% while the major transition increases to 78.1% and 82.6% respectively. The percentages of structural change occurring within the minor transition and major transition for heat-

Table 6.1 : Comparison of relative ellipticity changes of wild type and recombinant salmon fast muscle tropomyosins.

	Wild type tropomyosin		Non-heat treated Recombinant tropomyosin		Heat treated Recombinant tropomyosin	
	(%) Minor transition	(%) Major transition	(%) Minor transition	(%) Major transition	(%) Minor transition	(%) Major transition
First heating	16.4 ± 2.4	73.0 ± 3.3	16.8 ± 4.1	73.3 ± 1.2	9.7 ± 2.3	79.4 ± 4.5
Second heating	11.0 ± 2.4	80.0 ± 2.3	8.9 ± 3.2	82.6 ± 1.7	8.4 ± 2.8	83.1 ± 3.5

Relative ellipticity change within minor and major transitions of wild type, non-heat treated recombinant and heat treated recombinant in the first and the second runs. The percentage of each transition was estimated by expressing the change in ellipticity within each transition as a percentage of the total ellipticity change from 5-65°C. Buffer, 20mM potassium phosphate, 0.1M KCl, 1mM DTT, pH 7; heating rate, 30°C/hr; scan speed, 100nm/min; protein concentration, ~1mg/ml; light path, 0.5mm. Number of determinations, n >5; batches of protein, 5(wild type), 3 (heat treated recombinant) and 2 (heat treated recombinant).

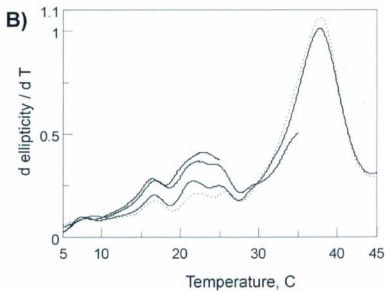
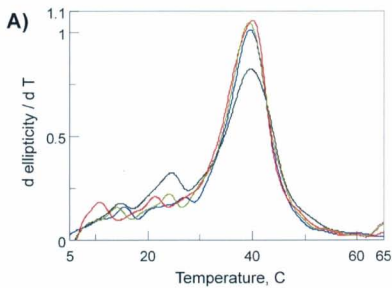
treated recombinant protein are 9.6% and 78.1%. These values are significantly different from those of native wild type and non heat-treated recombinant proteins, but are comparable to those if the latter two proteins have been previously heated.

6.2.1.1 Effect of different heating and cooling protocols on the minor transition of salmon fast muscle tropomyosin.

To learn whether periods of prolonged cooling, or a slower rate of cooling of thermally unfolded fast tropomyosin could return the minor transition, wild type tropomyosin was heated to 65°C and allowed to cool to 5°C differently: rapid cooling (sample was left in the CD with water running through the CD-cell jacket and the water bath was rapidly cooled back to 5°C within 10min by mixing with ice); slow cooling (samples were left to cool down to room temperature (~1hr) and then transferred to the fridge) followed by extended incubations for either 2hrs, 24hrs or 48hrs. Following a given cooling procedure the protein was reheated (Figure 6.3A). Buffer conditions were 0.1M KCl, 1mM DTT, and pH 7. The thermal melting profile of proteins, which had been cooled rapidly lacked a pronounced minor transition. Slow cooling and then extended incubation at low temperature for up to 48 hrs did not enhance the magnitude of the minor transition any further, although small shifts (~1-2°C) in the minor transition T_m values were evident. Further, the ellipticity value at 5°C upon rapid cooling was a slightly smaller negative number than that for the native protein (-178 mdeg for native vs -166 mdeg) possibly due to insufficient refolding time. However, all the samples subjected to a slow cooling process for 2hrs or more showed the same ellipticity values as the native protein. The

Figure 6.3 : The effect of different heating and cooling protocols on the minor transition of salmon fast muscle tropomyosin

- A) First derivatives of the ellipticity change at 222nm as a function of temperature are shown. Protein was heated to 65°C (black) and cooled to 5°C for different time periods before reheating: rapid cooling (sample was left in the CD with water running through the CD-cell jacket and the water bath was rapidly cooled (blue) back to 5°C within 10min by mixing with ice); slow cooling (samples were left to cool down to room temperature (~1hr) and then to 4°C in the fridge) and extended incubation for either 24hrs (red) or 48hrs (green). Buffer, 20mM potassium phosphate, 0.1M KCl, 1mM DTT, pH 7; heating rate, 60°C/hr; scan speed, 100nm/min; protein concentration, ~1mg/ml; light path, 0.5mm.
- B) First derivatives of the ellipticity change at 222nm as a function of temperature are shown. Starting from the lowest temperature a single protein sample was heated to 25°C, 35°C, 45°C (solid lines) and again 45°C (dotted line) with cooling back to 5°C between the heating steps. As soon as the sample reaches 5°C the next heating step was started. Run conditions are the same as in (A).



magnitudes of the major transitions were also noted to be higher in the case of previously heated proteins as compared to the native (Figure 6.3A).

To further study the reversibility of the minor transition, the wild type protein (0.1M KCl, 1mM DTT, pH 7) was subjected to heating and cooling cycles with 10°C incremental increases. Starting from the lowest temperature, protein was heated to 25°C, 35°C, 45°C and 55°C. Between each heating step, the protein was slowly cooled to 5°C before starting the next heating step (Figure 6.3B). Heating to 25°C and cooling to 5°C did not reduce the magnitude of the minor transition significantly. A major loss of the minor transition was observed after heating to 35°C. A slight reduction in the magnitude of the minor transition was evident upon further heating to 45°C and cooling to 5°C. Therefore, reversibility of the minor transition seems to be significantly lost after the protein has been heated to a temperature where unfolding of the region responsible for the minor transition is complete.

6.2.1.2. Thermostabilities of the two cyanogen bromide fragments.

To determine the regions of the salmon fast muscle tropomyosin sequence which give rise to the observed transitions, the thermal melting profiles of the two large cyanogen bromide fragments were analyzed. These were the amino-terminal half, CN1A (residues 11-127) and the carboxy-terminal half, CN1B (residues 142-281) of the protein. Figure 6.4 shows thermal melting profiles of both amino- and carboxy-terminal fragments

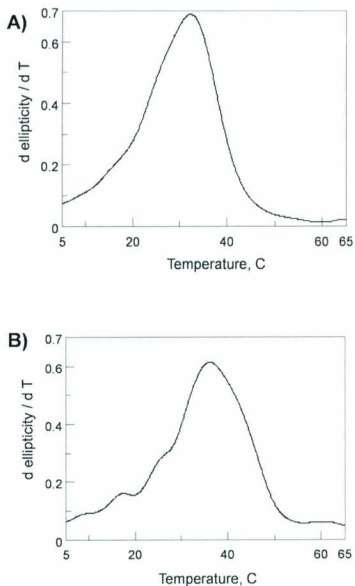


Figure 6.4 : Thermostability of the CNBr fragments of salmon fast muscle tropomyosin.

First derivative of the ellipticity change at 222nm as a function of temperature for A) CN1A (residues 11-127) and B) CN1B (residues 142-281). Buffer, 20mM potassium phosphate, 0.1M KCl, 1mM DTT, pH 7; heating rate, 60°C/hr; scan speed, 100nm/min; protein concentration, ~1mg/ml; light path, 0.5mm.

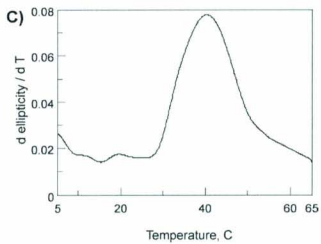
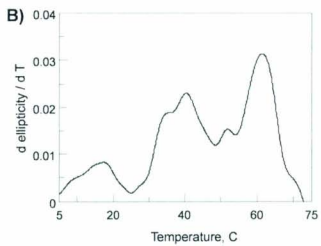
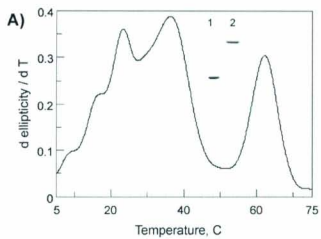
at 0.1M KCl, pH 7, 1mM DTT consisting of a single transition centered at 33°C and 36 °C respectively, corresponding to the major transition observed for the intact molecule. There was no evidence of the minor transition in either fragment in the above or various other buffer conditions that were tested such as in the presence of 1M KCl or 1M TMAO. This can be rationalized by the locally destabilized part of the protein being already unfolded in the peptides. Potekhin and Privalov 1982 showed that a cleavage of the protein within a cooperative block leads to destabilization of the regular structure of the complete block up unto its terminal points. A control experiment where native protein was treated with formic acid did not reduce or change the minor transition indicating that the result is not an effect of the formic acid used for the CNBr digestion (data not shown).

6.2.1.3 Thermostability of the oxidized protein

Thermal melting of the isoform was then performed with the oxidized protein (Figure 6.5A). With the cysteines oxidized, the unfolding profile is more complicated. This is mostly due to the appearance of a new transition centered at 60°C. The transitions at ~ 24°C and ~ 38°C are still apparent but, compared to what is observed in the presence of DTT, they are now more equal in magnitude (compare Fig. 6.1B and Fig 6.5A). The results show that the effect of oxidation is both stabilizing and destabilizing on the tropomyosin structure. It also agrees with the idea that the minor transition involves a region, which is affected by the presence or the absence of a disulphide bond. The region around Cys190 has been previously shown to unfold at low temperatures in the case of rabbit skeletal tropomyosin (Lehrer et. al., 1978, Potekhin et al. 1982). Further, the

Figure 6.5 : Effect of disulphide bond formation on the thermostability of salmon fast muscle tropomyosin in far and near UV range.

- A) First derivative of the ellipticity change at 222nm as a function of temperature for oxidized wild type salmon fast muscle tropomyosin. Buffer, 20mM potassium phosphate, 0.1M KCl, pH 7; heating rate, 60°C/hr; scan speed, 100nm/min; protein concentration, ~1mg/ml; light path, 0.5mm; inset, SDS PAGE of reduced (lane 1) and oxidized proteins (lane 2).
- B) First derivative of the ellipticity change at 280nm as a function of temperature for oxidized wild type salmon fast muscle tropomyosin. Buffer, 20mM potassium phosphate, 0.1M KCl, pH 7; heating rate, 30°C/hr; scan speed, 100nm/min; protein concentration, ~10mg/ml; light path, 5mm.
- C) First derivative of the ellipticity change at 280nm as a function of temperature for reduced wild type salmon fast muscle tropomyosin. Buffer, 20mM potassium phosphate, 0.1M KCl, 1mM DTT, pH 7; heating rate, 30°C/hr; scan speed, 100nm/min; protein concentration, ~10mg/ml; light path, 5mm.



oxidized CN1B fragment, as monitored in the far UV range, unfolded mainly at 60°C (this experiment was done by Donna Jackman, data not shown) indicating that the higher temperature transition observed with the oxidized intact protein corresponds to the unfolding of the carboxyl region of the molecule.

6.1.2.4 Near UV Circular Dichroism

The next step was to investigate the temperature dependent ellipticity change of the protein at 280nm (Figure 6.5B and C) under both reducing and oxidizing conditions. Tropomyosin (which is tryptophan-free) contains six tyrosines at the following positions: Tyr60, Tyr 162, Tyr 214, Tyr 221, Tyr 261 and Tyr 267. Five of the six are located in the carboxy-terminal half. Thus, the near-UV CD signal is a convenient means of probing the conformation of this part of the molecule. For the reduced protein, a single transition with a T_m of ~ 40°C was observed, which coincides with the major transition observed in far UV measurements. Under oxidized conditions, the low temperature unfolding was also evident, but at a slightly lower temperature (~18°C) than in the far UV range. Two other transitions are observed at ~40°C and ~60°C. In this case, however, the peak at 40°C is lower in magnitude as compared to that in the far UV range indicating that this transition may represent the unfolding of a region with proportionately fewer number of tyrosines, thus it may represent the unfolding of the amino-terminal half of the molecule, which has only one tyrosine.

6.2.2 Effect of pH, salt, trimethylene N-amino oxide, divalent cations, on the stability of salmon fast muscle tropomyosin.

The effect of solution pH on the conformational stability of wild type fast tropomyosin (0.1M KCl, 1mM DTT) is shown in Figure 6.6. Both transitions observed at neutrality (Figure 6.1B) are shifted to higher temperatures (30.7°C and 53.7°C respectively) at the lower pH of 6 (Figure 6.6A). At this pH, the minor transition is more pronounced and it may consist of more than one component. When the pH is increased to 8, the melting temperature of the major transition decreased to 36.3°C and the minor transition was less prominent or not detected (Figure 6.6B). As in the case at pH 7, previously heated wild type protein did not show a pronounced minor transition at pH 6. These results are summarized in Figure 6.6C.

Raising the concentration of neutral salt (KCl) from 0.1 to 1 M was noted to increase the T_m values of major transitions at both pH 7 and 6 (48.2°C and 59.9°C respectively) (Figure 6.7A). Minor transitions were broadened and consisted of two or more components at both pHs. In the presence of 1M TMAO, 0.1M KCl, T_m s of both transitions increased at pH 7 (35.1°C and 51.1 °C) (Figure 7B), but only that of minor transition at pH 6 (34.5°C) indicating that the stabilization by TMAO depends on the solvent conditions. For example, unlike KCl, TMAO does not provide additional stabilisation at pH 6. Further, in contrast to neutral salt, all transitions appeared sharper in the presence of 1M TMAO, such that they took place over a narrower temperature range. When present together, 1M TMAO and 1M KCl shifted all transitions to higher

Figure 6.6 : Effect of pH on the stability of salmon fast muscle tropomyosin

First derivative of the ellipticity change at 222nm as a function of temperature in the buffer 20mM PIPES, 0.1M KCl, 1mM DTT, pH 6 (A) or 20mM HEPES, 0.1M KCl, 1mM DTT, pH 8 (B); heating rate, 60°C/hr; scan speed, 100nm/min; protein concentration, ~1mg/ml; light path, 0.5mm; insets, second run. (C) The melting temperatures of minor and major transitions are plotted as a function of pH. Circle, major transition; diamond, minor transition.

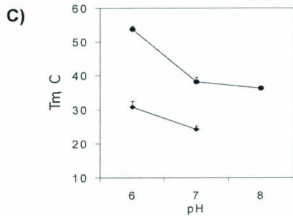
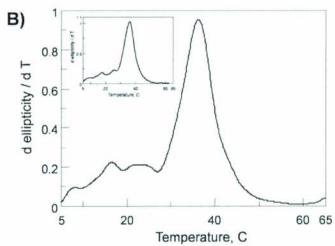
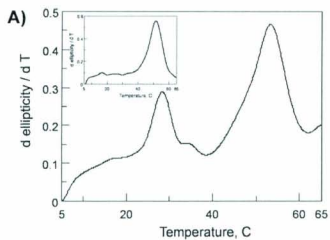
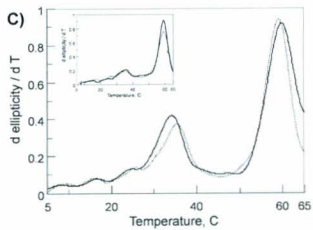
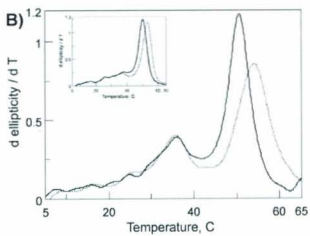
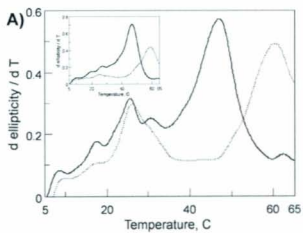


Figure 6.7 : Effect of salt and osmolyte on the stability of salmon fast muscle tropomyosin

First derivative of the ellipticity change at 222nm as a function of temperature for wild type salmon fast muscle tropomyosin in the presence of 1M KCl (A), 1M TMAO (B), 1M KCl and 1M TMAO (C). Buffer, 20mM PIPES / potassium phosphate, 1.0M KCl, 1mM DTT, pH 6 (dotted line) or 7 (solid line); heating rate, 60°C/hr; scan speed, 100nm/min; protein concentration, ~1mg/ml; light path, 0.5mm; insets, second heating.

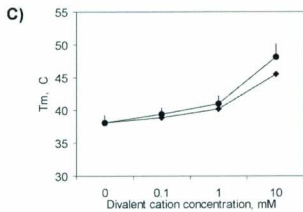
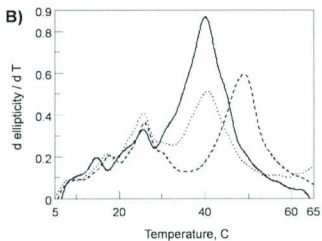
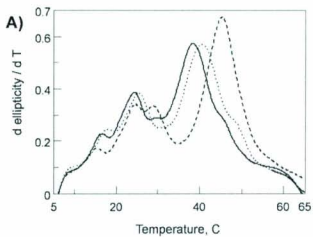


temperatures, with no significant difference between pH 6 and 7 as shown in Figure 6.7C (at pH 6 and 7 respectively: minor transitions, ~34.5 and 35.1 °C; major transitions, ~59.6 and 59.1°C). Interestingly, approximately 50% of the minor transition was reversible when the wild type fast tropomyosin was heated, cooled and reheated under these buffer conditions (Figure 6.7C, inset). The unfolding profiles of recombinant tropomyosins (heated and unheated) were similar to the wild type at varying pH, salt and TMAO conditions except for the minor transition of the heat-treated protein, which was less pronounced (data not shown).

The effect of divalent cations, specifically Ca^{2+} and Mg^{2+} , was investigated in 0.1M KCl, pH 7 (Figure 6.8A and B). The basal measurement for zero cation concentration was performed in the presence of 1mM EDTA to remove any residual cations (profile not shown). As the concentration of Ca^{2+} or Mg^{2+} was increased from zero to 1.0 mM, T_m values of the major transition were only slightly affected (38.9°C and 39.4°C at 0.1mM; 41 and 40.2°C at 1mM for Ca^{2+} and Mg^{2+} respectively). A more substantial change was observed when the cation concentration was raised to 10mM (48.1°C and 45.3°C respectively). In this instance, the minor transition consisted of two or more transitions. The results are summarized in Figure 6.8C. To confirm that the effect of Ca^{2+} and Mg^{2+} is not simply due to an increase in the ionic strength of the solution, the experiment was repeated in the presence of 0.13M neutral salt, which has the same ionic strength as 10mM divalent cation. The T_m value for the major transition increased only to 39.7°C (data not shown) indicating that divalent cations have a specific effect on tropomyosin

Figure 6.8 : The effect of divalent cations on the stability of salmon fast muscle tropomyosin.

First derivative of the ellipticity change at 222nm as a function of temperature in the presence of varying concentrations of Mg^{2+} (A) or Ca^{2+} (B), concentrations. Buffer, 20mM potassium phosphate, 0.1 mM (solid line), 1mM (dotted line) or 10 mM (dashed line), 0.1M KCl, 1mM DTT, pH 7; heating rate, 60°C/hr; scan speed, 100nm/min; protein concentration, ~1mg/ml; light path, 0.5mm. (C) The melting temperatures of the major transitions are plotted as a function of cation concentration. Circle, Ca^{2+} ; diamond, Mg^{2+} .



stability. Under none of the divalent cation concentrations was the minor transition observed when the proteins which had been once heated were used. Further, there were no significant differences in the mean residual ellipticities of the protein at 5°C as the pH, neutral salt, TMAO and divalent cation concentration were varied.

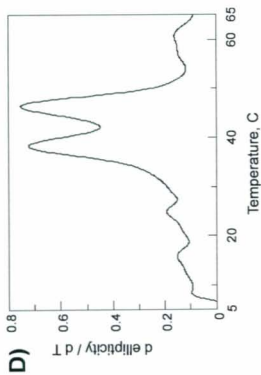
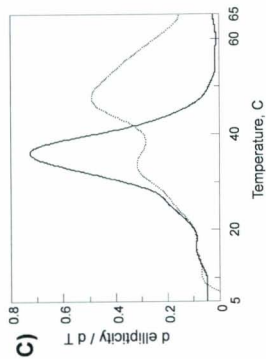
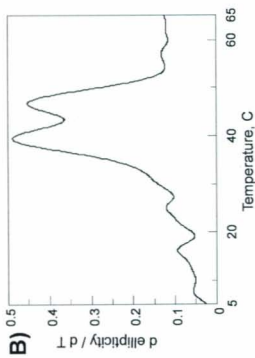
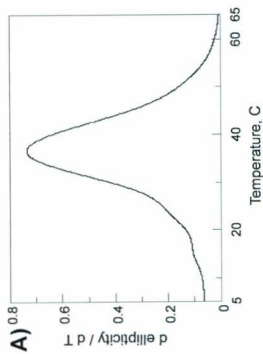
6.2.3 Thermostability of salmon cardiac and slow muscle tropomyosins

Structural stability of the salmon slow and cardiac muscle tropomyosins was studied as previously described for the salmon fast isoform. In the presence of 0.1M KCl, 1mM DTT, pH 7, a single transition with a T_m of 36.3°C was observed for cardiac muscle tropomyosin (Figure 6.9A), whereas two major transitions having T_m s of 38.6°C and 46.7°C were observed for the slow isoform (Figure 6.9B). The cardiac isoform, like the fast isoform, was completely unfolded by heating to 50°C. No further significant change in CD minima was detected for those two isoforms at temperatures above 50°C. Conversely, the slow isoform needed higher temperatures to achieve complete unfolding. In this instance the ellipticity at 222nm continued to decrease up to about 60°C. The mean residual ellipticity value at 5°C for cardiac and slow muscle tropomyosins ranged from 39000-40000 mdeg.cm².mol⁻¹ corresponding to a fractional helical value around 1.

As the buffer pH was increased to 8, stability of cardiac and slow isoforms was decreased. The T_m of the single transition in cardiac decreased to 35.2°C, and that of two major transitions in slow decreased to 36.4°C and 45°C respectively at 0.1M KCl,

Figure 6.9 : Thermostability of salmon cardiac and slow tropomyosins and the effect of pH.

First derivative of the ellipticity change at 222nm as a function of temperature for salmon cardiac, (A) & (C), and slow, (B) & (D), tropomyosins. Buffer, 20mM potassium phosphate / PIPES / HEPES, 0.1M KCl, 1mM DTT and pH 7 ((A) & (B)), pH 6 (dotted line in (C)) or pH 8 (solid line in (C) & (D)); heating rate, 60°C/hr; scan speed, 100nm/min; protein concentration, ~1mg/ml; light path, 0.5mm.



1mM DTT, pH 8 (Figure 6.9C). In the melting profile of cardiac isoform, two transitions were evident at pH 6: a minor transition with a T_m of 33.4°C and a major transition with a T_m of 47.2°C (Figure 6.9D). The profile for the slow isoform was more complicated. The protein appeared to be unfolding as a broad transition with a low amplitude starting around 30°C and extending beyond 65 °C (data not shown).

At 1M KCl, 1mM DTT, pH 7, both isoforms showed major transitions having higher T_m values (cardiac, 47°C; slow, 43.2°C and 55.3°C) however additional components were also noticeable (Figure 6.10A and B). The T_m values were also increased (cardiac, 48.5°C; slow, 48.4 and 56.5°C) in the presence of 1M TMAO, 0.1M KCl and the transitions were sharper than in its absence. (Figure 6.10C and D). The magnitude of this increase in the melting temperatures with added 1M neutral salt or 1M TMAO was similar to that obtained for the fast isoform (approximately 10°C increment). A summary of the melting temperatures of three salmonid isoforms as a function of pH, neutral salt and osmolytes is given in Table 6.2.

6.2.4 Sequence comparison of tropomyosin isoforms.

The primary structures of the three salmonid striated muscle tropomyosins were compared with each other and with that of rabbit alpha tropomyosin. Fifty three (of the 284) amino acids in salmonid striated TM are non-conserved. [This number is obtained by aligning the sequences of the three isoforms (fast, slow and cardiac)]. The most

Figure 6.10 : The effect of salt and TMAO on the stability of salmon cardiac and slow muscle tropomyosins.

First derivative of the ellipticity change at 222nm as a function of temperature for cardiac (A) and (C)) and slow,(B) and (D)) tropomyosins in the presence of 1M KCl ((A) and (B)) or 1M TMAO ((C) and (D)). Buffer, 20mM potassium phosphate, 1M KCl, 1mM DTT, pH 7; heating rate, 60°C/hr; scan speed, 100nm/min; protein concentration, ~1mg/ml; light path, 0.5mm.

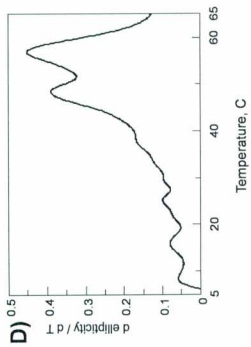
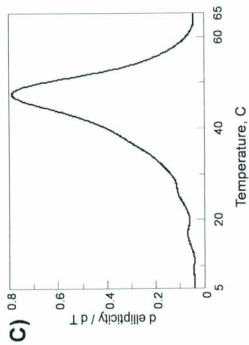
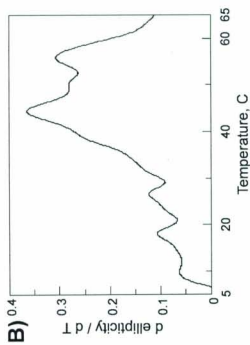
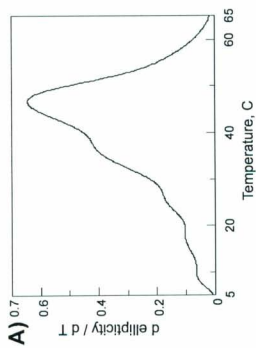


Table 6.2 : A summary of the melting temperatures of three salmonid fast, cardiac and slow tropomyosin isoforms.

	pH	0.1 M KCl	1M KCl	0.1 M KCl, 1M TMAO	1M KCl 1M TMAO
Fast	6	<i>30.7 ± 1.8</i>	<i>24.8 ± 0.7</i>	<i>34.5 ± 0.6</i>	<i>33.9 ± 1.1</i>
		53.7 ± 1.0	59.9 ± 0.9	53.7 ± 0.9	59.6 ± 0.3
	7	<i>24.2 ± 1.1</i>	<i>26.4 ± 1.3</i>	<i>35.1 ± 3.3</i>	<i>34.1 ± 2.5</i>
38.1 ± 1.3		48.2 ± 0.8	51.1 ± 3.6	59.1 ± 0.8	
	8	36.3 ± 0.1			
CN1A	7	33.5 ± 1.2			
CN1B	7	37.1 ± 0.7			
	6	-			
Slow	7	38.7 ± 1.1	43.2 ± 1.7	48.4 ± 0.3	
		46.7 ± 0.2	55.3 ± 0.8	56.5 ± 0.8	
	8	36.4 ± 2.9			
		45.0 ± 2.3			
	6	33.4 ± 0.1			
		47.2 ± 0.9			
Cardiac	7	36.3 ± 0.1	47.0 ± 0.3	48.5 ± 1.2	
	8	35.2 ± 0.7			

Number of batches of protein or fragment: fast muscle TM (five), slow muscle TM (two), cardiac muscle TM (two), CN1A (three) and CN1B (three). Note: only the melting temperature of the most prominent peak in a given unfolding profile is included in the table, even though evidence of additional components may have been observed. *Italics*, minor transition for fast muscle tropomyosin. Where n=2, ± indicates the range.

heterogeneous parts of the molecule are clustered in three regions of the molecule: (i) and (ii), in the amino-terminal half of the molecule, respectively between residues 17 - 49 (sixteen substitutions) and 73 - 87 (eight substitutions), and (iii), in the carboxyl half of the molecule between residues 172 - 216 (fourteen substitutions) (Figure 6.11). The latter region is of particular interest as it coincides with the region of local instability in the mammalian protein (Lehrer et al. 1978) and also includes disease-related point mutations (Thierfelder et al. 1994, Bing et al. 1997, Bing et al. 2000). In this part of the molecule, there are eleven substitutions between fast and cardiac muscle tropomyosins, five between fast and slow muscle tropomyosins and twelve between cardiac and slow muscle tropomyosins. Each salmonid tropomyosin contains two (fast), ten (cardiac) and five (slow) substitutions in this region when compared to rabbit alpha tropomyosin. The number of substitutions between four sequences in the other two regions are as follows:

variable region	fast vs cardiac	fast vs slow	fast vs rabbit	cardiac vs slow	cardiac vs rabbit	slow vs rabbit
17-49	8	13	5	15	6	14
73-87	5	4	2	7	6	4

All of the substitutions between the three salmonid tropomyosin isoforms that occur at a core position of the tropomyosin coiled-coil ("a" or "d" position), of which there are nine (2 x a and 7 x d): residues 25, 36, 39, 46, 74, 172, 179, 186 and 211, fall within the above mentioned three clusters (Figure 6.12). In five instances (residues 25, 74, 179, 186 and 211) the resident amino acid is either alanine or an hydroxylated amino acid. Some of

these substitutions that occur in the variable region (iii) have affected the fifth alanine cluster in the fast muscle tropomyosin isoform (Figure 6.13). The variable region (iii) contains four of the nine core position substitutions at three consecutive "d" positions, residues 172 (Ile in fast/rabbit/slow and Leu in cardiac), 179 (Thr in fast/slow and Ala in cardiac/rabbit) and 186 (Ser in fast/cardiac/rabbit and Ala in slow), and at an "a" position, residue 211 (Ala in fast/slow/rabbit & Ser in cardiac). As a result of these changes the fast muscle tropomyosin is completely devoid of a "d" position alanine in this region and therefore of the fifth alanine-cluster unlike the other three isoforms. Further, the residues at all the above three "d" positions of the fast muscle tropomyosin are predicted destabilising amino acids for the coiled-coil structure.

There are seven charge substitutions (although the "d" His at 39 in the 'slow' isoform may be deprotonated at neutrality) (Figure 6.12). Five of these bunch within residues 20 - 80 in the variable regions (i) and (ii). The residues are; 21 (Arg in fast, Glu in cardiac & Ala in slow), 39 (Leu in fast/cardiac & His in slow) 42 (Asp in fast/cardiac & Ala in slow), 49 (Lys in fast/slow & Asn in cardiac) and 77 (Thr in fast/cardiac & Lys in slow). The sixth is at residue 216 where glutamine in fast and slow isoforms is replaced by glutamic acid in cardiac. The other change is of particular interest as it falls in the overlap region: residue 276 (Asn in fast and His in slow/cardiac). An obvious consequence of these charge substitutions is a change in isoelectric points (pI) in a denaturing solvent: pI of the three salmonid muscle tropomyosins increases in the order, cardiac < fast < slow.

	CORE				'E'				'G'				CHARGE		
	F	S	C		F	S	C		F	S	C		F	S	C
25(d)	Ala	Ser	Ala	19	Leu	Leu	Ile	21	Arg	Ala	Arg	21(g)	Arg	Ala	Arg
36(a)	Ser	Ser	Cys	40	Glu	Asp	Glu	42	Asp	Ala	Glu	39(d)	Leu	His	Leu
39(d)	Leu	His	Leu	75	Glu	Asp	Glu	49	Lys	Lys	Asn	42(g)	Asp	Ala	Glu
46(d)	Leu	Met	Leu	145	Asp	Glu	Glu	63	Ser	Ala	Ala	49(g)	Lys	Lys	Asn
74(d)	Ala	Ala	Ser	201	Thr	Ser	Thr	77	Thr	Lys	Thr	77(g)	Thr	Lys	Thr
172(d)	Ile	Ile	Leu	229	Thr	Thr	Ser	84	Asp	Glu	Asp	216(f)	Gln	Gln	Glu
179(d)	Thr	Thr	Ala					175	Asp	Asp	Glu	276(c)	Asn	His	His
186(d)	Ser	Ala	Ser					210	Gln	Gln	Ser				
211(a)	Ala	Ala	Ser					245	Ser	Ser	Thr	Charge	+1	+3	- $\frac{1}{2}$
								252	Thr	Thr	Ser	(pH7)			

Figure 6.12: Amino acid sequence comparisons of salmonid tropomyosins.

Amino acid substitutions between salmonid fast (F), cardiac (C) and slow (S) tropomyosins at core, 'E', 'G' and charge positions. The predicted overall change in the charge at pH 7 as a result of charge substitutions is also shown.

Figure 6.13: Alanine clusters of tropomyosins

The 'a' and 'd' coiled-coil position residues of the three salmonid tropomyosin sequences are shown with alanine residues highlighted. The seven alanine clusters are indicated in red highlights. The 's' position alanines not involved in clustering with 'd' position alanines are indicated in yellow. Note: salmon fast muscle tropomyosin lacks the fifth cluster due to the substitutions at residues 179 and 186.

Fast	Cardiac	Slow	Rabbit	
a d	a d	a d	a d	
m i	m i	m i	m i	
m l	m l	m l	m l	
k a	k a	k a	k a	1
s a	s a	s a	s a	
k a	k a	k a	k a	
s l	c l	s h	s l	
l l	l l	l m	l l	
l t	l t	l t	l t	
l y	l y	l y	l y	
l a	l a	l a	l a	2
l s	l s	l s	l s	
v l	v l	v l	v l	
i v	i v	i v	i v	
l a	l a	l a	l a	3
l a	l a	l a	l a	
l a	l a	l a	l a	
s s	s s	s s	s s	
m i	m i	m i	m i	
a d	a d	a d	a d	
m g	m g	m g	m g	4
l l	l l	l l	l l	
l a	l a	l a	l a	
y v	y v	y v	y v	
l i	l i	l i	l i	
l t	l t	l t	l t	5
a s	a s	a s	a s	
c l	c l	c l	c l	
l v	l v	l v	l v	
l l	l l	l l	l l	
a y	s y	a y	a y	6
e y	e y	e y	e y	
i l	i l	i l	i l	
l l	l l	l l	l l	
a s	a s	a s	a s	
v l	v l	v l	v l	
i l	i l	i l	i l	
l q	l q	l q	l q	
y i	y i	y i	y i	7
l l	l l	l l	l l	
m i	m l	m i	m i	

The number of substitutions, between the three salmonid tropomyosins, at non-conserved inner ("e" or "g") positions, which are involved in ionic interactions between two helices in the coiled-coil, is sixteen (6 x "e" and 10 x "g") (Figure 6.12). Of these, there is a change in charge (either positive to neutral or negative to neutral) at four "g" residues (see Figure 6.12, at residues 21, 42, 49 and 77). Consequently, one ion pair ("g" to "e") interaction is lost in slow (res. 21 Ala to 26 Glu) and cardiac (res. 49 Asn to 54 Glu). Thus, the fast variant is predicted to form more attractive interactions (for a dimeric molecule) compared to the other two isoforms. However, it contains a smaller number of attractive interactions than rabbit alpha tropomyosin on account of a substitution at position 77 (Thr in fast and Lys in rabbit). The number of repulsive "g" - "e" interactions is the same for each salmonid protein, which are six.

Finally, it is worth noting that the fast and cardiac muscle tropomyosins each contain a closely-spaced pair of glycines (Figure 6.12), which are separated from each other in the primary structure by two amino acids in fast (at residues 24 and 27) and three in cardiac (at residues Gly 83 and 87). Further, these are absent in slow muscle tropomyosin and rabbit alpha tropomyosin. To our knowledge, the former pair (Gly 24 and 27) and the Gly 87 are unique to fast and cardiac muscle tropomyosins respectively.

6.2.5 Constructing a phylogenetic tree for tropomyosin

A phylogenetic tree based on the tropomyosin amino acid sequences was constructed (Figure 6.14) to understand the origin of the three salmonid tropomyosin isoforms and their evolutionary relationship with each other. There are four tropomyosin genes that

Figure 6.14: The phylogenetic analysis of tropomyosin

A phylogenetic tree was constructed for tropomyosin based on amino acid sequences using the MEGA 4 program for building phylogenetic trees with Poisson model, Neighbour joining algorithm and 1000 bootstrap replicates. Tropomyosin sequence information was obtained from NCBI and the accession numbers are as follows: House mouse alpha, CAA46043; House mouse beta; X12650; House mouse slow, AAA03725; Human alpha, AAA61225; Human beta, CAA29971; Human slow, P06753; Rabbit alpha, AAB34957; Rabbit beta, P58776; Chicken alpha, AAN75276; Chicken beta, AAA49117; African clawed frog alpha, Q01173; African clawed frog beta, AAA18100; African clawed frog cardiac, AAA91763; Atlantic salmon fast, AAB36559; Brown trout cardiac, CAA91434; Brown trout slow, CAA91251; Zebra fish alpha, AAH62870; Zebra fish beta, NP_001002119; Dog fish shark, AAK38348; Yesso scallop, BAB17858; Fruitfly, NP_996216. The chicken cardiac sequence was taken from Forry-Scaudies et al. 1990. Note: Salmon slow and cardiac sequences were obtained from brown trout slow and cardiac muscles respectively (Jackman et al 1996).



have been characterized in vertebrates: (1) TPM-1 (alpha), prominently found in mammalian cardiac muscle and in fast skeletal muscle; (2) TPM-2 (beta), found in skeletal muscle; (3) TPM-3 (slow twitch alpha), abundant in slow skeletal muscle and (4) TPM-4 (cardiac), specific to cardiac muscle (Lees-Miller et al., 1991, Cutticchia and Pearson, 1993). Fruitfly and scallop tropomyosins were included in the tree as an out-group. Two main branches diverging from an ancestral tropomyosin gene are evident; each later on diverged into two groups: (i) alpha and slow twitch alpha, and (ii) beta and cardiac. In other words, first, the ancestral cardiac and beta tropomyosins separated from ancestral alpha and slow twitch alpha tropomyosins and then they further separated to make four genes. Therefore, cardiac muscle tropomyosin is evolutionarily more related to beta tropomyosin than the alpha or slow twitch alpha tropomyosin. At the same time slow twitch alpha is more related to alpha than the other two isoforms. As expected, based on the evolutionary tree, salmonid fast tropomyosin clusters with alpha tropomyosins indicating that its origin is the TPM-1 gene. Salmonid cardiac muscle tropomyosin groups with the TPM-4 gene product whereas salmonid slow muscle tropomyosin with TPM-3 gene product.

6.3 Discussion

This chapter describes evidence for the divergence of tropomyosin from Atlantic salmon as an adaptation to the cold environment. These fishes are cold-water dwellers. Salmonid tropomyosins are less resistant to thermal denaturation than the mammalian proteins

(William and Swenson 1981). It follows that strategies for low-temperature adaptation should be 'encoded' within the respective primary structures, determined previously (Heeley et al. 1995). Towards this end, discussion will mainly focus on the isoforms, which exist as homodimers in the natural setting, i.e. those variants that are present in fast skeletal muscle and heart. The properties of salmonid slow skeletal muscle tropomyosin are harder to evaluate due to the fact that there are two isoforms (thereby allowing for the possibility of heterodimer formation) of which only one has been sequenced.

It is evident, as well as from a recent report (Goonasekara et al. 2007), that the salmon fast muscle tropomyosin, which is the only salmonid isoform that produces a low temperature transition (Figure 6.1B), is destabilised in each half of its structure relative to rabbit (William and Swenson 1981). This is consistent with the positioning of regions in the coiled-coil that contain clusters of substitutions. Two such clusters occur in the amino-terminal half of the molecule. Another, namely residues 172 – 216, resides in a section of the molecule that is known to be unstable.

Beginning with the cluster between residues 172-216, the region of tropomyosin around Cys190 has been suggested in a number of previous studies to have an inherent instability. Using fluorescent probes (Lehrer 1978, Graceffa and Lehrer 1980, Betteridge and Lehrer 1983) and spin labels attached to Cys190 (Graceffa and Lehrer 1984), and enzyme digestion (Ueno 1984), rabbit skeletal tropomyosin was observed to show a pre-transition in the 30-45°C temperature range, which was related to a local unfolding at a

region closer to Cys190. This transition was dependent on the state of oxidation and only observed with the oxidized protein in the case of rabbit (William and Swenson 1981). The presence of a disulphide linkage between the two cysteines increases the instability in this region making the unfolding more cooperative whilst stabilizing other parts of the molecule (Lehrer 1978, William and Swenson 1981, O'Shea et al. 1989, Hodges et al. 1990, Engel et al. 1991). Similarly, in both far and near UV regions, the minor transition of salmon fast muscle tropomyosin was more cooperative if the molecule was oxidized (compare Figures 6.1B and 6.5A), indicating that it involves a low stability region in the vicinity of Cys190. Moreover, as denoted by the 60°C transition, the carboxyl half of the molecule was more stable in the oxidized protein than in the reduced (Figure 6.5A and B). Therefore, the effect of oxidation is both stabilizing and destabilizing. The distinction of the minor transition of the fish protein is; although it is similar in the proportion of unfolding to the pre-transition of mammalian counterpart (~20%), it is more cooperative, observed at a lower temperature and detected even in the reduced form (Figure 6.1B).

Looking into the sources for this instability, substitutions within the variable segment between residues 172 – 210, between salmonid isoforms and rabbit alpha deserve attention. Of these, the core ('d') position replacements at 179 and 186, near Cys 190 are of particular interest. These two sites together with Ala 183 at the adjacent 'a' position, constitute the fifth 'Alanine cluster' of the protein giving flexibility to the coiled-coil (Figure 6.13) (Brown et al. 2001, Singh and Hitchcock-DeGregori 2003, Singh and Hitchcock-DeGregori 2006). Replacement of these core positions with residues of greater

hydrophobicity and packing effect, such as leucine and valine, have been proposed to cause the molecule to be less flexible but more stable (Singh and Hitchcock-DeGregori 2003, Kwok and Hodges 2004, Singh and Hitchcock-DeGregori 2006). At the same time, alanine is more favored at a core 'd' position than a branched polar residue like threonine (Triplet et al. 2000). In the fast isoform, both alanines at 179 and 186 are substituted to destabilizing threonine and serine respectively and as a result it is devoid of the particular 'alanine cluster'. On the other hand, all the other isoforms have one alanine at either 179 (in rabbit alpha and cardiac) or 186 (in slow) 'd' positions therefore retaining the cluster. Thus, the replacement of a key alanine by a destabilizing residue appears to have accentuated the response of the unstable region around Cys190 in the fast isoform to heat, effecting a cooperative transition as opposed to one which proceeds more uniformly with changing temperature such as in the case of rabbit skeletal tropomyosin. Since the "d" residues on either side of Thr179 in fast tropomyosin are the same in rabbit alpha (Ile172 and Ser186) and since there is only one other substitution in this section between the two molecules (Ala191 in rabbit and Ser in fast), the isomorphism at 179 is, in our opinion, the best candidate for this accentuated instability.

Turning to the amino-terminal half, the CN1A (residues 11- 127) peptide of salmon fast muscle tropomyosin was less stable than CN1B (residues 142- 281) (Figure 6.5); the opposite to what was reported for rabbit alpha tropomyosin (William and Swenson 1981). A conspicuous distinction between the fish and rabbit proteins in this regard is the presence, in the former, of a 'glycyl pair' (fast, at residues 24 and 27; cardiac, at residues

Gly 83 and 87). In addition, there is a change in the number of "g" to "e" interactions (Figure 6.12). For the dimeric molecules, rabbit alpha tropomyosin will potentially form two more interactions than fast muscle tropomyosin and four more than cardiac muscle tropomyosin. The significance of two 'core' substitutions at 36 (Ser in fast and rabbit, Cys in cardiac) and 74 (Ala in fast and rabbit, Ser in cardiac) (Figure 6.12) is not clear because the presence of a polar side chain at both interfacial positions is not exclusive to fish. These glycines combined with an electrostatic component appear to be the main candidates for modulation of stability in the first half of the molecule.

A possible mechanism for thermal denaturation and renaturation of fast tropomyosin can be described as follows. Unfolding begins with a local chain separation and an associated loss of coiled coil helix in a region close to Cys 190 when a temperature around 25°C is reached (minor transition). As inferred by the similar T_m values of each CNBr fragment, which were close to 40°C, under reducing conditions, the initial unfolding is followed by the cooperative melting of the complete molecule towards the two termini (major transition). At temperatures above 50°C the protein is mostly in a random coil configuration (Figure 6.1A). The fact that previously heated protein displays only the major transition (Figure 6.1A, inset) may lead one to think that, in this case, the region that unfolds at the minor transition is denatured. However, the heat-denatured protein attains the same mean residue ellipticity as the native protein upon slow cooling (for 2hrs) indicating that it is not the case. This suggests that the heated protein regains its complete secondary structure upon refolding but adopts a conformation, which is slightly

different from the native form. Previous CD studies on mammalian tropomyosin unfolding and refolding have suggested that an intermediate state, partially containing conventional alpha helix, is formed before the maximal amount of coiled coil is attained (Greenfield and Hitchcock-DeGregori 1993). In the case of salmon fast muscle tropomyosin, it can be thought that when the protein is heated and allowed to refold, the region involved in the minor transition remains as a conventional alpha helix rather than refolding to a complete coiled coil. Since the new conformation is also highly helical, it shows the same molar ellipticity as the native form at 5°C. This conventional alpha helical structure in the new conformation is stable at room temperature and remains folded until the main transition. This is also evident from the increase in relative ellipticity change observed in the major transition comparable to the decrease in the minor transition after the protein is heated, cooled and reheated (Table 6.1). Longer cooling periods produce no further changes (Figure 6.3A) in the melting profiles thus suggesting that the molecule does not reacquire its native state, which is consistent with the lack of a minor transition in heat-treated recombinant tropomyosin (Figure 6.2A). Further, this loss of the minor transition appears to be occurring after the protein is heated to about 35°C at which unfolding of the low stability region is complete (Figure 6.3B). The effect is accentuated when the protein is heated to elevated temperatures, at which point the complete molecule is fully unfolded.

Recombinant salmon fast muscle tropomyosin is identical to the wild type in sequence except for the absence of the amino-terminal acetylation (Jackman et. al., 1996). This

modification is of particular importance for a number of tropomyosin properties. Repulsion between the two positively charged methionines is predicted to destabilize the amino-terminal region of the molecule. As a result recombinant tropomyosin does not show an effective end-to-end polymerization (Hitchcock-DeGregori and Heald, 1987; Urbanchikova and Hitchcock-DeGregori, 1994; Jackman et al., 1996). The similarity in the thermal melting profiles observed for wild type and non heat-treated recombinant tropomyosins suggests that the two proteins are equivalent in conformational stability despite the lack of terminal acetyl group (Figure 6.2). The lack of a minor transition in heat-treated recombinant tropomyosin is therefore attributed to heating to temperatures around 80°C during isolation. A study using amino-terminal peptides showed low fractional helical contents and lower stabilities for unacetylated peptides compared to acetylated peptides (Greenfield et al. 1994). However, such effects of acetylation on the stability and helical content would be masked by the greater length and high helical content of the complete intact tropomyosin coiled coil.

The effects of pH and neutral salt (Figures 6.6 and 6.7A) can be interpreted in terms of the models for coiled-coil tropomyosin structure by McLachlan and Stewart 1975; Hodges et al. 1975 and Sodek et al. 1978. The coiled-coil structure of tropomyosin is stabilized by interchain electrostatic (between ionic amino acids in positions 'e' and 'g') and hydrophobic (between apolar amino acids in positions 'a' and 'd') interactions. Since tropomyosin has a pI value of 4.6, it has a net negative charge at pH 7. Therefore, decreasing the pH or increasing salt, reduces or shields the negative charges, thereby

minimizing repulsive interactions between the chains (William and Swenson 1981). Further, the presence of additional unfolding steps is more evident at 1M KCl and pH 6. It appears that some cooperative blocks are stabilized to a higher extent by high salt and low pH. Therefore under these conditions, additional transitions are observed. Given the low stability and the pH dependence, the minor transition of fast tropomyosin can be thought to occur in a region with a high proportion of excess negative charges. One of these regions is between 173-196 where there are only three positive charges for eleven negative charges (Williams et al. 1981; Lehrer 1978). Interestingly, the minor transition of the fast tropomyosin greatly diminishes at pH 8. Further, perhaps for the same reason, rabbit cardiac muscle tropomyosin did not show a minor transition in low or no salt buffers (Betteridge et al. 1983). The disappearance of the minor transition may be a consequence of greater instability in that part of the molecule at high pH or low salt buffer, causing it to undergo the transition at much lower temperatures, thus undetected from the background. Otherwise, the lowered melting temperatures of the main transition may be masking the minor transition.

The osmolyte and the divalent cations are considered to be kosmotropes. Kosmotropes are highly soluble and hydrogen bond extensively with water. They stabilize the structure of macromolecules by reducing hydration of denatured protein surfaces, thereby tending to prevent the denaturing process (Yancey and Somero 1979, Arakawa and Timasheff 1985, Lin and Timasheff 1994, Zou et al. 2002). The additive effects of KCl and TMAO on tropomyosin structure can be attributed to their different mechanisms of protein

stabilization. The 50% reversibility of the minor transition observed in the presence of 1M KCl and 1M TMAO (Figure 6.7C) appears to favor the protein properly refolding to its native conformation. In the muscle cell, molecules like chaperones aid the folding process of proteins. When the protein is refolding in non-cellular conditions, the presence of protein stabilizing agents may be required to mask unfavorable repulsive interactions and to facilitate maximal coiled coil formation. The onset of increased stability by divalent cations occurs at concentrations which are much lower than that required for significant stabilization by salt. This implies specific interactions between Ca^{2+} , Mg^{2+} and tropomyosin.

Finally, from this study it is apparent that the three major muscle tropomyosin isoforms of salmonids: fast, slow and cardiac, have arisen from three separate genes: TPM-1, TPM-3 and TPM-4 respectively (Figure 6.14). The expression of a beta tropomyosin isoform encoded from the TPM-2 gene was not evident among salmonid tropomyosins although it is abundantly found in slow twitch muscles in other vertebrate groups. We were interested in the possibility that the minor isoform in slow muscle tropomyosin is a beta form. Considering the fact that beta tropomyosin contains two cysteines, slow skeletal muscle tropomyosin was reacted with iodoacetate and then analyzed the carboxymethylated and control tropomyosins electrophoretically. No differential shift in mobility was observed for the two isoforms (data not shown) indicating that unless these fishes synthesize a beta tropomyosin with only one cysteine per chain, this isoform is absent in the adult salmon striated muscle. However, the possibility that a beta isoform

may be developmentally regulated such that it is replaced by a different isoform in the adult organism still exists.

Chapter 7. General Discussion

This thesis profiles a new proteolysed version of tropomyosin encompassing residues 7 – 284. In view of the fact that the cleavage site falls within a conserved region, the digestion procedure should be applicable to all muscle tropomyosins and the product can be prepared in large quantities. The digested material proved useful in probing the structural and functional roles of tropomyosin's amino-terminal region. Especially exciting is the fact that this new shortened tropomyosin can be reconstituted into thin filaments at both high and low Ca^{2+} concentrations. This had not been demonstrated with previous tropomyosin lacking the first nine amino acids (Cho et al. 1990, and Moraczewska and Hitchcock-DeGregori 2000).

As outlined elsewhere, the hexapeptide which is removed by Omp T occurs in a 'crowded' region of the thin filament. Firstly, it occurs within the overlap site of tropomyosin. Secondly, the tail section of troponin T extends all of the way from the core of the troponin complex to this site (Figure 1.1F). As yet, there is no consensus as to how much of tropomyosin is in physical contact with the tail. But new information is obtained when Omp T digested tropomyosin is brought to bear on the problem. This information was acquired using two independent methods: affinity chromatography and sedimentation assays. In each instance, the measured parameter (either chromatographic elution or induction of binding to F-actin) was disrupted (Figure 4.1) or abolished (Figure 4.2), in the case of the shortened protein relative to one which is full length. The

inference, at least from the methods used here, is that the hexapeptide (including the terminal acetyl group) is 'required' for the full association of tropomyosin with troponin T.

This raises the question of whether the amino-terminal region of tropomyosin interacts directly or indirectly with troponin T. In the latter scenario, troponin T would be envisaged to bind solely to the carboxy-terminal region of tropomyosin with the amino-terminal region serving merely as a scaffold, to facilitate the interaction. While this possibility can not be ruled out entirely, it appears that it is not the whole story. The finding that Omp T-digested tropomyosin has weakened affinity for the N-TnT peptide, compared to the full-length molecule (Figure 4.1) is indicative of a direct linkage. And this is consistent with the observation that N-TnT accentuates troponin I induction of F-actin binding of carboxy-terminally truncated tropomyosin (Heeley et al. 1987) but not that of amino-terminally shortened tropomyosin (Figure 4.6). These findings can be interpreted in terms of troponin-T bridging the overlap by forming an interaction with the amino-terminal portion of tropomyosin, that this, at least in part, direct.

How much of tropomyosin's amino-terminal region is involved in troponin T binding? The 1987 crystallographic study of White et al., in which glutaraldehyde cross-linked crystals of tropomyosin soaked with either troponin or N-TnT, showed that the troponin T tail covered the first 10-15 amino acids of tropomyosin. Although co-localisation (resolution, 17Å) could only infer that an interaction is taking place, when the current

observations are combined with those obtained previously (White et al. 1987), it is clear that the binding site is short in length; particularly when compared to the extensive interaction that occurs between the carboxyl-terminal region of tropomyosin and N-TnT (Jackson et al. 1975, Pearlstone and Smillie 1982). That said, we can not define the exact limits of the binding site. Nor can we say that the amino-terminal hexapeptide represents most, or all, of this site. Indeed, the involvement of the hexapeptide in troponin-T binding may only be to maintain the conformation of residues 7 – 15, as the hexapeptide might be unavailable to bind to troponin T on account of its participation in overlap formation. If this is valid, a corollary would be that Omp T digestion has destabilized a troponin T binding site slightly downstream of the hexapeptide either by loss of covalent structure or the generation, at pH 7, of a positively charged alpha-amino group, or both. That unacetylated tropomyosin (residues 1 – 284) exhibits weakened affinity for N-TnT (Fig 4.1) can be rationalised in terms of a local destabilization (Greenfield et al. 1994 and Brown et al. 2001), one which can not be detected by CD but which is sufficient to disturb a small binding site. This issue, that of the fine architecture of the thin filament, may only be truly worked out by analyzing the overlap complex in atomic detail. To conclude, we propose that the tail portion of troponin T is able to interact with two successive tropomyosins in the thin filament. The majority of the binding surface is supplied by the tropomyosin to which the core of the troponin complex is anchored, which was already known. But this thesis provides new evidence which indicates that the troponin T tail binds to a short segment within the adjoining tropomyosin.

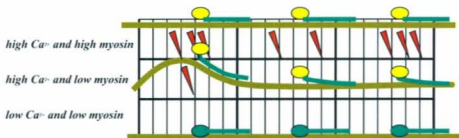
The two 'ends' (as defined by the first and the last ten amino acids) of muscle tropomyosin differ in terms of net charge at pH 7, sequence conservation (Mak et al 1980 and Sanders and Smillie 1985) and structure (Greenfield et al 2006). The amino-terminal region bears a net positive charge while the carboxyl-terminal region a net negative charge at pH 7. The former end is evolutionarily conserved whereas the latter end is less conserved. As mentioned before, the carboxyl-terminal end is less folded than the other. In this thesis we have shown more differences in the properties of the two ends of tropomyosin.

Firstly, the comparison of F-actin affinities of Omp T and carboxypeptidase digested tropomyosins under the same buffer compositions, clearly showed that removing six residues from the amino-terminus is more deleterious than removing eleven residues from the carboxyl-terminus. In the presence of added calcium (pCa 4), troponin-induced binding to F-actin was diminished to a greater extent with amino-terminally shortened tropomyosin (Figure 4.2) as compared to the carboxy-terminally shortened tropomyosin (Heeley et al 1987) even though the number of removed residues is smaller. Further, the N-TnT fragment showed no effect on the induction of Omp T-digested tropomyosin binding to F-actin (Figure 4.6), but this was not the case with carboxypeptidase-digested tropomyosin (Heeley et al 1987).

Next, in ATPase experiments carried out at pCa 4, thin filaments containing Omp T-digested tropomyosin activated myosin to a greater extent than fully integral thin

filaments (Figure 5.3), whereas thin filaments composed of carboxypeptidase-treated tropomyosin generated lesser activation than the native filaments (Heeley et al 1989a). Thus, the removal of each end of tropomyosin appears to have opposing effects in regulation. From these findings, we suggest that the amino-terminal region of tropomyosin promotes the turned-off state of thin filament (Figure 7.1), indirectly, via its interaction with N-TnT fragment. Disruption of this interaction, in the case of Omp T-digested tropomyosin, would be expected to interrupt the line of continuity within the thin filament. It follows that this could decrease troponin-induced tropomyosin binding to F-actin as well as myosin ATPase inhibition exerted by the N-TnT fragment. Further, these effects appear to be more pronounced at low pCa and low myosin concentrations. At high pCa, there are two portions of troponin; TnI and N-TnT fragment, contributing to the stability of the turned-off state of thin filament, thereby inhibiting myosin ATPase activity. Of the two, the inhibition of only the latter is affected by the removal of the amino-terminal hexapeptide of tropomyosin; therefore, the consequences of this defect are less significant, because, TnI alone could exert almost the full inhibition. However, in the calcium bound form of thin filament, interactions between the troponin core and tropomyosin are weakened and, therefore, TnI inhibition is released. Although, the interaction between the TnT tail and tropomyosin overlap is not affected directly by added calcium, it is partly disrupted in the case of Omp T-digested protein due to its lack of first six residues. Therefore, at low pCa, the effects of removing this hexapeptide on troponin-induced tropomyosin binding to F-actin and myosin ATPase inhibition become more prominent.

A) Thin filament system containing wild type tropomyosin



B) Thin filament system containing Omp T-digested tropomyosin

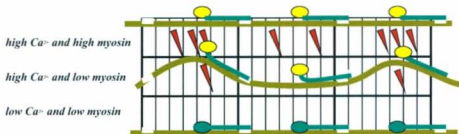


Figure 7.1: A model depicting the consequence of removing amino-terminal six residues of tropomyosin on the state of the thin filament

The model shows the changes in the positioning of regulatory proteins; tropomyosin and troponin, relative to actin upon binding of ligands (calcium and myosin). Each individual rectangle represents an actin monomer. The brown line shows a flexible continuous tropomyosin chain and, in the case of Omp T-digested tropomyosin, the white gap in the filament shows the missing hexapeptide (the length of the gap is exaggerated for illustrative purposes). Troponin is indicated by either red triangle (calcium free) or yellow (calcium bound). Myosin heads are shown by red triangles. Note that there are more regulatory units in the thin filaments containing Omp T-digested tropomyosin (B) in the turned-on state as compared to those in the native system (A).

The above-presented proposal is also compatible with myosin-S1-ADP binding experiments. Again, the consequence of removing the hexapeptide was opposite to that incurred by removal of the carboxyl end (Pan et al. 1989). The increased affinity of myosin-S1-ADP for thin filaments containing Omp T-digested protein (Figure 5.4) is indicative of the equilibrium regulatory units in this system being shifted more towards the turned-on state. At this point however, we can not explain why this effect is only observed at high pCa, unlike in ATPase experiments. It could be an effect of different nucleotides used in the two experiments, ADP versus ATP.

An alternative explanation for the role of the amino-terminal hexapeptide of tropomyosin is that this region itself is an inhibitory element of the thin filament. However, the above statement is unlikely to be true because this hexapeptide has no sequence homology with any known actin-binding site (Cho et al. 1990). Therefore, we conclude that the amino-terminal region of tropomyosin provides a binding surface for troponin T, through which it serves an inhibitory role in the regulation of myosin ATPase activity.

Above, we discussed the role of the amino-terminal end of tropomyosin, a region of the coiled-coil with high sequence conservation. The variability among tropomyosin sequences confers specialization of the molecule to a particular muscle, although this is not always obvious. Details of sequence heterogeneity, therefore, are the key to understanding structural and functional adaptations of tropomyosin in correlation with the

environment. The structural adaptation of a tropomyosin coiled-coil operating in a low-temperature regime is discussed below.

Atlantic salmon is a cold-water fish containing three main tropomyosin isoforms; each originates from a separate gene and is confined to one type of striated muscle (fast skeletal, slow skeletal and cardiac) (Heeley et al 1995). Unlike mammals, this fish does not utilize a tropomyosin isoform encoded by the beta gene (Figure 6.14). These salmon tropomyosins are less conformationally stable than rabbit skeletal tropomyosin (William and Swenson 1981, Jackman et al 1996), consistent with the idea that they have adapted to their environment. Of particular interest, in this respect, is the isoform in fast skeletal muscle, which displays a unique unfolding at room temperature (Figure 6.1). The loss of a core Ala and its replacement by a branched, polar side-chain (the isomorphism at residue 179, alanine to threonine) (Figure 6.11) in this protein appears to have 'accentuated' the thermal-induced unfolding of a low stability region around Cys190 (Lehrer 1978). The fast isoform and the cardiac isoform contain another strategy to life in the cold waters of the Atlantic; again in context of a coiled coil, appears to be the inclusion of pairs of closely-spaced glycines (Figure 6.12). As a result the amino terminal half of the former isoform is destabilized relative to the carboxyl half, which is the opposite of what has been detected with rabbit skeletal tropomyosin. The disparity in the susceptibilities of salmon fast muscle and rabbit skeletal tropomyosins to *Omp T* (Figure 3.2) also supports the above suggestion that the tropomyosin amino-terminal region from fish is less stable than that from mammal. Thus, amino acid substitutions at key positions

in the coiled-coil have changed the stabilities of tropomyosin, which in turn affect its functions, in accordance to the environment.

Future directions

As a continuation of the myosin ATPase regulation by the thin filament system containing the Omp T-digested tropomyosin at steady state, it would be interesting to perform these experiments at pre-steady state using a fast mixing (stop-flow) apparatus. This would also allow an opportunity to determine the cooperative unit size of this system. The knowledge about the cooperative unit size of this system will provide insight into the extent that the removal of the first six residues affects continuity of the thin filament.

It will also be of interest to identify key residues within the amino-terminal hexapeptide that are more crucial to tropomyosin function. In this regard, the charged amino acids, which might be important for interactions with the amino-terminal peptide of troponin-T, would be prime candidates. This can be achieved by making full-length tropomyosins that have single or a few substitutions at key positions, like the ones mentioned above, using site directed mutagenesis. Similarly, the way to confirm the effect of core substitutions (179, alanine to threonine; 186, alanine to serine; 211 alanine to serine) in the fifth period of tropomyosin on its conformational stability is to mutate those residues in the salmonid tropomyosin sequences back to alanines and analyze the changes in their conformational stabilities using CD. The mutants can also be investigated for their actin

affinities to see if those substitutions have an impact on actin binding, as was previously observed with the F-actin affinity of the fast isoform at room temperature. The influence of the glycyl pair on the stability of the amino terminal half of the molecule could also be examined the same way by mutating Gly24 and Gly27 to Asp and Ala respectively, as in the rabbit alpha tropomyosin. These studies will provide insight into the key isomorphisms in the primary structures of salmonid tropomyosins that have enabled them to adapt to a cold environment.

Publications and papers presented at conferences.

1. Goonasekara, C. L., Gallivan, L., Jackman, D., & Heeley, D. H. (2007). Some binding properties of Omp T protease digested muscle tropomyosin. *J Muscle Res Cell Motil*, 28, 175-182.
2. Goonasekara, C. L., Heeley, D. H. (2008) Effects of removal of the amino terminal six amino acids of tropomyosin on the regulatory properties of the striated muscle thin filament, *Eur J Biol Chem* (to be submitted).
3. Goonasekara, C. L., Mudalige A. W., Heeley, D. H. (2008) Conformational and regulatory properties of striated muscle tropomyosins from salmonid fish, *Protein Sci* (to be submitted).
4. Goonasekara, C. L., Heeley, D. H. (2008) F-actin Binding And Regulatory Properties Of An Amino-terminally Truncated Tropomyosin. 52nd Annual meeting of Biophysical Society, Long Beach, California.
5. Goonasekara, C. L., Jackman, D., Heeley, D. H. (2007) An amino terminally truncated tropomyosin. 51th Annual meeting of Biophysical Society, Baltimore.

6. Goonasekara, C. L., Martin, G. R., Heeley, D. H. (2006) Analysis of the conformational stability of a tropomyosin isoform from a cold water fish. 50th Annual meeting of Biophysical Society, Salt Lake city.

7. Goonasekara, C. L., Gallivan, L., Heeley, D. H. (2005), Investigation of the interaction between tropomyosin and troponin, 6th European symposium of the protein society, Barcelona.

References

- Aidley, D. J. (1971). The comparative physiology of muscle. *The physiology of excitable cells* (pp. 304-306). Cambridge, UK: Cambridge university press.
- Al-Khayat, H. A., Yagi, N., & Squire, J. M. (1995). Structural changes in actin-tropomyosin during muscle regulation: Computer modelling of low-angle X-ray diffraction data. *J Mol Biol*, 252, 611-632.
- Allen, G. (1989). Laboratory techniques in biochemistry and molecular biology. In R. H. Burdon, & P. H. V. Knippenberg (Eds.), (2nd ed., pp. 56-57). Amsterdam: Elsevier Science publishers.
- Amphlett, G. M., Syska, H., & Perry, S. V. (1976). The polymorphic forms of tropomyosin and troponin I in developing rabbit skeletal muscle. *FEBS Letts*, 63, 22-26.
- Anderson, P. A. W., Malouf, N. N., Oakeley, A. E., Pagani, E. D., & Allen, P. D. (1991). Troponin T isoform expression in humans: A comparison among normal and failing heart, fetal heart and adult and fetal skeletal muscle. *Circ Res*, 69, 1226-1233.
- Arakawa, T., & Timasheff, S. N. (1985). The stabilization of proteins by osmolytes. *Biophys J*, 47, 411-414.

- Arata, T., Aihara, T., Ueda, K., Nakamura, M., & Ueki, S. (2007). Calcium structural transition of troponin in the complexes, on the thin filament, and in muscle fibres, as studied by site-directed spin-labelling EPR. *Adv Exp Med Biology*, 592, 125-136.
- Astbury, W. T., Reed, R., & Spark, L. C. (1948). An X-ray and electron microscope study of tropomyosin. *Biochem J*, 43, 282-287.
- Bailey, K. (1946). Tropomyosin: A new symmetric protein component of muscle. *Nature*, 157, 368-369.
- Bailey, K. (1948). Tropomyosin: A new symmetric protein component of muscle. *Biochem J*, 43, 271-275.
- Bailey, K. (1951). End group assay in some proteins of the keratin-myosin group. *Biochem J*, 49, 23-27.
- Basi, G. S., & Storti, R. V. (1986). Structure and DNA sequence of the tropomyosin I gene from drosophila metalogaster. *J Biol Chem*, 261, 817-827.
- Betcher-Lange, S. L., & Lehrer, S. S. (1978). Pyrene excimer fluorescence in rabbit skeletal alpha-alpha-tropomyosin labeled with N-(1-pyrene) maleimide. *J Biol Chem*, 253, 3757-3760.
- Bettersidge, D. R., & Lehrer, S. S. (1983). Two conformational states of didansylcysteine-labeled rabbit cardiac tropomyosin. *J Mol Biol*, 167, 481-496.

- Billeter, R., Heizmann, C. W., Howald, H., & Jenny, E. (1982). Alpha and beta-tropomyosin in typed single fibres of human skeletal muscle. *FEBS Letts*, 132, 133-136.
- Bing, W., Knott, A., Redwood, C., Esposito, G., Purcell, I., Watkins, H., et al. (2000). Effect of hypertrophic cardiomyopathy mutations in human cardiac muscle alpha-tropomyosin (Asp175Asn and Glu180Gly) on the regulatory properties of human cardiac troponin determined by in vitro motility assay. *J Mol Cell Cardiol*, 32, 1489-1498.
- Bing, W., Redwood, C., Purcell, I., Esposito, G., Watkins, H., & Marston, S. (1997). Effects of two hypertrophic cardiomyopathy mutations in alpha-tropomyosin, Asp175Asn and Glu180Gly, on calcium regulation of thin filament motility. *Biochem Biophys Res Commun*, 236, 760-764.
- Bivin, D. B., Stone, D. B., Schneider, D. K., & Mendelson, R. A. (1991). Cross-helix separation of tropomyosin molecules in acto-tropomyosin as determined by neutron scattering. *Biophys J*, 59, 880-888.
- Bonder, E. M., Fishkind, D. J., & Mooseker, M. S. (1983). Direct measurement of critical concentrations and assembly rate constants at the two ends of an actin filament. *Cell*, 34, 491-502.
- Boussouf, S. E., & Geeves, M. A. (2007). Tropomyosin and troponin cooperativity on the thin filament. *Adv Exp Med Biology*, 592, 99-109.

- Bradford, M. M. (1976). A rapid and sensitive method for the quantitation of microgram quantities of proteins utilizing the principle of protein dye binding. *Anal Biochem*, 72, 248-254.
- Brahms, S., & Brahms, J. (1980). Determination of protein secondary structure in solution by vacuum ultraviolet circular dichroism. *J Mol Biol*, 138, 149-178.
- Bremel, R. D., Murray, J. M., & Weber, A. (1972). Manifestations of cooperative behaviour in the regulated actin filament during actin-activated ATP hydrolysis in the presence of calcium. *Cold Spring Harbor Symp Quan Biol*, 37, 267-275.
- Bremel, R. D., & Weber, A. (1972). Cooperation within actin filament in vertebrate skeletal muscle. *Nat New Biol*, 238, 97-101.
- Brisson, J. R., Golosinska, K., Smillie, L. B., & Sykes, B. D. (1986). Interaction of tropomyosin and troponin-T: A proton nuclear magnetic resonance study. *Biochemistry*, 25, 4548-4555.
- Bronson, D. D., & Schachat, F. H. (1982). Heterogeneity of contractile proteins. *J Biol Chem*, 257, 3937-3944.
- Brown, J. H., Kim, K. H., Jun, G., Greenfield, N. J., Dominguez, R., Volmann, N., et al. (2001). Deciphering the design of the tropomyosin molecule. *Proc Natl Acad Sci USA*, 98, 8496-8501.
- Brown, J. H., & Cohen, C. (2005). Regulation of muscle contraction by tropomyosin and troponin: How structure illuminates function. *Adv Protein Chem*, 71, 121-159.

- Bullard, B., Mercola, D. A., & Mommaerts, W. F. H. M. (1976). The origin of tyrosyl circular dichroism of tropomyosin. *Biochim Biophys Acta*, 434, 90-99.
- Butters, C. A., Willadsen, K. A., & Tobacman, L. S. (1993). Cooperative interactions between adjacent troponin-tropomyosin complexes may be transmitted through the actin filament. *J Biol Chem*, 268, 15565-15570.
- Byers, D. M., & Kay, C. M. (1983). Hydrodynamic properties of bovine cardiac troponin-I and troponin-T. *J Biol Chem*, 258, 2951-2954.
- Carlier, M. F. (1991). Actin: Protein structure and filament dynamics. *J Biol Chem*, 266, 1-4.
- Carlier, M. F., Criquet, P., Pantaloni, D., & Korn, E. D. (1986a). Interaction of cytochalasin D with actin filaments in the presence of ADP and ATP. *J Biol Chem*, 261, 2041-2050.
- Carlier, M. F., Pantaloni, D., & Korn, E. D. (1986b). The effects of Mg²⁺ at the high-affinity and low-affinity sites on the polymerization of actin and associated ATP hydrolysis. *J Biol Chem*, 261, 10785-10792.
- Chalovich, J. M. (2002). Regulation of striated muscle contraction: A discussion. *J Muscle Res Cell Motil*, 23, 353-361.
- Chalovich, J. M., Chock, P. B., & Eisenberg, E. (1981). Mechanism of action of troponin . tropomyosin. inhibition of actomyosin ATPase activity without inhibition of myosin binding to actin. *J Biol Chem*, 256, 575-578.

- Chao, Y. Y. H., & Holtzer, A. (1975). Spin-label studies of tropomyosin. *Biochemistry*, *14*, 2164-2170.
- Cho, Y., Liu, J., & Hitchcock-DeGregori, S. E. (1990). The amino terminus of muscle tropomyosin is a major determinant for function. *J Biol Chem*, *265*, 538-545.
- Chong, P. C., & Hodges, R. S. (1982). Photochemical cross-linking between rabbit skeletal troponin and alpha-tropomyosin. attachment of the photoaffinity probe N-(4-azidobenzoyl-[2-3H]glycyl)-S-(2-thiopyridyl)-cysteine to cysteine 190 of alpha-tropomyosin. *J Biol Chem*, *257*, 9152-9160.
- Clayton, L., Reinach, L. C., Chumbley, G. M., & MacLeod, A. R. (1988). Organization of the hTMnm gene: Implication for the evolution of muscle and non-muscle tropomyosins. *J Mol Biol*, *201*, 507-515.
- Cooper, J. A., Buhle, E. L., Walker, S. B., Tsong, T. Y., & Pollard, T. D. (1983). Kinetic evidence for a monomer activation step in actin polymerization. *Biochemistry*, *22*, 2193-2202.
- Cooper, T. M., & Woody, R. W. (1990). The effect of conformation on the CD of interacting helices: A theoretical study of tropomyosin. *Biopolymers*, *30*, 657-676.
- Coue, M., & Korn, E. D. (1985). Interaction of plasma gelsolin with G-actin and F-actin in the presence and absence of calcium ions. *J Biol Chem*, *260*, 15033-15041.
- Craig, R., & Lehman, W. (2002). The ultrastructural basis of actin filament regulation. *Results Probl Cell Differ*, *36*, 149-169.

- Crick, F. H. C. (1953). The packing of alpha helices: Simple coiled-coils. *Acta Crystallogr*, 6, 689-697.
- Cummins, P., & Perry, S. V. (1973). The subunits and biological activity of polymorphic forms of tropomyosin. *Biochem J*, 133, 765-777.
- Cummins, P., & Perry, S. V. (1974). Chemical and immunochemical characteristics of tropomyosin from striated and smooth muscle. *Biochem J*, 141, 43-49.
- Cuticchia, A. J., & Pearson, P. L. (1993). Human gene mapping: A compendium. Baltimore: Johns Hopkins University Press.
- Davies, R. E., & Hill, A. V. (1964). Adenosine triphosphate breakdown during single muscle contractions. *Proc R Soc Lond B Biol Sci*, 160, 480-485.
- Dekker, N., Ruud, C. C., Kramer, A., & Egmond, M. R. (2001). Substrate specificity of the integral membrane protease omp T determined by spatially addressed peptide libraries. *Biochemistry*, 40, 1694-1701.
- DeRosier, D. J., & Moore, P. B. (1970). Reconstruction of three-dimensional images from electron micrographs of structures with helical symmetry. *J Mol Biol*, 52, 355-362.
- Drees, B., Brown, C., Barrel, B. G., & Bretscher, A. (1995). Tropomyosin is essential in yeast, yet the TPM1 and TPM2 products perform distinct functions. *J Cell Biol*, 128, 383-392.

- Eaton, B. L., Kominz, D. R., & Eisenberg, E. (1975). Correlation between the inhibition of the acto-heavy meromyosin ATPase and the binding of tropomyosin to F-actin: Effects of Mg²⁺, KCl, troponin I and troponin C. *Biochemistry*, *14*, 2718-2725.
- Eaton, B. L. (1976). Tropomyosin binding to F-actin induced by myosin heads. *Science*, *192*, 1337-1339.
- Ebashi, S. (1963). Third component participating in the superprecipitation of natural acto myosin. *Nature*, *200*, 1010.
- Ebashi, S. (1972). Separation of troponin into its three components. *J Biochem (Tokyo)*, *72*, 787-790.
- Ebashi, S., & Ebashi, F. (1964). A new protein component participating in the superprecipitation of myosin B. *J Biochem*, *55*, 604-613.
- Ebashi, S., & Kodama, A. (1965). A new protein factor promoting aggregation of tropomyosin. *J Biochem*, *58*, 107-108.
- Edwards, B. F. P., & Sykes, B. D. (1978). Assignment and characterization of the histidine resonances in the proton nuclear magnetic resonance spectra of rabbit tropomyosins. *Biochemistry*, *17*, 684-689.
- Edwards, B. F. P., & Sykes, B. D. (1980). Nuclear magnetic resonance evidence for the coexistence of several conformational states of rabbit cardiac and skeletal tropomyosins. *Biochemistry*, *19*, 2577-2583.

- Edwards, B. F. P., & Sykes, B. D. (1981). Analysis of cooperativity observed in pH titrations of proton nuclear magnetic resonances of histidine residues of rabbit cardiac tropomyosin. *Biochemistry*, *20*, 4193-4198.
- Eisenberg, E., & Kielley, W. W. (1974). Troponin-tropomyosin complex. column chromatographic separation and activity of the three, active troponin components with and without tropomyosin present. *J Biol Chem*, *249*, 4742-4748.
- Elliott, A., & Offer, G. (1978). Shape and flexibility of the myosin molecule. *J Mol Biol*, *123*, 505-519.
- Elzinga, M., Collins, J. H., Kuehl, W. M., & Adelstein, R. S. (1973). Complete amino-acid sequence of actin of rabbit skeletal muscle. *Proc Natl Acad Sci USA*, *70*, 2687-2691.
- Engel, J., Fasold, H., Hulla, F. W., Waechter, F., & Wegner, A. (1977). The polymerization reaction of muscle actin. *Mol Cell Biochem*, *18*, 3-13.
- Engel, M., Williams, R. W., & Erickson, B. W. (1991). Designed coiled-coils proteins: Synthesis and spectroscopy of two 78-residue alpha-helical dimers. *Biochemistry*, *30*, 3161-3169.
- Engelhardt, V. A., & Lyubimova, M. N. (1939). Myosin and adenosinetriphosphatase. *Nature*, *144*, 668.

- Farah, C. S., Miyamoto, C. A., Ramos, C. H., da Silva, A. C., Quaggio, R. B., Fujimori, K. (1994). Structural and regulatory functions of the NH₂ and COOH terminal regions of skeletal muscle troponin I. *J Biol Chem*, 269, 5230-5240.
- Flicker, P. F., Phillips, G. N., & Cohen, C. (1982). Troponin and its interactions with tropomyosin : An electron microscope study. *J Mol Biol*, 162, 495-501.
- Forry-Schaudies, S., Gruber, C. E., & Hughes, S. H. (1990a). Chicken cardiac tropomyosin and a low molecular weight nonmuscle tropomyosin are related to alternative splicing. *Cell Growth Differ*, 1, 473-481.
- Forry-Schaudies, S., Maihle, N. J., & Hughes, S. H. (1990b). Generation of skeletal, smooth and low molecular weight non-muscle tropomyosin isoforms from the chicken tropomyosin I gene. *J Mol Biol*, 211, 321-330.
- Franzini-Armstrong, C., & Peachey, L. D. (1981). Striated muscle-contractile and control mechanisms. *J Cell Biol*, 91, 166s-186s.
- Frieden, C., Lieberman, D., & Gilbert, H. R. (1980). A fluorescent probe for conformational changes in skeletal muscle G- actin. *J Biol Chem*, 255, 8991-8993.
- Gagné, S. M., Monica, S. T., Li, X., Smillie, L. B., & Sykes, B. D. (1995). Structures of the troponin C regulatory domains in the apo and calcium-saturated states. *Nat Struct Biol*, 2, 784-789.
- Gazith, J., Himmelfarb, S., & Harrington, W. F. (1970). Studies on the subunit structure of myosin. *J Biol Chem*, 245, 15-22.

- Gershman, L. C., Newman, J., Selden, L. A., & Estes, J. E. (1984). Bound-cation exchange affects the lag phase in actin polymerization. *Biochemistry*, 23, 2199-2203.
- Goonasekara, C. L., Gallivan, L., Jackman, D., & Heeley, D. H. (2007). Some binding properties of Omp T protease digested muscle tropomyosin. *J Muscle Res Cell Motil*, 28, 175-182.
- Graceffa, P., & Dominguez, R. (2003). Crystal structure of monomeric actin in the ATP state. Structural basis of nucleotide-dependent actin dynamics. *J Biol Chem*, 278, 34172-34180.
- Graceffa, P., & Lehrer, S. S. (1980). The excimer fluorescence of pyrene-labeled tropomyosin. A probe of conformational dynamics. *J Biol Chem*, 255, 11296-11300.
- Graceffa, P., & Lehrer, S. S. (1983). Two conformational states of tropomyosin. A spin labeled study. *Biophys J*, 37a
- Graceffa, P., & Lehrer, S. S. (1984). Dynamic equilibrium between the two conformational states of spin labeled tropomyosin. *Biochemistry*, 23, 2606-2612.
- Greaser, M. L., & Gergely, J. (1971). Reconstitution of troponin activity from three protein components. *J Biol Chem*, 246, 4226-4233.
- Greaser, M. L., & Gergely, J. (1973). Purification and properties of the components from troponin. *J Biol Chem*, 248, 2125-2133.

- Greenfield, N., & Fasman, G. D. (1967). Computed circular dichroism spectra for the evaluation of protein conformation. *Biochemistry*, 8, 4108-4116.
- Greenfield, N. J., Huang, Y. J., Swapna, G. V. T., Bhattacharya, A., Rapp, B., Singh, A., et al. (2006). Solution NMR structure of the junction between tropomyosin molecules: Implications for actin binding and regulation. *J Mol Biol*, 364, 80-96.
- Greenfield, N. J., Stafford, W. F., & Hitchcock-DeGregori, S. E. (1994). The effect of N-terminal acetylation on the structure of an N-terminal tropomyosin peptide and alpha-tropomyosin. *Protein Sci*, 3, 402-410.
- Greenfield, N. J., & Hitchcock-DeGregori, S. E. (1993). Conformational intermediates in the folding of a coiled-coil model peptide of the N-terminus of tropomyosin and alpha-alpha-tropomyosin. *Protein Sci*, 2, 1263-1273.
- Greenfield, N. J., Monterline, G. T., Farid, R. S., & Hitchcock De-Gregori, S. E. (1998). The structure of the N-terminus of striated muscle alpha-tropomyosin in a chimeric peptide: Nuclear magnetic resonance structure and circular dichroism studies. *Biochemistry*, 37, 7834-7843.
- Greenfield, N. J., Swapna, G. V., Huang, Y., Palm, T., Graboski, S., Montelione, G. T. (2003). The structure of the carboxy terminus of striated alpha-tropomyosinin solution reveals an unusual parallel arrangement of interacting alpha-helices. *Biochemistry*, 42, 614-619.

- Greshman, L. C., Newman, J., Selden, L. A., & Estes, J. E. (1984). Bound-cation exchange affects the lag phase in actin polymerization. *Biochemistry*, 23, 2199-2203.
- Gunning, P., Gordon, M., Wade, R., Gailman, R., Lin, C., & Hardeman, E. (1990). Differential control of tropomyosin mRNA levels during myogenesis suggests the existence of an isoform competition-autoregulatory compensation mechanism. *Dev Biol*, 138, 443-453.
- Hai, H., Sano, K. I., Maeda, K., Maeda, Y., & Miki, M. (2002). Ca²⁺- and SI-induced conformational changes of reconstituted skeletal muscle thin filaments observed by fluorescence energy transfer spectroscopy: Structural evidence for three states of thin filament. *J Biochem (Tokyo)*, 131, 407-418.
- Hammell, R. L., & Hitchcock De-Gregori, S. E. (1996). Mapping the functional domains within the carboxyl terminus of alpha-tropomyosin encoded by the alternatively splice ninth exon. *J Biol Chem*, 271, 4236-4242.
- Hammell, R. L., & Hitchcock De-Gregori, S. E. (1997). The sequence of the alternatively spliced sixth exon of alpha-tropomyosin is critical for cooperative actin binding but not for interaction with troponin. *J Biol Chem*, 272, 22409-22416.
- Hanson, J., & Huxley, H. E. (1953). Structural basis of the cross-striations in muscle. *Nature*, 172, 530-532.
- Harrington, W. F., & Rodgers, M. E. (1984). Myosin. *Annu Rev Biochem*, 53, 35-73.

- Hartshorne, D. J., & Dreizen, P. (1972). Studies on the subunit composition of troponin. *Cold Spring Harbor Symp Quant Biol*, 37, 225-234.
- Hartshorne, D. J., & Mueller, H. (1968). Fractionation of troponin into two distinct proteins. *Biochem Biophys Res Commun*, 31, 647-653.
- Hartshorne, D. J., & Mueller, H. (1969). The preparation of tropomyosin and troponin from natural actomyosin. *Biochim Biophys Acta*, 175, 301-319.
- Hartshorne, D. J., & Pyun, H. Y. (1971). Calcium binding by the troponin complex, and the purification and properties of troponin A. *Biochim Biophys Acta*, 229, 698-711.
- Haselgrove, J. C. (1972). X-ray evidence for a conformational change in the actin containing filaments of vertebrate striated muscle. *Cold Spring Harbor Symp Quant Biol*, 37, 341-352.
- Hayashi, T., & Ip, W. (1976). Polymerization polarity of actin. *J Mechanochem Cell Motil*, 3, 163-169.
- Heald, R. W., & Hitchcock-DeGregori, S. E. (1988). The structure of the amino terminus of tropomyosin is critical for binding to actin in the absence and presence of troponin. *J Biol Chem*, 263, 5254-5259.
- Heeley, D. H., Belknap, B., & White, H. D. (2006). Maximal activation of skeletal muscle thin filaments requires both rigor myosin S1 and calcium. *J Biol Chem*, 281, 668-676.

- Heeley, D. H., & Hong, C. (1994). Isolation and characterization of tropomyosin from fish muscle. *Comp Biochem Physiol*, 108, 95-106.
- Heeley, D. H. (1994). Investigation of the effects of phosphorylation of rabbit striated muscle alpha-tropomyosin and rabbit skeletal muscle troponin-T. *Eur J Biochemistry*, 221, 129-137.
- Heeley, D. H., Beiger, T., Waddleton, D. M., Hong, C. D., Jackman, M., McGowan, C., et al. (1995). Characterisation of fast, slow and cardiac muscle tropomyosins from salmonid fish. *Eur J Biochem*, 232, 226-234.
- Heeley, D. H., Belknap, B., & White, H. D. (2002). Mechanism of regulation of phosphate dissociation from actomyosin-ADP-Pi by thin filament proteins. *Proc Natl Acad Sci USA*, 99, 16731-16736.
- Heeley, D. H., Dhoot, D. K., Frearson, N., Perry, S. V., & Vrbova, G. (1983). The effect of cross innervation on the tropomyosin composition of rabbit skeletal muscle. *FEBS Letts*, 152, 282-286.
- Heeley, D. H., Golonska, K., & Smillie, L. B. (1987). The effects of troponin T fragments T1 and T2 on the binding of nonpolymerizable tropomyosin to F-actin in the presence and absence of troponin I and troponin C. *J Biol Chem*, 262, 9971-9977.
- Heeley, D. H., Smillie, L. B., & Lohmeier-Vogel, E. M. (1989a). Effects of deletion of tropomyosin overlap on regulated actomyosin subfragment I ATPase. *Biochem J*, 258, 831-836.

- Heeley, D. H., Watson, M. H., Mac, A. S., Dubord, P. L., & Smillie, B. (1989b). Effect of phosphorylation on the interaction and functional properties of rabbit striated muscle alpha-tropomyosin. *J Biol Chem*, 264, 2424-2430.
- Helfman, D. M., Cheley, S., Kuismanen, E., Finn, A., & Yamamaki-Katoaka, Y. (1986). Nonmuscle and muscle tropomyosins are expressed from a single gene by alternate splicing and polyadenylation. *Mol Cell Biol*, 6, 3582-3595.
- Hennessey, J. P., & Johnson, C. J. (1981). Information content in the circular dichroism of proteins. *Biochemistry*, 20, 1085-1094.
- Herzberg, O., & James, M. N. G. (1985). Structure of the calcium regulatory muscle protein troponin-C at 2.8 Å resolution. *Nature*, 313, 253-259.
- Herzberg, O., Moul, J., & James, M. N. (1986). A model for the Ca²⁺-induced conformational transition of troponin C. A trigger for muscle contraction. *J Biol Chem*, 261, 2638-2644.
- Hill, T. L. (1980). Bioenergetic aspects and polymer length distribution in steady-state head-to-tail polymerization of actin or microtubules. *Proc Natl Acad Sci USA*, 77, 4803-4807.
- Hill, T. L., Eisenberg, E., & Greene, L. (1980). Theoretical model for the cooperative equilibrium binding of myosin subfragment 1 to the actin-troponin-tropomyosin complex. *Proc Natl Acad Sci USA*, 77, 3186-3190.

- Hitchcock-DeGregori, S. E., & An, Y. (1996). Integral repeats and a continuous coiled coil are required for binding of striated muscle tropomyosin to the regulated actin filament. *J Biol Chem*, 271, 3600-3603.
- Hitchcock-DeGregori, S. E., & Heald, R. W. (1987). Altered actin and troponin binding of amino-terminal variants of chicken striated muscle alpha-tropomyosin expressed in *Escherichia coli*. *J Biol Chem*, 262, 9730-9735.
- Hitchcock-DeGregori, S. E., Song, Y., & Greenfield, N. J. (2002). Functions of tropomyosin's periodic repeats. *Biochemistry*, 41, 15036-15044.
- Hitchcock-DeGregori, S. E., Song, Y., & Moraczewska, J. (2001). Importance of internal regions and the overall length of tropomyosin for actin binding and regulatory function. *Biochemistry*, 40, 2104-2112.
- Hitchcock-DeGregori, S. E., & Varnell, T. A. (1990). Tropomyosin has discrete actin-binding sites with sevenfold and fourteenfold periodicities. *J Mol Biol*, 214, 885-896.
- Hitchcock-DeGregori, S. E., Greenfield, N. J., & Singh, A. (2007). Tropomyosin: Regulator of actin filaments. *Adv Exp Med Biology*, 592, 87-98.
- Hodges, R. S., Sodek, J., Smillie, L. B., & Jurasek, L. (1972). Tropomyosin: Amino acid sequence and coiled-coil structure. *Cold Spring Harbor Symp Quant Biol*, 37, 299-310.

- Hodges, R. S., Zhou, N. E., Kay, C. M., & Semchuk, P. D. (1990). Synthetic model proteins: Contribution of hydrophobic residues and disulfide bonds to protein stability. *Peptide Res*, 3, 123-137.
- Holmes, K. C. (1995). The actomyosin interaction and its control by tropomyosin. *Biophys J*, 68, 2S-7S.
- Holmes, K. C., Popp, D., Gebhard, W., & Kabsch, W. (1990). Atomic model of the actin filament. *Nature*, 347, 44-49.
- Holtzer, M. E., Holtzer, A., & Skolnik, J. (1983). Alpha helix to random coil transition of two chain, coiled coils: Theory and experiments for thermal denaturation of alpha tropomyosin at acidic pH. *Macromolecules*, 16, 462-465.
- Holtzer, M. E., Kumar, S., & Holtzer, A. (1989). The CD of two-chain coiled coils: Experiments on tropomyosin and tropomyosin segments in the tyrosine / disulphide spectral region. *Biopolymers*, 28, 1597-1612.
- Houdusse, A., Love, M. L., Dominguez, R., Grabarek, Z., & Cohen, C. (1997). Structures of four Ca^{2+} -bound troponin C at 2.0 Å resolution: Further insights into the Ca^{2+} -switch in the calmodulin superfamily. *Structure*, 5, 1695-1711.
- Huxley, A. F., & Niedergerke, R. (1954). Interference microscopy of living muscle fibres. *Nature*, 173, 171-173.
- Huxley, A. F., & Simmons, R. M. (1971). Proposed mechanism of force generation in striated muscle. *Nature*, 233, 533-558.

- Huxley, H. E. (1969). The mechanism of muscular contraction. *Science*, 164, 1356-1366.
- Huxley, H. E. (1972). Structural changes in the actin- and myosin- containing filaments during contraction. *Cold Spring Harbor Symp Quan Biol*, 37, 361-376.
- Huxley, H. E. (1957). The double array of filaments in cross-striated muscle. *J Biophys Biochem Cytol*, 25, 631-648.
- Huxley, H. E. (1963). Electron microscope studies on the structure of natural and synthetic protein filaments from striated muscle. *J Mol Biol*, 7, 281-308.
- Huxley, H. E., & Hanson, J. (1954). Changes in the cross-striations of muscle contraction and their structural interpretation. *Nature*, 173, 973-976.
- Ishi, Y., & Lehrer, S. S. (1991). Two-site attachment of troponin to pyrene-labeled tropomyosin. *J Biol Chem*, 266, 6894-6903.
- Jackman, D. M., Waddeleton, D. M., Youngusband, B., & Heeley, D. H. (1996). Further characterization of fast, slow and cardiac muscle tropomyosins from salmonid fish. *Eur J Biochem*, 242, 363-371.
- Jackson, P., Amphlett, G. W., & Perry, S. V. (1975). The primary structure of troponin T and the interaction with tropomyosin. *Biochem J*, 151, 85-97.
- Johnson, K. A., & Taylor, E. W. (1978). Intermediate states of subfragment 1 and actosubfragment 1 ATPase. *Biochemistry*, 17, 3432-3442.

- Johnson, P., & Smillie, L. B. (1975). Rabbit skeletal alpha-tropomyosin are in register. *Biochem Biophys Res Commun*, 82, 1013-1018.
- Johnson, P., & Smillie, L. B. (1977). Polymerizability of rabbit skeletal tropomyosin: Effects of enzymic and chemical modifications. *Biochemistry*, 16, 2264-2269.
- Kabsch, W., Mannherz, H. G., Suck, D., Pai, E. F., & Holmes, K. C. (1990). Atomic structure of the actin: DNase I complex. *Nature*, 347, 37-44.
- Kimura, C., Maeda, K., Maeda, Y., & Miki, M. (2002). Ca²⁺S1-induced movement of troponin T on reconstituted skeletal muscle thin filaments observed by fluorescence energy transfer spectroscopy. *J Biochem (Tokyo)*, 132, 93-102.
- Kluwe, L., Maeda, K. A., Miegel, A., Fujita-Becker, S., Maeda, Y., Talbo, G., et al. (1995). Rabbit skeletal muscle alpha-tropomyosin expressed in baculovirus-infected insect cells possesses the authentic N-terminus structure and functions. *J Muscle Res Cell Motil*, 16, 103-110.
- Kobayashi, T., Kobayashi, M., & Collins, J. H. (2001). Ca(2+)-dependent, myosin subfragment 1-induced proximity changes between actin and the inhibitory region of troponin I. *Biochim Biophys Acta*, 1549, 148-154.
- Kondo, H., & Ishiwata, S. (1976). Uni-directional growth of F-actin. *J Biochem (Tokyo)*, 79, 159-171.
- Kretsinger, R. H., & Nockolds, C. E. (1973). Carp muscle calcium-binding protein. II. Structure determination and general description. *J Biol Chem*, 248, 3313-3326.

- Krishnan, K. S., Brandts, J. F., & Lehrer, S. S. (1978). Effects of an interchain disulfide bond on tropomyosin structure : Differential scanning calorimetry. *FEBS Letters*, *91*, 206-208.
- Kunz, W., Henle, J., & Ninham, B. W. (2004). 'Zur lehre von der wirkung der salze' (about the science of the effect of salts): Franz hofmeister's historical papers. *Curr Opin Coll Interface Sci*, *9*, 19-37.
- Kwok, S. C., & Hodges, R. S. (2004). Stabilizing and destabilizing clusters in the hydrophobic core of long two-stranded alpha-helical coiled-coils. *J Biol Chem*, *279*, 21576-21588.
- Laemmli, U. K. (1970). Cleavage of structural proteins during the assembly of the head of bacteriophage T4. *Nature*, *227*, 680-685.
- Landis, C., Back, N., Homsher, E., & Tobacman, L. S. (1999). Effects of tropomyosin internal deletions on thin filament function. *J Biol Chem*, *274*, 31279-31285.
- Landis, C. A., Bobkova, A., Homsher, E., & Tobacman, L. S. (1997). The active state of the thin filament is destabilized by an internal deletion in tropomyosin. *J Biol Chem*, *272*, 14051-14056.
- Lees-Miller, J. P., Goodwin, L. O., & Helfman, D. M. (1990a). Three novel brain tropomyosin isoforms are expressed from the rat alpha-tropomyosin gene through the use of alternative promoters and alternative RNA processing. *Mol Cell Biol*, *10*, 1729-1742.

- Lees-Miller, J. P., & Helfman, D. V. (1991). The molecular basis for tropomyosin isoform diversity. *Bioassays*, 13, 429-437.
- Lees-Miller, J. P., Yan, A., & Helfman, D. M. (1990b). Structure and complete nucleotide sequence of the gene encoding rat fibroblast tropomyosin 4. *J Mol Biol*, 213, 339-405.
- Lehman, W., Craig, R., & Vibert, P. (1994a). Ca^{2+} -induced tropomyosin movement in *limulus* thin filaments revealed by three-dimensional reconstruction. *Nature*, 368, 65-67.
- Lehman, W., Rosal, M., Hatch, V., Korman, V., Horowitz, R., Van Eyk, J. (2000). Tropomyosin control of thin filament activity revealed by electron microscopy and 3D reconstruction. *Biophys J*, 78a, 908-917.
- Lehman, W., Vibert, P., Uman, P., & Craig, R. (1994b). Steric blocking mechanism visualized in relaxed vertebrate muscle thin filaments. *J Mol Biol*, 251, 191-196.
- Lehrer, S. S. (1975). Intramolecular crosslinking of tropomyosin via disulphide bond formation: Evidence for chain register. *Proc Natl Acad Sci USA*, 71, 3377-3381.
- Lehrer, S. S. (1978). Effects of an interchain disulfide bond on tropomyosin structure: Intrinsic fluorescence and circular dichroism studies. *J Mol Biol*, 118, 209-226.
- Lehrer, S. S. (1994). The regulatory switch of the muscle thin filament: Ca^{2+} or myosin heads? *J Muscle Res Cell Motil*, 15, 232-236.

- Lehrer, S. S., & Geeves, M. A. (1998). The muscle thin filament as a classical cooperative/allosteric regulatory system. *J Mol Biol*, 277, 1081-1089.
- Lehrer, S. S., Golitsina, N. L., & Geeves, M. A. (1997). Actin-tropomyosin activation of myosin subfragment 1 ATPase and thin filament cooperativity. the role of tropomyosin flexibility and end-to-end interactions. *Biochemistry*, 36, 13449-13454.
- Lehrer, S. S., Graceffa, P., & Betteridge, D. (1981). Conformational dynamics of tropomyosin in solution: Evidence for two conformational states. *Ann NY Acad Sci*, 366, 285-299.
- Lehrer, S. S., & Kerwar, G. (1972). Intrinsic fluorescence of actin. *Biochemistry*, 11, 1211-1217.
- Lehrer, S. S., & Morris, E. P. (1982). Dual effects of tropomyosin and troponin-tropomyosin on actomyosin subfragment 1 ATPase. *J Biol Chem*, 257, 8073-8080.
- Lehrer, S. S., & Morris, E. P. (1984). Comparison of the effects of smooth and skeletal tropomyosin on skeletal actomyosin subfragment 1 ATPase. *J Biol Chem*, 259, 2070-2072.
- Levine, B. A., Patchell, V. B., & Perry, S. V. (1999). Troponin I and conformational changes in actin. *J Muscle Res Cell Motil*, 20, 828-829.
- Li, M. X., Spyropoulos, L., & Sykes, B. D. (1999). Binding of cardiac troponin-I₁₄₇₋₁₆₃ induces a structural opening in human cardiac troponin-C. *Biochemistry*, 38, 8289-8298.

- Li, M. X., Wang, X., & Sykes, B. D. (2004). Structural based insights into the role of troponin in cardiac muscle pathophysiology. *J Muscle Res Cell Motil*, 25, 559-579.
- Li, Y., Mui, S., Brown, J. H., Strand, J., Reshetnikova, L., Tobacman, L. S., et al. (2002). The crystal structure of the C-terminal fragment of striated-muscle -tropomyosin reveals a key troponin T recognition site. *Proc Natl Acad Sci USA*, 99, 7378-7383.
- Li, Z., Gergely, J., & Tao, T. (2001). Proximity relationships between residue 117 of rabbit skeletal troponin-I and residues in troponin-C and actin. *Biophys J*, 81, 321-333.
- Libri, D., Lemonnier, M., Meinel, T., & Fiszman, M. Y. (1989). A single gene codes for the beta subunits of smooth and skeletal muscle tropomyosin in the chicken. *J Biol Chem*, 264, 2935-2944.
- Lin, J. J., Warren, K. S., Wamboldt, D. D., Wang, T., & Lin, J. L. (1997). Tropomyosin isoforms in non-muscle cells. *Int Rev Cytol*, 170, 1-38.
- Lin, T. I., & Dowben, R. M. (1983). Studies on the spatial arrangement of muscle thin filament proteins using fluorescence energy transfer. *J Biol Chem*, 258, 5142-5150.
- Lin, T. Y., & Timasheff, S. N. (1994). Why do some organisms use a urea-methylamine mixture as osmolyte? thermodynamic compensation of urea and trimethylamine N-oxide interactions with protein. *Biochemistry*, 33, 12695-12701.

- Lorenz, M., Popp, D., & Holmes, K. C. (1993). Refinement of the F-actin model against X-ray fiber diffraction data by the use of a directed mutation algorithm. *J Mol Biol*, 234, 826-836.
- Lowey, S., Slayter, H. S., Weeds, A. G., & Baker, H. (1969). Substructure of the myosin molecule : I. Subfragments of myosin by enzymic degradation. *J Mol Biol*, 42, 1-6.
- Luo, Y., Wu, J. L., Li, B., Langsetmo, K., Gergely, J., & Tao, T. (2000). Photocrosslinking of benzophenone-labeled single cysteine troponin I mutants to other thin filament proteins. *J Mol Biol*, 296, 899-910.
- Lymn, R. W., & Taylor, E. W. (1971). Mechanism of adenosine phosphate hydrolysis by actomyosin. *Biochemistry*, 10, 4617-4624.
- MacLeod, A. R., & Gooding, C. (1988). Human hTMA gene: Expression in muscle and non-muscle tissue. *Mol Cell Biol*, 8, 433-440.
- MacLeod, A. R., Talbot, K., Smillie, L. B., & Houliker, C. (1987). Characterization of a cDNA defining a gene family encoding TM30pl, a human fibroblast trpomyosin. *J Mol Biol*, 194, 1-10.
- Maita, T., Yajima, E., Nagata, S., Miyanishi, T., Nakayama, S., & Matsuda, G. (1991). The primary structure of skeletal muscle myosin heavy chain: IV. Sequence of the rod, and the complete 1,938-residue sequence of the heavy chain. *J Biochem (Tokyo)*, 110, 75-87.

- Mak, A. S., Golonska, K., & Smillie, L. B. (1983). Induction of nonpolymerizable tropomyosin binding to F-actin by troponin and its components. *J Biol Chem*, 258, 14330-14334.
- Mak, A. S., & Smillie, L. B. (1981a). Non-polymerizable tropomyosin: Preparation, some properties and F-actin binding. *Biochem Biophys Res Commun*, 101, 208-214.
- Mak, A. S., & Smillie, L. B. (1981b). Structural interpretation of the two-site binding of troponin on the muscle thin filament. *J Mol Biol*, 149, 541-550.
- Malnic, B., Farah, C. S., & Reinach, F. C. (1998). Regulatory properties of the NH₂- and COOH-terminal domains of troponin T. ATPase activation and binding to troponin I and troponin C. *J Biol Chem*, 273, 10594-10601.
- Marshall, J. M., Holtzer, H., Finck, H., & Pepe, F. (1959). The distribution of protein antigens in striated myofibrils. *Exp Cell Res*, 7, 219-233.
- Martins, S. M., Chapeaurouge, A., & Ferreira, S. T. (2002). Equilibrium unfolding and conformational plasticity of troponin I and T. *Eur J Biochem*, 269, 5484-5491.
- Maytum, R., Lehrer, S. S., & Geeves, M. A. (1999). Cooperativity and switching within the three-state model of muscle regulation. *Biochemistry*, 38, 1102-1110.
- McCarter, J. D., Stephens, D., Shoemaker, K., Rosenberg, S., Kirsh, J. F., & Georgiou, G. (2004). Substrate specificity of the *Escherichia coli* outer membrane protease OmpT. *J Bacteriol*, 186, 5919-5925.

- McKay, R. T., Tripet, B. P., Hodges, R. S., & Sykes, B. D. (1997). Interaction of the second binding region of troponin I with the regulatory domain of skeletal muscle troponin C as determined by NMR spectroscopy. *J Biol Chem*, 272, 28494-28500.
- McKillop, D. F. A., & Geeves, M. A. (1993). Regulation of the interaction between actin and myosin subfragment 1: Evidence of three states of the thin filament. *Biophys J*, 65, 693-701.
- McLachlan, A. D., & Stewart, M. (1975). Tropomyosin coiled-coil interactions: Evidence for an unstaggered structure. *J Mol Biol*, 98, 293-304.
- McLachlan, A. D., & Stewart, M. (1976). The 14-fold periodicity in alpha-tropomyosin and the interaction with actin. *J Mol Biol*, 103, 271-298.
- McLaughlin, P. J., Gooch, J. T., Mannherz, H. G., & Weeds, A. G. (1993). Structure of gelsolin segment 1-actin complex and the mechanism of filament severing. *Nature*, 364, 685-692.
- Mihashi, K. (1972). Thermal modification of structure of tropomyosin. II. Fluorescence depolarization of tropomyosin-fluorescein isothiocyanate conjugate; a change in the rotational relaxation time near physiological temperature. *J Biochem (Tokyo)*, 71, 597-605.
- Miki, M. (1990). Resonance energy transfer between points in a reconstituted skeletal muscle thin filament. A conformational change of the thin filament in response to a change in Ca^{2+} concentration. *Eur J Biochem*, 187, 155-162.

- Miki, M. (2007). Conformational changes in reconstituted skeletal muscle thin filaments observed by fluorescence spectroscopy. *Adv Exp Med Biology*, 592, 111-124.
- Miki, M., Hai, H., Saeki, K., Shitaka, Y., Sano, K. I., Maéda, Y., et al. (2004). Fluorescence resonance energy transfer between points on actin and the C-terminal region of tropomyosin in skeletal muscle thin filaments. *J Biochem (Tokyo)*, 136, 39-47.
- Miki, M., & Kihashi, K. (1979). Conformational change of the reconstituted thin filaments-fluorescence energy transfer and fluorescence polarization measurements. *Seibutsu-Butsuri*, 19, 135-140.
- Miki, M., Kobayashi, T., Kimura, H., Hagiwara, A., Hai, H., & Maeda, Y. (1998a). Ca²⁺-induced distance change between points on actin and troponin in skeletal muscle thin filaments estimated by fluorescence energy transfer spectroscopy. *J Biochem (Tokyo)*, 123, 324-331.
- Miki, M., Miura, T., Sano, K. I., Kimura, H., Kondo, H., Ishida, H., et al. (1998b). Fluorescence resonance energy transfer between points on tropomyosin and actin in skeletal muscle thin filaments: Does tropomyosin move? *J Biochem (Tokyo)*, 123, 1104-1111.
- Milligan, R. A., Whittaker, M., & Safer, D. (1990). Molecular structure of F-actin and location of surface binding sites. *Nature*, 348, 217-221.

- Milligan, R. A., & Flicker, P. F. (1987). Structural relationships of actin, myosin, and tropomyosin revealed by cryo-electron microscopy. *J Cell Biol*, 105, 29-39.
- Mo, J., Holtzer, M. E., & Holtzer, A. (1990). The thermal denaturation of nonpolymerizable alpha,alpha tropomyosin and its segments as a function of ionic strength. *Biopolymers*, 30, 921-927.
- Molina, M. I., Kropp, K. E., Gulick, J., & Robbins, J. (1987). The sequence of an embryonic myosin heavy chain gene and isolation of its corresponding cDNA. *J Biol Chem*, 262, 6478-6488.
- Monmaerts, W. F. H. M. (1952). The molecular transformations of actin. III. The participation of nucleotides. *J Biol Chem*, 198, 469-475.
- Montarras, D., Fiszman, M. Y., & Gross, F. (1981). Characterization of the tropomyosin present in various chick embryo muscle types and in muscle cells differentiated in vitro. *J Biol Chem*, 256, 4081-4086.
- Monteiro, P. B., Lataro, R. C., Ferro, J. A., & Reinach, F. C. (1994). Functional alpha tropomyosin produced in *Escherichia coli*. A dipeptide extension can substitute the amino terminal acetyl-group. *J Biol Chem*, 269, 10461-10466.
- Moore, G. E., & Schachat, F. H. (1985). Molecular heterogeneity of histochemical fibre types: A comparison of fast fibres. *J Muscle Res Cell Motil*, 11, 176-185.
- Moore, P. B., Huxley, H. E., & DeRosier, D. J. (1970). Three-dimensional reconstruction of F-actin, thin filaments and decorated thin filaments. *J Mol Biol*, 50, 279-288.

- Moraczewska, J., & Hitchcock-DeGregori, S. E. (2000). Independent functions for the N- and C-termini in the overlap region of tropomyosin. *Biochemistry*, *39*, 6891-6897.
- Morris, E. P., & Lehrer, S. S. (1984). Troponin-tropomyosin interactions. Fluorescence studies of the binding of troponin, troponin T and chymotryptic troponin T fragments to specifically labeled tropomyosin. *Biochemistry*, *23*, 2214-2220.
- Mozo-Villarias, A., & Ware, B. R. (1985). Actin oligomers below the critical concentration detected by fluorescence photobleaching recovery. *Biochemistry*, *24*, 1544-1548.
- Murray, J. M., Knox, M. K., Trueblood, C. E., & Weber, A. (1982). Potentiated state of the tropomyosin actin filament and nucleotide-containing myosin subfragment 1. *Biochemistry*, *21*, 906-915.
- Murray, J. M., Weber, A., & Knox, M. K. (1981). Myosin subfragment 1 binding to relaxed actin filaments and steric model of relaxation. *Biochemistry*, *20*, 641-649.
- Muthuchamy, M., Rethinasamy, P., & Wieczorek, D. F. (1997). Tropomyosin structure and function – new insights. *Trends Cardiovas Med*, *7*, 124-128.
- Nagy, B. (1977). Circular dichroic and perturbation spectra of aromatic chromophores in rabbit tropomyosin. *J Biol Chem*, *252*, 4557-4563.
- Nagy, B., & Jencks, W. P. (1980). Optical rotatory dispersion of G-actin. *Biochemistry*, *19*, 987-996.

- Nakamura, S., Yamamoto, K., Hashimoto, K., & Ohtsuki, I. (1981). Effect of chymotryptic troponin T subfragments on the Ca^{2+} sensitivity of superprecipitation. *J Biochem (Tokyo)*, 89, 1639-1641.
- Narita, A., Yasunaga, T., Ishikawa, T., Mayanagi, K., & Wakabayashi, T. (2001). Ca^{2+} -induced switching of troponin and tropomyosin on actin filaments as revealed by electron cryo-microscopy. *Journal of Molecular Biology*, 308, 241-261.
- Newman, J., Estes, J. E., Selden, L. A., & Gershman, L. C. (1985). Presence of oligomers at subcritical actin concentrations. *Biochemistry*, 24, 1538-1544.
- O'shea, E. K., Rutkowski, R., & Kim, P. S. (1989). Evidence that the leuzine zipper is a coiled coil. *Science*, 243, 538-542.
- Oda, T., Makino, K., Yamashita, I., Namba, K., & Maéda, Y. (1998). Effect of the length and effective diameter of F-actin on the filament orientation in liquid crystalline sols measured by X-ray fiber diffraction. *Biophys J*, 75, 2672-2681.
- Ohtsuki, I. (1974). Localization of troponin in thin filament and tropomyosin paracrystal. *J Biochem*, 75, 753-765.
- Ohtsuki, I. (1975). Distribution of troponin components in the thin filament studied by immunoelectron microscopy. *J Biochem (Tokyo)*, 77, 633-639.
- Ohtsuki, I. (1979). Molecular arrangement of troponin-T in the thin filament. *J Biochem (Tokyo)*, 86, 491-497.

- Ohtsuki, I. (2007). Troponin: Structure, function and dysfunction. *Adv Exp Med Biology*, 592, 21-36.
- Ohtsuki, I., Masaki, T., Nonomura, Y., & Ebashi, S. (1967). Periodic distribution of troponin along the thin filament. *J Biochem (Tokyo)*, 61, 817-819.
- Ohtsuki, I., Yamamoto, K., & Hashimoto, K. (1981). Effect of two C-terminal side chymotryptic troponin T subfragments on the Ca^{2+} sensitivity of superprecipitation and ATPase activities of actomyosin. *J Biochem (Tokyo)*, 90, 259-261.
- Oikawa, K., Kay, C. M., & McCubbin, W. D. (1968). The ultraviolet circular dichroism of muscle proteins. *Biochem Biophys Acta*, 168, 164-167.
- Onoyama, Y., & Ohtsuki, I. (1986). Effect of chymotryptic troponin T subfragments on the calcium ion-sensitivity of ATPase and superprecipitation of actomyosin. *J Biochem (Tokyo)*, 100, 517-519.
- Otterbein, L. R., Graceffa, P., & Dominguez, R. (2001). The crystal structure of uncomplexed actin in the ADP state. *Science*, 293, 708-711.
- Pan, B. S., Gordon, A. M., & Luo, Z. (1989). Removal of tropomyosin overlap modifies cooperative binding of myosin S-1 to reconstituted thin filaments of rabbit striated muscle. *J Biol Chem*, 264, 8495-8498.
- Parry, D. A. D. (1975). Analysis of the primary sequence of α -tropomyosin from rabbit skeletal muscle. *J Mol Biol*, 98, 519-535.

- Parry, D. A. D. (1981). Analysis of the amino acid sequence of a tropomyosin-binding fragment from troponin-T. *J Mol Biol*, 146, 259-263.
- Parry, D. A. D., & Squire, J. M. (1973). Structural role of tropomyosin in muscle regulation: Analysis of the X-ray diffraction patterns from relaxed and contracting muscles. *J Mol Biol*, 75, 33-34.
- Pato, M. D., Mak, A. S., & Smillie, L. B. (1981a). Fragments of rabbit striated muscle alpha-tropomyosin: Preparation and characterization. *J Biol Chem*, 256, 593-601.
- Pato, M. D., Mak, A. S., & Smillie, L. B. (1981b). Fragments of rabbit striated muscle alpha-tropomyosin: Binding to troponin T. *J Biol Chem*, 256, 602-607.
- Pearlstone, J. R., Carpenter, M. R., Johnson, P., & Smillie, L. B. (1976). Amino-acid sequence of tropomyosin-binding component of rabbit skeletal muscle troponin. *Proc Natl Acad Sci USA*, 73, 1902-1906.
- Pearlstone, J. R., & Smillie, L. B. (1982). Binding of troponin-T fragments to several types of tropomyosin. Sensitivity to Ca^{2+} in the presence of troponin-C. *J Biol Chem*, 257, 10587-10592.
- Pearlstone, J. R., & Smillie, L. B. (1981). Identification of a second binding region on rabbit skeletal troponin-T for α -tropomyosin. *FEBS Letts*, 128, 119-122.
- Pearlstone, J. R., & Smillie, L. B. (1985). The interaction of rabbit skeletal muscle troponin-T fragments with troponin-I. *Can J Biochem Cell Biol*, 63, 212-218.

- Perry, S. V. (1955). Proteins in muscular contraction. *Lect Sci Basis Med*, 5, 314-320.
- Perry, S. V. (2001). Vertebrate tropomyosin: Distribution, properties and function. *J Muscle Res Cell Motil*, 22, 5-49.
- Perry, S. V. (2003). What is the role of tropomyosin in the regulation of muscle contraction? *J Muscle Res Cell Motil*, 24, 593-596.
- Phillips, G. N. J., Filler, J. P., & Cohen, C. (1986). Tropomyosin crystal structure and muscle regulation. *J Mol Biol*, 192, 111-113.
- Phillips, G. N. J., Lattman, E. E., Cummins, P., Lee, K. Y., & Cohen, C. (1979). Crystal structure and molecular interaction of tropomyosin. *Nature*, 278, 413-417.
- Phillips, G. N. J., Fillers, J. P., & Cohen, C. (1980). Motions of tropomyosin. Crystal as metaphor. *Biophys J*, 32, 485-502.
- Pieples, K., & Wiczorek, D. F. (1999). Characterization and expression of tropomyosin 30 (TM3). *Biophys J*, 76a, 41.
- Pieples, K., & Wiczorek, D. F. (2000). Tropomyosin increases striated muscle diversity. *Biochemstry*, 39, 8291-8297.
- Pollard, T. D., Almo, S., Quirk, S., Vinson, V., & Lattman, E. E. (1994). Structure of actin binding proteins: Insights about function at atomic resolution. *Annu Rev Cell Biol*, 10, 207-249.

- Pollard, T. D., & Mooseker, M. S. (1981). Direct measurement of actin polymerization rate constants by electron microscopy of actin filaments nucleated by isolated microvillus cores. *J Cell Biol*, 88, 654-659.
- Pont, M. J., & Woods, E. F. (1971). Denaturation of tropomyosin by guanidine hydrochloride. *Int J Protein Res*, 3, 177-183.
- Poole, K., Evans, J. V., Rosenbaum, G., Lorenz, M., & Holmes, K. C. (1995). The effect of crossbridges on the calcium sensitivity of the structural change of the regulated thin filament. *Biophys J*, 68a, 365.
- Potekhin, S. A., & Privalov, P. L. (1978). Heat denaturation of alpha-tropomyosin and its fragments. *Biofizika*, 23, 219-223.
- Potekhin, S. A., & Privalov, P. L. (1982). Co-operative blocks in tropomyosin. *J Mol Biol*, 159, 519-535.
- Potter, J. D. (1982). Purification and identification of alpha and beta tropomyosins. *Methods Enzymol*, 85, 241-263.
- Potter, J. D., & Gergely, J. (1975). The calcium and magnesium binding sites on troponin and their role in the regulation of myofibrillar adenosine triphosphatase. *J Biol Chem*, 250, 4628-4633.
- Prendergast, F. G., & Potter, J. D. (1979). Solution conformation and hydrodynamic properties of rabbit skeletal troponin T. *Biophys J*, 25a, 250.

- Rayment, I., Rypniewski, W. R., Schmidt-Base, K., Smith, R., Tomchick, D. R., Benning, M. M., et al. (1993). Three-dimensional structure of myosin subfragment-1: A molecular motor. *Science*, 261, 50-58.
- Robertson, S. P., Johnson, J. D., & Potter, J. D. (1981). The time-course of Ca^{2+} exchange with calmodulin, troponin, parvalbumin, and myosin in response to transient increases in Ca^{2+} . *Biophys J*, 34, 559-569.
- Rosol, M., Lehman, W., Craig, R., Landis, C., Butters, C., & Tobacman, L. S. (2000). Three-dimensional reconstruction of thin filaments containing mutant tropomyosin. *Biophys J*, 78, 908-917.
- Rould, M. A., Wan, Q., Joel, P. B., Lowey, S., & Trybus, K. M. (2006). Crystal structures of expressed non-polymerizable monomeric actin in the ADP and ATP states. *J Biol Chem*, 281, 31909-31919.
- Ruiz-Opazo, N., & Ginard, G. B. (1987). Alpha-tropomyosin gene organization. Alternative splicing of duplicated isotype specific exons accounts for the production of smooth and striated muscle isoforms. *J Biol Chem*, 262, 4755-4765.
- Salviati, G., Betto, R., & Danieli Betto, D. (1982). Polymorphism of myofibrillar proteins of rabbit skeletal muscle fibres. *Biochem J*, 207, 261-272.
- Sambrook, J., Fritsch, E. F., Maniatis, T. (1989) Molecular cloning: a laboratory manual, (2 nd ed., pp1.63-1.72, 6.46-6.49). USA. Cold Spring Harbor Laboratory Press.

- Satoh, A., & Mihashi, K. (1972). Thermal modification of structure of tropomyosin. I. Changes in the intensity and polarization of the intrinsic fluorescence (tyrosine). *J. Biochem (Tokyo)*, *71*, 597-605.
- Saxena, V. P., & Wetlaufer, D. B. (1971). A new basis for interpreting the circular dichroic spectra of proteins. *Proc Natl Acad Sci USA*, *68*, 969-972.
- Schaertl, S., Lehrer, S. S., & Geeves, M. A. (1995). Separation and characterization of the two functional regions of troponin involved in muscle thin filament regulation. *Biochemistry*, *34*, 15890-15894.
- Schaub, M. C., & Perry, S. V. (1969). The relaxing protein system of striated muscle. Resolution of the troponin complex into inhibitory and calcium ion-sensitizing factors and their relationship to tropomyosin. *Biochem J*, *115*, 993-1004.
- Schutt, C. E., Myslik, J. C., Rozycki, M. D., Goonesekere, N. C. W., & Lindberg, U. (1993). The structure of crystalline profilin-actin. *Nature*, *365*, 810-816.
- Sia, S. K., Li, M. X., Spyropoulos, L., Gagné, S. M., Liu, W., Putkey, J. A., et al. (1997). Structure of cardiac muscle troponin C unexpectedly reveals a closed regulatory domain. *J Biol Chem*, *272*, 18216-18221.
- Singh, A., & Hitchcock-DeGregori, S. E. (2003). Local destabilization of the tropomyosin coiled-coil gives the molecular flexibility required for actin binding. *Biochemistry*, *42*, 14114-14121.

- Singh, A., & Hitchcock-DeGregori, S. E. (2006). Dual requirement for flexibility and specificity for binding of the coiled-coil tropomyosin to its target, actin. *Structure*, *14*, 43-50.
- Slupsky, C. M., & Sykes, B. D. (1995). NMR solution structure of calcium-saturated skeletal muscle troponin C. *Biochemistry*, *34*, 15953-15964.
- Smillie, L. B. (1979). Structure and functions of tropomyosins from muscle and nonmuscle sources. *Trends Biochem Sci*, *4*, 151-154.
- Smillie, L. B. (1996). Tropomyosin. In M. Barany (Ed.), *Biochemistry of smooth muscle contraction* (pp. 63-75). New York: Academic press.
- Smith, D. A., & Geeves, M. A. (2003). Cooperative regulation of myosin-actin interactions by a continuous flexible chain II: Actin-tropomyosin-troponin and regulation by calcium. *Biophys J*, *84*, 3168-3180.
- Smith, P. R., Fowler, W. E., Pollard, T. D., Aebi, U., & Huxley, H. E. (1983). Structure of the actin molecule determined from electron micrographs of crystalline actin sheets with a tentative alignment of the molecule in the actin filament. *J Mol Biol*, *167*, 641-660.
- Sodek, J., Hodges, R. S., & Smillie, L. B. (1978). Amino acid sequence of rabbit skeletal muscle alpha-tropomyosin. the COOH-terminal half (residues 142 to 284). *J Biol Chem*, *253*, 1129-1136.

- Sodek, J., HoDges, R. S., Smillie, L. B., & Jurasek, L. (1972). Amino-acid sequence of rabbit skeletal tropomyosin and its coiled-coil structure. *Proc Natl Acad Sci USA*, 69, 3800-3804.
- Spudich, J. A., Huxley, H. E., & Finch, J. T. (1972). Regulation of skeletal muscle contraction: II. Structural studies of the interaction of the tropomyosin-troponin complex with actin. *J Mol Biol*, 72, 619-620.
- Spudich, J. A., & Watt, S. (1971). The regulation of rabbit skeletal muscle contraction. I. Biochemical studies of the interaction of the tropomyosin-troponin complex with actin. *J Biol Chem*, 246, 4866-4871.
- Stefancsik, R., Jha, P. K., & Sarkar, S. (1998). Identification and mutagenesis of a highly conserved domain in troponin T responsible for troponin I binding: Potential role for coiled coil interaction. *Proc Natl Acad Sci USA*, 95, 957-962.
- Steinbach, J. H., Schubert, D., & Eldridgs, L. (1980). Changes in cat muscle contractile proteins after prolonged inactivity. *Expl Neur*, 67, 655-669.
- Stewart, M. (1975b). Tropomyosin: Evidence for no stagger between the chains. *FEBS Letts*, 53, 5-7.
- Stewart, M. (2001). Structural basis for bending tropomyosin around actin in muscle thin filaments. *Proc Natl Acad Sci USA*, 98, 8165-8166.
- Stewart, M., & McLachlan, A. D. (1975a). Fourteen actin binding sites on tropomyosin? *Nature*, 257, 331-333.

- Stone, D., & Smillie, L. B. (1978). The amino acid sequence of rabbit skeletal alpha-tropomyosin. The NH₂-terminal half and complete sequence. *J Biol Chem*, 253, 1137-1148.
- Stone, D., Sodek, J., Johnson, P., & Smillie, L. B. (1975). *Proc 9th FEBS Meeting*, 31, 125-136.
- Straub, F. B. (1942). Actin. *Stud Szeged*, 2, 3-15.
- Straub, F. B., & Feuer, G. (1950). Adenosinetriphosphate. The functional group of actin. *Biochim Biophys Acta*, 4, 455-470.
- Strynadka, N. C. J., Cherney, M., Sielecki, A. R., Li, M. X., Smillie, L. B., & James, M. N. G. (1997). Structural details of a calcium-induced molecular switch: X-ray crystallographic analysis of the calcium-saturated N-terminal domain of troponin C at 1.75 Å resolution. *J Mol Biol*, 273, 238-255.
- Strzelecka-Golaszewska, H. (1973). Relative affinities of divalent cations to the site of the tight calcium binding in G-actin. *Biochim Biophys Acta*, 310, 60-69.
- Strzelecka-Golaszewska, H., Pröchniewicz, E., & Drabikowski, W. (1978). Interaction of actin with divalent cations. 2. Characterization of protein-metal complexes. *Eur J Biochem*, 88, 229-237.
- Sugimura, K., & Nishihara, T. (1988). Purification, characterisation and primary structure of *Escherichia coli* protease VII with specificity for paired basic residues: Identity of protease VII and OmpT. *J Bacteriol*, 170, 5625-5632.

- Sundaralingam, M., Bergstrom, R., Strasburg, G., Rao, S. T., Roychowdhury, P., Greaser, M., et al. (1985). Molecular structure of troponin C from chicken skeletal muscle at 3-Å resolution. *Science*, 227, 945-948.
- Takeda, S., Kobayashi, T., Taniguchi, H., Hayashi, H., & Maéda, Y. (1997). Structural and functional domains of the troponin complex revealed by limited digestion. *Eur J Biochem*, 246, 611-617.
- Takeda, S., Yamashita, A., Maeda, K., & Maéda, Y. (2003). Structure of the core domain of human cardiac troponin in the Ca²⁺-saturated form. *Nature*, 424, 35-41.
- Talbot, J. A., & Hodges, R. S. (1981). Synthetic studies on the inhibitory region of rabbit skeletal troponin I. Relationship of amino acid sequence to biological activity. *J Biol Chem*, 256, 2798-2802.
- Tanokura, M., Tawada, Y., & Ohtsuki, I. (1982). Chymotryptic subfragments of troponin T from rabbit skeletal muscle. I. Determination of the primary structure. *J Biochem (Tokyo)*, 91, 1257-1265.
- Tanokura, M., Tawada, Y., Ono, A., & Ohtsuki, I. (1983). Chymotryptic subfragments of troponin T from rabbit skeletal muscle. Interaction with tropomyosin, troponin I and troponin C. *J Biochem (Tokyo)*, 93, 331-337.
- Tao, T., Gong, B. J., & Leavis, P. C. (1990). Calcium-induced movement of troponin-I relative to actin in skeletal muscle thin filaments. *Science*, 247, 1339-1341.

- Tao, T., Lamkin, M., Lehrer, S. S., & Morris, E. P. (1983). Excitation energy transfer studies of the proximity between tropomyosin and actin in reconstituted skeletal muscle thin filaments. Computer simulation study on the extent of energy transfer from a single Tm-bound donor to multiple actin-bound acceptors. *Biochemistry*, *22*, 3059-3066.
- Thierfelder, L., Watkins, H., MacRae, C. A., Lamas, R. McKenna, W.J., Vosberg, H., Siedman, J. G., et al. (1994). Alpha-tropomyosin and cardiac troponin-T mutations cause familial hypertrophic cardiomyopathy: A disease of the sarcomere. *Cell*, *77*, 701-712.
- Tobacman, L. S., & Butters, C. A. (2000). A new model of cooperative myosin-thin filament binding. *J Biol Chem*, *275*, 27587-27593.
- Tobacman, L.S., Nihli, M., Butters, C. A, Heller, M., Hatch, V., Craig, R., Lehman, W. & Homsher, E. (2002) The Troponin Tail Domain Promotes a Conformational State of the Thin Filament That Suppresses Myosin Activity. *J Biol Chem*, *277*, 27636-27642.
- Tobacman, L. S., & Korn, E. D. (1983). The kinetics of actin nucleation and polymerization. *J Biol Chem*, *258*, 3207-3214.
- Townsend, P. J., Barton, P. J. R., Yacoub, M. H., & Farza, H. (1995). Molecular cloning of human cardiac troponin T isoforms: Expression in developing and failing heart. *J Mol Cell Cardiol*, *27*, 2223-2236.

- Triplet, B., Wagshal, K., Lavigne, P., Mant, C. T., & Godges, R. S. (2000). Effects of side-chain characteristics on stability and oligomerisation state of a de novo-designed model coiled-coil: 20 amino acid substitutions in position "d". *J Mol Biol*, 300, 377-402.
- Ueno, H. (1984). Local structural changes in tropomyosin detected by a trypsin-probe method. *Biochemistry*, 23, 4791-4798.
- Ueno, H., Tawada, Y., & Ooi, T. (1976). Properties of non-polymerizable tropomyosin obtained by carboxypeptidase A digestion. *J Biochem (Tokyo)*, 80, 283-290.
- Urbancikova, M., & Hitchcock-DeGregori, S. E. (1994). Requirement of amino terminal modification for striated muscle alpha tropomyosin function. *J Biol Chem*, 269, 24310-24315.
- Van Eard, J. P., & Takahashi, K. (1975). The amino acid sequence of bovine cardiac troponin-C. comparison with rabbit skeletal troponin-C. *Biochem. Biophys. Res. Comm*, 64, 122-127.
- Vibert, P., Craig, R., & Lehman, W. (1997). Steric-model for activation of muscle thin filaments. *J Mol Biol*, 266, 8-14.
- Vinogradova, M. V., Stone, D. B., Malanina, G. G., Karatzaferi, C., Cooke, R., Mendelson, R. A., et al. (2005). Ca²⁺-regulated structural changes in troponin. *Proc Natl Acad Sci USA*, 102, 5038-5043.

- Walsh, T. P., Trueblood, C. E., Evans, R., & Weber, A. (1984). Removal of tropomyosin overlap and the cooperative response to increasing calcium concentrations of the acto-subfragment-1 ATPase. *J Mol Biol*, 182, 265-269.
- Weber, A., & Murray, J. M. (1973). Molecular control mechanisms in muscle contraction. *Physiol Rev*, 53, 612-673.
- Weeds, A. G., & Lowey, S. J. (1971). Substructure of the myosin molecule: II. The light chains of myosin. *J Mol Biol*, 61, 701-725.
- Weeds, A. G., & Pope, B. (1977). Studies on the chymotryptic digestion of myosin. Effects of divalent cations on proteolytic susceptibility. *J Mol Biol*, 111, 129-157.
- Weeds, A. G., & Taylor, R. S. (1975). Separation of subfragment-1 isoenzymes from rabbit skeletal muscle myosin. *Nature*, 257, 54-56.
- Wegner, A. (1976). Head to tail polymerization of actin. *J Mol Biol*, 108, 139-150.
- Wegner, A. (1977). The mechanism of ATP hydrolysis by polymer actin. *Biophys Chem*, 7, 51-58.
- Wegner, A. (1982). Treadmilling of actin at physiological salt concentrations. An analysis of the critical concentrations of actin filaments. *J Mol Biol*, 161, 607-615.
- Wegner, A., & Engel, J. (1975). Kinetics of the cooperative association of actin to actin filament. *Biophys Chem*, 3, 215-225.

- Wegner, A., & Isenberg, G. (1983). 12-fold difference between the critical monomer concentrations of the two ends of actin filaments in physiological salt conditions. *Proc Natl Acad Sci USA*, *80*, 4922-4925.
- Wegner, A., & Neuhaus, J. (1981). Requirement of divalent cations for fast exchange of actin monomers and actin filament subunits. *J Mol Biol*, *153*, 681-693.
- Whitby, F. G., & Phillips, G. N. J. (2000). Crystal structure of tropomyosin at 7 angstroms resolution. *Proteins*, *38*, 49-59.
- White, H. D. (1982). Special instrumentation and techniques for kinetic studies of contractile systems. *Methods Enzymol*, *85*, 698-708.
- White, H. D., Belknap, B., & Webb, M. R. (1997). Kinetics of nucleoside triphosphate cleavage and phosphate release steps by associated rabbit skeletal actomyosin, measured using a novel fluorescent probe for phosphate. *Biochemistry*, *36*, 11828-11836.
- White, S. P., Cohen, C., & Phillips, G. N. (1987). Structure of co-crystals of tropomyosin and troponin. *Nature*, *325*, 826-828.
- Wieczorek, D. F., Smith, C. W. J., & Nadal-Ginard, B. (1988). The rat alpha-tropomyosin gene generates a minimum of six different mRNAs coding for striated, smooth and nonmuscle isoforms by alternative splicing. *Mol Cell Biol*, *8*, 679-694.

- Wilkinson, J. M., Perry, S. V., Cole, H. A., & Trayer, I. P. (1972). The regulatory proteins of the myofibril. Separation and biological activity of the components of inhibitory-factor preparations. *Biochem J*, 127, 215-228.
- Wilkinson, J. M. (1974). The preparation and properties of the components of troponin B. *Biochim Biophys Acta*, 359, 379-388.
- Wilkinson, J. M., & Grand, R. J. (1975). The amino acid sequence of troponin I from rabbit skeletal muscle. *Biochem J*, 149, 493-496.
- Williams, D. L., Greene, L. E., & Eisenberg, E. (1984). Comparison of effects of smooth and skeletal muscle tropomyosins on interactions of actin and myosin subfragment 1. *Biochemistry*, 23, 4150-4155.
- Williams, D. L., & Swenson, C. A. (1981). Tropomyosin stability: Assignment of thermally induced conformational transitions to separate regions of the molecule. *Biochemistry*, 20, 3856-3864.
- Woodrum, D. T., Rich, S. A., & Pollard, T. D. (1975). Evidence for biased bidirectional polymerization of actin filaments using heavy meromyosin prepared by an improved method. *J Cell Biol*, 67, 231-237.
- Woods, E. F. (1966). Dissociation of tropomyosin by urea. *J Mol Biol*, 16, 581-584.
- Woods, E. F. (1967). Molecular weight and subunit structure of tropomyosin B. *J Biol Chem*, 242, 2859-2871.

- Woods, E. F. (1969). Studies on the denaturation of tropomyosin and light meromyosin. *Int J Protein Res*, 1, 29-43.
- Woods, E. F. (1976). The conformational stabilities of tropomyosin. *Aus J Biol Sci*, 29, 405-418.
- Xu, C., Craig, R., Tobacman, L. S., Horowitz, R., & Lehman, W. (1999). Tropomyosin positions in regulated thin filaments revealed by cryoelectron microscopy. *Biophys J*, 77, 985-992.
- Yagi, N., & Matsubara, I. (1989). Structural changes in the thin filament during activation studied by X-ray diffraction of highly stretched skeletal muscle. *J Mol Biol*, 208, 359-363.
- Yamawaki-Katoaka, Y., & Helfman, D. M. (1985). Rat embryonic fibroblast tropomyosin 1. cDNA and complete primary amino acid sequence. *J Biol Chem*, 260, 14440-14445.
- Yancey, P. H., & Somero, G. N. (1979). Counteraction of urea destabilization of protein structure by methylamine osmoregulatory compounds of elasmobranch fishes. *Biochem J*, 183, 317-323.
- Yang, Y. Z., Korn, E. D., & Eisenberg, E. (1979). Cooperative binding of tropomyosin to muscle and acanthamoeba actin. *J Biol Chem*, 254, 7137-7140.

Zou, Q., Bennion, J., Daggett, V., & Murphy, K. P. (2002). The molecular mechanism of stabilization of proteins by TMAO and its ability to counteract the effects of urea. *J Am Chem Soc*, 124, 1192-1202.

